

**Kinetics and Engineering of Solid Acid Catalyzed Selective
Toluene Nitration**

THESIS

Submitted in partial fulfilment
of the requirements for the degree of
DOCTOR OF PHILOSOPHY

by

INKOLLU SREEDHAR

Under the Supervision of

Dr. K. V. Raghavan

Chairman, Recruitment and Assessment Centre, DRDO



**BIRLA INSTITUTE OF TECHNOLOGY AND SCIENCE
PILANI (RAJASTHAN) INDIA**

2007

**Kinetics and Engineering of Solid Acid Catalyzed Selective
Toluene Nitration**

THESIS

Submitted in partial fulfilment
of the requirements for the degree of
DOCTOR OF PHILOSOPHY

by

INKOLLU SREEDHAR

Under the Supervision of

Dr. K. V. Raghavan

Chairman, Recruitment and Assessment Centre, DRDO



**BIRLA INSTITUTE OF TECHNOLOGY AND SCIENCE
PILANI (RAJASTHAN) INDIA**

2007

**BIRLA INSTITUTE OF TECHNOLOGY AND SCIENCE
PILANI (RAJASTHAN)**

CERTIFICATE

This is to certify that the thesis entitled “**Kinetics and Engineering of Solid Acid Catalyzed Selective Toluene Nitration**” submitted by **Inkollu Sreedhar** ID. No. **2002PHXF028** for award of Ph.D. Degree of the Institute, embodies the original work done by him under my supervision.

Signature in full of the Supervisor-----

Name in capital block letters: Dr. K. V. RAGHAVAN

Designation: Chairman, Recruitment and Assessment Centre, DRDO

Date:

ACKNOWLEDGEMENTS

It gives me great pleasure and opportunity to express my deep sense of gratitude and indebtedness to my research supervisor, Dr. K.V. Raghavan, Chairman, RAC, DRDO, Delhi for his meticulous guidance, valuable suggestions and constant encouragement and inspiring discussions throughout this investigation. I consider myself highly fortunate and privileged to be associated with him during this research period. It is an honour to work under such an inspiring personality and this thesis would not have seen the light of the day without his support and care.

I am highly grateful to BITS, Pilani for providing all the required support to complete my research work. My sincere thanks to Prof. L.K. Maheshwari, the Vice-Chancellor of the institute for allowing me to pursue my research work. My special thanks to Prof. V.S. Rao, Director, BITS, Pilani - Hyderabad Campus for all his support, encouragement and inspiring words.

I am highly thankful to Prof. Ravi Prakash, Dean, Research and Consultancy Division and his team for their support and constant monitoring throughout my research work. Thanks are also accorded to Prof. G. Sundar, Dean, Practice School Division for his support. My special thanks to Prof. B. R. Natarajan, Dean, DLPD for his kind support.

I wish to express my profound regards to Prof. B.V. Babu and Dr. Arvind Kumar Sharma who are the members of Doctoral Advisory Committee (DAC) for their kind suggestions, enquiries and moral support.

Special acknowledgements to Director, Indian Institute of Chemical Technology (IICT) for providing all the necessary facilities and infrastructure to complete my research work. I am highly indebted to Dr. M. Ramakrishna, Scientist F, IICT for his invaluable suggestions, inputs and critical evaluation throughout my research work. Thanks are also

accorded to Dr. S.J. Kulkarni and Mr. K. Ravindranath Scientists EII, IICT for their support and providing the necessary facilities. My special thanks to Dr. N. Narender, Scientist C, IICT for his joyful support, encouragement and affectionate words. I express my profound thanks to Mr. K. Suresh Kumar Reddy, my co-research scholar for all his help, company and moral support throughout this research period. I would also like to thank Dr. K. Krishna Mohan, Post Doctoral Fellow and Mrs. C.N. Rohita, JTA, IICT for their timely help. Acknowledgements are due to all members of the Reaction Engineering Laboratory and staff of various analytical sections of IICT for their support.

My special acknowledgements to all the Practice School faculty of Hyderabad centre for their moral support. Thanks are also due to the staff of our Hyderabad Campus Office for their assistance.

I am greatly indebted to my parents I. Ramachandra Rao and I.V. Syamalamba for their incessant moral support, affection and encouragement. This work would not have been completed without the delightful support and company of my wife Rajeswari and children Srivarsha and Sri Anshul. My heartfelt thanks to my brother Dr. I. Srinivasa Rao and sisters R.V. Ramadevi, B. Padmaja, to my brothers-in-law R.D. Prasad, B.Panduranga Rao and my nephews Ravi Teja, Anudeep, nieces Akhila and Hema. Their love and affection have been the catalyst for what I am today. I am also highly thankful to my father-in-law and mother-in-law for their constant encouragement and support.

Last but not the least, it gives me immense pleasure to express my sincere thanks to one and all who have helped me directly or indirectly to successfully complete my research work.

ABSTRACT

The present investigations have focused on process, kinetics and reaction engineering studies on solid acid catalyzed toluene nitration in stirred tank reactor operated on batch and semi batch modes. They cover vital aspects of nitration viz., its thermodynamic feasibility, material and energy accountability, mixing, dispersion and phase inversion of HNO₃-toluene system and their impact on reactant conversion and product distribution, minimizing the catalyst inhibition effects of water formed during the reaction and its removal from the reaction front and size specificity and dealumination tendencies of the catalyst. Their understanding greatly contributed to the generation of new knowledge on solid catalyzed toluene nitration.

Toluene nitration as a liquid-liquid-solid system poses tremendous challenges for process standardization. The multiprocess parameter standardization as attempted in this work is unique in terms of the wide spread of process factors and unfolding their complex relationship with reactant conversion and product distribution. Heightening of *para*-selectivity in toluene nitration has always posed scientific challenges in view of the complex mechanism of nitronium ion formation and electrophilic substitution on an already substituted toluene. An attempt has been made in this work to adopt a two level standardization process in which the regioselectivity which is inherent to the catalyst is first brought to the fore and then *para*-selectivity is further heightened by suitably adjusting the acidity level of the microreaction environment in and around the catalyst particle to facilitate the transformation of lattice aluminium from tetrahedral to octahedral format.

In agitated solid-liquid-liquid dispersions, chemical reaction and multiphase mass transfer can occur simultaneously. Evaluation of their relative rates provides the key to the understanding of the controlling mechanism. An attempt has been made to experimentally determine the apparent rate of toluene nitration in a semi-batch mode of operation. After a detailed analysis of external and internal mass transfer resistances, the acid catalyzed toluene nitration is found to be kinetically controlled for the conditions employed in the semi batch nitration studies.

Keywords: Toluene Nitration, Zeolite Catalyst, *Para*-selectivity, Thermodynamic Aspects, Agitated Dispersions, Dispersion Morphology, Lattice Aluminium Transformation, Catalyst Microenvironment, Liquid-Liquid System, Liquid-Liquid-Solid System, Process Standardization, Catalyst Characterization, Stability, Regenerability, Mass Transfer Effects.

TABLE OF CONTENTS

ACKNOWLEDGEMENTS	i
ABSTRACT	iii
TABLE OF CONTENTS	v
LIST OF TABLES	x
LIST OF FIGURES	xii
LIST OF SYMBOLS	xiv
ABBREVIATIONS / ACRONYMS	xviii
1 INTRODUCTION	1
1.1 AROMATIC NITRATIONS	1
1.1.1 Historical	1
1.1.2 The Nitration Process	1
1.1.3 Toluene Nitration	3
1.1.4 Reported Reaction Mechanisms	4
1.1.5 Nitrating Agents	6
1.2 GREEN AROMATIC NITRATION	7
1.2.1 Solid Acid Catalysts	7
1.2.2 Classification	8
1.2.3 Zeolites	9
1.2.4 Special Features of Zeolites	11
1.2.4.1 Acidity	11
1.2.4.2 Shape Selectivity of Zeolites	12
1.2.5 Zeolite Beta	13
1.2.6 Solid Super Acids	15
1.3 RECENT ADVANCES IN GREEN NITRATIONS	16

1.4 REACTION ENGINEERING ASPECTS	19
1.4.1 Laboratory Reactors for Kinetic Studies	19
1.5 KINETIC AND THERMAL STUDIES FOR MIXED ACID NITRATIONS	21
1.6 FOCUS AND SCOPE OF PRESENT INVESTIGATIONS	23
1.7 LIMITATIONS OF RESEARCH STUDY	24
2 THERMODYNAMIC, PHYSICAL AND TRANSPORT PARAMETERS EVALUATION	26
2.1 THERMODYNAMIC PARAMETERS	26
2.1.1 Reaction Chemistry and Product Distribution	27
2.1.2 Reported Thermodynamic Properties of Reactants and Products	27
2.1.3 Reaction Feasibility	28
2.1.4 Standard Entropy Change of the Reaction	29
2.1.5 Evaluation of Heat of Reaction from Standard Heats of Formation Data	30
2.2 ESTIMATION METHODOLOGIES OF VARIOUS PHYSICAL AND TRANSPORT PARAMETERS	30
2.2.1 Estimation of Viscosity of Immiscible Liquid Mixture	30
2.2.2 Estimation of Sauter Mean Diameter	31
2.2.3 Estimation of Phase Inversion Point	32
2.2.4 Estimation of Interfacial Area	33
2.2.5 Estimation of Diffusivity	33
3 EXPERIMENTAL FACILITIES AND PROCEDURES	35
3.1 EXPERIMENTAL	35
3.1.1 Materials and Methods	35
3.1.2 Experimental Set-Up and Procedure	35
3.2 ANALYTICAL FACILITIES AND PROCEDURES	36
3.2.1 GC Analysis	36
3.2.2 X-Ray Diffraction	37
3.2.3 Thermal Analysis	37
3.2.4 Scanning Electron Microscopy	37

3.2.5	Fourier Transform Infrared Spectroscopy	38
3.2.6	Solid State Nuclear Magnetic Resonance Spectroscopy	38
3.2.7	Temperature Programmed Desorption of Ammonia	38
3.2.8	Surface Area Measurement	39
3.2.9	Reaction Calorimetry for Thermochemical Investigations	40
4	CATALYST SELECTION AND CHARACTERIZATION	41
4.1	SELECTION OF A SOLID ACID CATALYST	41
4.1.1	Reported Studies	41
4.1.1.1	Aromatic Nitrations	41
4.1.1.2	Nitration of Toluene	42
4.1.2	Selection of Catalyst	43
4.2	CATALYST CHARACTERIZATION	45
4.2.1	X-ray Diffraction Studies (XRD)	45
4.2.2	FT-IR Studies	47
4.2.3	Scanning Electron Microscopy	49
4.2.4	Thermal Analysis	49
4.2.5	Solid State NMR Spectroscopy	51
4.2.6	Catalyst Stability and Regenerability	52
4.2.6.1	Catalyst Stability	52
4.2.6.2	Catalyst Regenerability	57
4.3	DEALUMINATION OF CATALYST	63
4.3.1	Effect of HNO ₃ Concentration	63
4.3.2	Effect of Prolonged Exposure	65
4.4	LATTICE ALUMINIUM TRANSFORMATIONS IN H-BETA CATALYST	65
5	PROCESS STUDIES	68
5.1	MATERIAL AND ENERGY BALANCES	68
5.1.1	Material Balances in a Typical Batch Nitration of Toluene	69
5.1.2	Material Balances in Semi batch Nitration of Toluene	70
5.1.3	Energy Balance for a Typical Toluene Nitration in Batch mode	71
5.1.4	Evaluation of Thermal Data through Reaction Calorimetry	73

5.2 MIXING AND DISPERSION EFFECTS	
ON TOLUENE NITRATION	74
5.2.1 Morphology of HNO ₃ -Toluene Dispersions	74
5.2.2 Delineation of Dispersion Regimes	74
5.2.3 Phase Inversion in Toluene-HNO ₃ Dispersions	75
5.2.4 Effect of Toluene-HNO ₃ Dispersion Morphology on Nitration	77
5.2.5 Agitation Effects	78
5.3 EFFECT OF CRITICAL PROCESS PARAMETERS	80
5.3.1 Effect of Toluene-Nitric Acid Molar ratio	80
5.3.2 Effect of Reaction Water Removal	80
5.3.3 Effect of Temperature	81
5.3.4 Effect of Concentration of Nitric Acid	82
5.3.5 Effect of Boil-Up Rate	82
5.4 TWO PRONGED APPROACH TO	
HEIGHTENING <i>PARA</i> -SELECTIVITY	83
5.4.1 Reported Approaches	83
5.4.2 A Two Level Standardization Process for Heightening <i>Para</i> -	
Selectivity	84
5.4.2.1 Level I Standardization	85
5.4.2.2 Level II Standardization	87
5.4.2.3 Semi Batch experimentation	88
5.4.2.4 Solid State NMR Studies	89
5.5 BEST COMBINATION OF PROCESS PARAMETERS	92
6 MASS TRANSFER AND KINETICS	93
6.1 REPORTED LITERATURE ON MULTIPHASE PROCESSES	93
6.2 SCOPE OF PRESENT WORK	95
6.3 MECHANISTIC ASPECTS OF TOLUENE NITRATION	95
6.4 MASS TRANSFER PROCESS IN AGITATED	
LIQUID-LIQUID SYSTEMS	97
6.5 MASS TRANSFER CHARACTERISTICS OF	
LIQUID-SOLID SYSTEMS	99

6.6 EVALUATION OF APPARENT REACTION KINETICS UNDER SEMI BATCH MODE OF OPERATION	101
6.7 ASSESSMENT OF RELATIVE CONTRIBUTION OF MASS TRANSFER AND KINETIC EFFECTS	103
6.8 EVALUATION OF KINETIC CONSTANTS	106
7 SUMMARY AND CONCLUSIONS	108
CONTRIBUTIONS FROM THE STUDY	111
SCOPE OF FUTURE WORK	112
REFERENCES	114
APPENDIX A: Photographs of Experimental Set-Up	126
Reaction Calorimeter	127
PUBLICATIONS FROM THE STUDY	128
BRIEF BIOGRAPHY OF THE CANDIDATE	130
BRIEF BIOGRAPHY OF THE SUPERVISOR	130

LIST OF TABLES

Table 1.1	Acid strengths of some typical acids	8
Table 1.2	Classification of solid acid catalysts	9
Table 1.3	Classification of zeolites on the basis of the effective pore diameter	10
Table 1.4	Characteristics of zeolites	10
Table 1.5	Bond distances in zeolite beta	15
Table 1.6	Physical properties of various isomers of nitrotoluene	17
Table 1.7	Dimensions of different molecules in their minimum energy configuration	17
Table 1.8	Reported kinetic parameters	22
Table 1.9	Thermokinetic and safety parameters	22
Table 2.1	Thermodynamic properties of reactants and products	28
Table 4.1	Reported comparative performance of various catalysts for toluene nitration	43
Table 4.2	Reported structural characteristics of H-Beta	45
Table 4.3	Influence of catalyst regeneration and recycle on toluene conversion and <i>para</i> -selectivity	58
Table 4.4	Dealumination of catalyst	64
Table 4.5	Effect of catalyst recycle on dealumination at lower toluene volume fraction	64
Table 4.6	Effect of exposure time on dealumination	65
Table 5.1	Semi batch nitration at an acid dosing rate of 30 ml/h	70
Table 5.2	Thermodynamic properties of reactants and products	71
Table 5.3	Estimation of thermal data	73
Table 5.4a	Sauter mean diameters and interfacial areas at	

	various volume fractions of organic phase	76
Table 5.4b	Sauter mean diameters and interfacial areas at various volume fractions of aqueous phase	76
Table 5.5	Contrasting effects of agitation speed on nitric acid-toluene dispersions	79
Table 5.6	Effect of toluene to nitric acid molar ratio on product distribution	80
Table 5.7	Temperature effect on product distribution	81
Table 5.8	Comparison of reactivities and isomer distribution using various nitrating agents and catalysts	84
Table 5.9a	Effect of acid dosing rate	85
Table 5.9b	Effect of catalyst on <i>para</i> selectivity in semi batch nitration of Toluene	86
Table 5.9c	Effect of nitric acid dosing rate-time interactions	88
Table 5.9d	Effect of time after dosing on <i>para</i> -selectivity	89
Table 6.1	Calculated mass transfer coefficients at various volume fractions of organic phase	99
Table 6.2	Computed kinetic and mass transfer contributions	104
Table 6.3	Effect of temperature on the rate constant	107

LIST OF FIGURES

Fig. 1.1	Formation of Lewis acid sites	11
Fig. 1.2	Simultaneous existence of Bronsted and Lewis sites	11
Fig. 1.3	Shape selectivity of zeolites	13
Fig. 1.4	Structure of zeolite beta (poly type A)	14
Fig. 1.5	Structure of zeolite beta (poly type B)	14
Fig. 1.6	Model structure of a super acid	15
Fig. 1.7	Laboratory reactors and their operation modes	20
Fig. 3.1	Experimental set-up for batch and semi-batch modes of toluene nitration	36
Fig. 4.1	Effect of catalyst on toluene conversion and <i>para</i> -selectivity	44
Fig. 4.2	XRD pattern of freshly prepared zeolite H-beta (S/A=22)	46
Fig. 4.3	FT-IR plot of freshly prepared H-beta (S/A = 22)	48
Fig. 4.4	DTA/TGA plot of freshly prepared H-beta (S/A = 22)	50
Fig. 4.5	^{Al} 27 MAS NMR spectrum of freshly prepared zeolite H-beta catalyst	51
Fig. 4.6	XRD patterns at various mole ratios of toluene and nitric acid-batch nitration	53
Fig. 4.7	XRD patterns of H-beta catalyst after batch nitration continued for 24 h under low (N24) and high (T24) volume fractions of toluene	54
Fig. 4.8	DTA / TGA profiles of H-beta catalyst after batch nitration of toluene continued for 24 h under low and high volume fraction of toluene	55
Fig. 4.9	FTIR plot after batch toluene nitration continued for 24 h under low and high toluene volume fraction	56
Fig. 4.10	XRD patterns of H-beta catalyst in semi batch nitration	

	with nitric acid dosing rate 30 ml/h upto 3 cycles	59
Fig. 4.11	XRD patterns of H-beta catalyst in semi batch nitration	
	with nitric acid dosing rate of 60 ml/h upto 3 cycles	60
Fig. 4.12	TGA analysis after 3 cycles of semi batch nitration at	
	acid dosing rates of 30 ml/h and 60 ml/h	61
Fig. 4.13	FTIR plot after 3 cycles of semi batch nitration with	
	nitric acid dosing rates 30 and 60 ml/h	62
Fig. 4.14	Solid state ²⁷ Al MAS-NMR spectra of zeolite	
	H-beta (a) freshly prepared zeolite (b) after semi batch	
	nitration at 30 ml/h HNO ₃ dosing rate for 3h	66
Fig. 4.15	Solid state ²⁷ Al MAS-NMR spectra of recycled zeolite	
	H-Beta catalyst in semi batch nitration at 30 ml / h	
	HNO ₃ dosing rate for 3 h; a, after 1 st recycle, b, after	
	2 nd recycle and c, after 3 rd recycle	67
Fig. 5.1	Material balance of a typical batch nitration of toluene	69
Fig. 5.2	Energy balance of a typical batch nitration of toluene	72
Fig. 5.3	Effect of Dispersion morphology on conversion	
	and selectivity	78
Fig. 5.4	Effect of boil-up rate on % toluene conversion and	
	aqueous phase removal rate	82
Fig. 5.5	Solid state ²⁷ Al MAS-NMR spectra of zeolite	
	H-beta (a) fresh zeolite (b) after semi batch nitration	
	at 30 and 60 ml/h HNO ₃ dosing rate for 3h	91
Fig. 6.1	Model representing multiphase mass transfer in	
	toluene nitration	97
Fig. 6.2	Arrhenius plot	107

LIST OF SYMBOLS

A	Heat transfer area, m^2
a	Interfacial area per unit volume, m^2/m^3
$A30$	After 1 st recycle at acid dosing rate of 30 ml/h
$AC60$	After 1 st recycle at acid dosing rate of 60 ml/h
A_m	Surface area of adsorbate molecule, m^2
a_p	Surface area of catalyst, m^2/kg
B	Percent weight of solids
$B30$	After 2 nd recycle at acid dosing rate of 30 ml/h
$BC60$	After 2 nd recycle at acid dosing rate of 60 ml/h
BEA	Beta
C	BET Constant
$C30$	After 3 rd recycle at acid dosing rate of 30 ml/h
C_A	Concentration of A at time t, mol/lit
C_{AE}	Exit concentration of A, mol/lit
C_{AO}	Initial concentration of A, mol/lit
C_{AS}	Saturated concentration of A, mol/lit
$CC60$	After 3 rd recycle at acid dosing rate of 60 ml/h
C_{HNO_3}	Concentration of nitric acid, mol/lit
C_{pr}	Specific heat of reaction mixture at constant pressure
D	Diffusivity, m^2/s
d_{32}	Sauter mean diameter, mm
D_a	Diameter of impeller, m
D_{ArH}	Diffusivity of aromatic compound, m^2/s
D_{eff}	Effective diffusivity, m^2/s
dN_A/dt	Rate of accumulation, mol/s

d_p	Particle diameter, m
E	Activation energy, kJ
F	Freshly prepared catalyst
F_A	Molar output flow rate of A, mol/h
F_{AO}	Molar input flow rate of A, mol/h
g	Acceleration due to gravity, m ² /s
H_o	Hammett acidity
k_1	Intrinsic 1 st order rate constant, s ⁻¹
k_2	Second order rate constant, lit/mol/s
k_{L2}	Liquid-liquid mass transfer coefficient, m/s
$k_{r,app}$	Apparent reaction rate constant, s ⁻¹
k_{SL}	Particle-liquid mass transfer coefficient, m/s
$L2$	Organic phase
$L-L$	Liquid-Liquid
m	<i>meta</i>
M	Molecular weight, g/mol
Mor	Mordenite
mp	Melting point, °C
m_r	mass of reaction mixture, kg
N	Avogadro number, mol ⁻¹
n	Reaction order
n_a	Impeller speed, rpm
nbp	Normal boiling point, °C
n_D	Refractive index
N_{ReI}	Impeller Reynolds number
N_s	Critical speed of impeller, s ⁻¹
o	ortho
p	<i>para</i>
P	Power dissipated by stirrer, W
P_c	Critical pressure, atm
P_o	Standard vapor pressure, atm

r_A	Rate of reaction w.r.t A
$r_{A,app}$	Apparent rate of reaction, mol/lit.s
R	Gas constant, J/mol.K
S/A	Silica / Alumina ratio
$S2-NT$	<i>ortho</i> -nitrotoluene
$S4-NT$	<i>para</i> -nitrotoluene
S_{BET}	BET Surface area, m ²
Sc	Schmidt number
S^o	Standard entropy, J/mol.K
T	Absolute temperature, K
T	Ratio between collision and coalescence frequencies
t_b	Temperature of oil bath, °C
t_r	Temperature of reaction mixture, °C
U	Overall heat transfer coefficient, W/m ² K
u	slip velocity, m/s
V_A	Volume fraction of aqueous phase
V_{ads}	Volume of gas adsorbed at pressure P, m ³
V_b	Molar volume, lit/mol
V_c	Critical volume, lit
V_d	Volume of dispersed phase, m ³
$V-L-L-S$	Vapor-Liquid-Liquid-Solid
$V-L-S$	Vapor-Liquid-Solid
V_m	Volume of gas adsorbed for monolayer coverage, m ³
V_o	Initial volume of reaction mixture, lit
v_o	volumetric flow rate, lit/h
V_T	Volume fraction of toluene
We	Weber number
We_I	Impeller Weber number
x	mole fraction
X_i	Percent conversion w.r.t i
X_m	moles of N ₂ adsorbed

ΔG_f°	Standard Gibbs free energy of formation, kJ/mol
$\Delta G^\circ_{reaction}$	Standard Gibbs free energy change of reaction, kJ/mol
ΔH_c	Heat of condensation, kJ/mol
ΔH_f°	Standard heat of formation, kJ/mol
ΔH_{rxn}°	Standard heat of reaction, kJ/mol
ΔS°_{rxn}	Standard entropy change of reaction, J/mol.K
ΔT_{ad}	Adiabatic temperature rise, °C
$\Delta \rho$	Density difference between particle and liquid, kg/m ³
ε_d	Volume fraction of dispersed phase
η	Effectiveness factor
μ	Viscosity, kg/m.s
μ_c	Viscosity of continuous phase, kg/m.s
μ_i	Viscosity of component i, kg/m.s
μ_m	Viscosity of mixture, kg/m.s
ρ	Density, kg/m ³
ρ_c	Density of continuous phase, kg/m ³
ρ_p	Particle density, kg/m ³
σ	Interfacial tension, N/m
τ	space time, s
ν	Kinematic viscosity, m ² /s

ABBREVIATIONS / ACRONYMS

BR	Boil-up rate, °C
DNT	Dinitrotoluene
DTA	Differential Thermal Analysis
EDX	Energy Dispersive X-Ray Analysis
fp	Flash Point, °C
FTIR	Fourier Transform Infrared Spectroscopy
GC	Gas Chromatography
MAS	Magic Angle Spinning
MNT	<i>meta</i> -nitrotoluene
MTSR	Maximum Temperature of Synthetic Reaction, °C
NMR	Nuclear Magnetic Resonance
ONT	<i>ortho</i> -nitrotoluene
PNT	<i>para</i> -nitrotoluene
RC	Reaction Calorimeter
rpm	revolutions per minute
SEM	Scanning Electron Microscopy
STR	Stirred Tank Reactor
TGA	Thermogravimetric Analysis
TMR _{ad}	Time to Maximum Rate under adiabatic conditions, s
TPD	Temperature Programmed Desorption
XRD	X-ray Diffraction
vd	Vapor Density

CHAPTER 1

INTRODUCTION

1.1 AROMATIC NITRATIONS

1.1.1 Historical

Aromatic nitro compounds and their derivatives are used as solvents, analytical reagents and are important intermediates in organic synthesis of perfumes, drugs, pesticides and explosives [1]. They can be reduced to primary amines, which are valuable intermediates in the synthesis of dyes, pharmaceuticals, photographic developers and antioxidants [2].

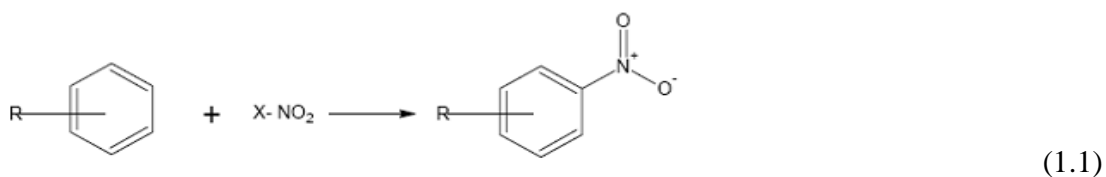
Nitration of organic compounds has attracted substantial research interest as evidenced by the large body of published literature. The earliest report on nitration was from Mitscherlich in 1834 [2]. He treated hydrocarbons derived from coal tar with fuming nitric acid to obtain nitrated products. In 1835 Laurent worked on the nitration of naphthalene, the most readily available pure aromatic hydrocarbon in pure form at that time [2]. It was in only in 1845 that Hofmann and Muspratt reported on the nitration of benzene to mono- and dinitrobenzenes by using a mixture of nitric and sulfuric acids [2]. Bechamp's iron production process, which made aniline more readily available, was published in 1854, and the discovery of aniline mauve by Perkin in 1856 revolutionised the european aniline dye industry. Process development and scale up of the nitration and reduction processes, initiated by Perkin and continued by many others, resulted in the trade price of a kg of aniline dropping from 50 Fr in 1858 to 10 Fr in 1863 and a significant increase in its production to 5,00,000 TPA level by 1985 [3].

1.1.2. The Nitration Process

The number of naturally occurring nitroaromatic compounds is small; the first to be recognized was chloramphenicol, an important compound extracted from soil mold *streptomyces venezuelae* and whose structure was identified in 1949. This and the earlier

discovery of the antibacterial activity of nitrofurans stimulated investigations on the role of nitro group in achieving pharmacological activity.

The process of nitration can be defined as an irreversible introduction of one or more nitro (NO₂) groups into an aromatic nucleus by replacement of a hydrogen atom. It can be represented as an electrophilic substitution reaction:



Introduction of the nitro group inhibits further electrophilic substitution and accordingly dinitration rarely occurs under the conditions used for mononitration. The more vigorous conditions required for dinitration are excess stronger acid and higher temperatures.

The nitration reaction is strongly exothermic, as exemplified by mononitration of benzene ($H = -117$ kJ/mol) and naphthalene ($H = -209$ kJ/mol) and is probably one of the most hazardous industrially operated unit processes. The exothermic heat can enhance the ability of nitric acid to degrade the organic materials exothermally to gaseous products with explosive violence [4].

Though nitration is the dominant method for introducing the nitro group into aromatic systems, indirect methods like oxidation of nitroso or amino compounds, replacement of diazonium groups, rearrangement of nitramines and nucleophilic displacement reactions have also been reported in the literature. They have lesser industrial significance. Conventionally aromatic nitro compounds are produced by liquid phase nitration reactions employing mixed acids viz., sulfuric acid and nitric acid mixture [5-6]. Many important nitro compounds are produced by sulfonating, halogenating, or aminating the primary starting materials and subjecting them to nitration as a subsequent operation.

The nitration can be carried out on both batch and continuous modes. Lower tonnage requirements upto 6000 litres are usually met by batch process in stirred reactors designed to accommodate a variety of products. The exothermic process requires efficient cooling of the reactor contents by jacket as well as internal cooling or both. Continuous processes employ a single or a cascade of agitated reactors for large tonnage products. They are attractive from safety, economy and temperature control considerations. However they require closely defined operating parameters and effective control management.

Nitrations of aromatic compounds are high yield processes, with more than 80% of the production cost accounted by the raw materials. Two major areas that have received attention are the sulfuric acid recycle as an integral part of nitration process and isomer control and separation.

1.1.3 Toluene Nitration

Mononitration of toluene can be executed in batch or continuous mode. In a typical batch process, the toluene is fed into the nitrator and cooled to about 25°C. The nitrating acid (52-56 wt% H₂SO₄, 28-32 wt% HNO₃ and 12-20 wt% H₂O) is added slowly below the surface of the toluene and the temperature of the reaction mixture is maintained at 25°C by adjusting the feed rate of the nitrating acid and the amount of cooling. After full addition of acid, the reactor temperature is raised slowly to 35-40°C. On completion, the reaction mixture is transferred to a separator where the spent acid is withdrawn from the bottom and is reconcentrated. The crude product is several times washed with dilute caustic followed by water. The product is steam distilled to remove excess toluene and then dried by distilling the remaining traces of water. The resulting product contains 55-60 wt% *o*-nitrotoluene, 3-4 wt% *m*-nitrotoluene and 35-40 wt% *p*-nitrotoluene. The yield of mononitrotoluenes is 96%. The separation of isomers is carried out by a combination of fractional distillation and crystallization. The distillate as obtained from the former at a head temperature of 96-97°C at 1.6 kPa (12mm Hg) is fairly pure *o*-nitrotoluene and can be purified further by crystallization. Similar strategy is employed for separation of *meta* isomer from a mixture of *m*- and *p*- nitrotoluenes.

1.1.4 Reported Reaction Mechanisms

Isomer Distribution in Toluene Nitration

Electrophilic aromatic substitution through nitration enables the replacement of hydrogen atom by an electrophile viz., nitronium ion from nitric acid. Performing the electrophilic substitution on an already substituted toluene raises the problem of regioselectivity. Functional groups like amino donate their unshared electrons to the pi system of the aromatic compound giving rise to four resonance structures. In case of toluene nitration, the nitrogen atom is not capable to donate electron density to the pi system thereby providing three resonance contributors. For this reason *metanitrotoluene* is produced in much smaller proportion to the *ortho* and *para* counter parts. *Ortho* and *para* attacks are preferred here because their resonance structures include one tertiary carbocation while all the resonance structures for the meta attack have secondary carbocations only. In conventional mixed acid based nitration proceeds with predominant formation of o-isomer (58.4%) followed by p-isomer (37.25) and m-isomer. Nelson and Brown [7] reported that the *o*, *p*, and *m* isomer distribution in toluene nitration does not appear to be altered significantly by changes in concentration of nitrating agent(s). Berliner [8] reported that variation in reaction conditions including nitrating agents can have a marked effect on isomer distribution. Hammond [9] postulated that the regioselectivity of final product distribution reflects the relative stabilities of the corresponding arenium ions.

Electrophilic Substitutions Regulations

The mechanism of electrophilic substitutions in aromatic nitrations has been studied over the last 50 years. Ingold -Hughes proposed the nitronium ion as the active species in aromatic nitrations [10]. The mechanism of nitration depends on the nitrating species and operating conditions [11]. Though NO_2^+ was suggested to be the nitrating species as early as in 1903, its presence was substantiated only in 1946. In 1950, employing Raman spectra. Ingold - Hughes confirmed its presence in the solid phase. The overall mechanism that can accommodate all the events associated with toluene nitration can be described by:



The reaction (3) is reported to be rate determining for toluene nitration. The presence of NO_2^+ was detected spectroscopically in very strong acid media [12]. Kenner [13] proposed that electron charge transfer may play an important role in the mechanism of nitronium ion formation. This was substantiated by Nagakura and Tanaka [14] using molecular orbital theory. In mid 1950, stable σ complexes were isolated. These complexes originated from the molecules with several substituents. The arenonium nature of these species was established by NMR and a suitable reaction mechanism was proposed [15-16]. In 1986, Feng et al. [17] suggested that the radical pair recombination mechanism will be favored for nitration whenever the ionization potential of the aromatic hydrocarbons is much less than that of NO_2 . Substituents or reaction conditions that raise the ionization potential of the aromatic compound to a value higher than that of NO_2 is to prevent radical pair formation by electron transfer. Two schemes have been proposed to establish this mechanism.

The nitration with nitric acid in organic solvents is found to be of zero-order with respect to substrates when 10-fold excess of nitric acid is employed. The rate determining step is the formation of NO_2^+ and the nitration is zero order with respect to the aromatic compound [6]. Nitric acid heterolysis is reported to accelerate with an increase of polarity of the medium. Schofield [18] proposed the formation of the first intermediate through an encounter pair between NO_2^+ ion and an aromatic molecule held in a solvent shell very closely. The two species do not interact with each other [15a] and require a lifetime to produce a σ complex. This could explain the low substrate selectivity. The kinetic role of π -complexes of aromatic hydrocarbons in nitration has not been elucidated yet. Olah et al. pointed out that the Wheeland structure is not a transition state but a stable intermediate [15b]. In 1994 Ebersson et al. [19] proposed that electrophilic aromatic nitration by NO_2^+

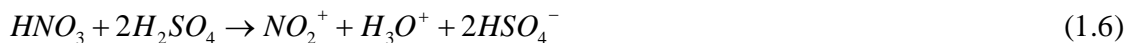
ion takes place via an initial electron transfer, followed by recombination of an intermediate radical pair. They experimentally proved the photoexcitation of ArH-tetramethane employing tetranitromethane.

1.1.5. Nitrating Agents

Liquid Acids and Others

For reasons of practicability and economic viability, industrial scale nitration is usually carried out with a mixture of nitric and sulfuric acids (mixed acid), and occasionally with aqueous nitric acid in combination with acetic acid or acetic anhydride or nitrogen oxides. The strength of the nitrating agent (X-NO₂) decreases with decreasing electronegativity of X [20]: nitronium (e.g., BF₄-NO₂⁺) > nitracidium (OH₂⁺-NO₂) > nitronium chloride (Cl-NO₂) > acetyl nitrate (AcO-NO₂) > nitric acid (HO-NO₂) > ethyl nitrate (C₂H₅O-NO₂).

As stated earlier, the nitronium ion is the active species in case of mixed acids, it is formed by :



A typical mixed nitrating agent for large scale aromatic mononitration consists of 20% nitric acid, 60% sulfuric acid and 20% water; this is referred to as 20/60/20 acid mixture. In this case, nitration mass exists in two phases viz., the organic phase consisting of precursor and nitrated product and the aqueous phase comprising of mixed acid. Efficient agitation is required to maximize the contact between the phases and to minimize the resistance to mass transfer. Stronger nitric acid leads to oxidative side reactions whereas higher temperature leads to decreased nitronium ion concentration.

Amongst the powerful nitrating agents, nitrogen dioxide - ozone mixture [21] provides an interesting case study. Selective production of mononitrated products is difficult in this case because of powerful nature of nitrating agent. Other option is to promote *in situ* generation of nitric acid using metal nitrates and organic acid which requires tedious work up procedures. On the basis of the above reports, it is clear that there is a need for

more regioselective control of nitration using nitric acid as a nitrating agent to obtain higher conversion and selectivity.

1.2. GREEN AROMATIC NITRATIONS

1.2.1. Solid Acid Catalysts

Solid acid catalysis has attracted worldwide attention in view of its potential advantages over many homogeneously catalyzed nitrations. The solid acid catalysts can be designed to give higher activity, selectivity, regenerability and longer life. Substantial progress has been made in this direction during the last two decades. Acid strengths in terms of Hammett acidity scale of some typical acids [22] are compared in Table 1.1. It shows the ability of solid acids to generate as much acidity levels of liquid acids like H₂SO₄. Their economical attractiveness is yet to be fully established. Accumulation or elimination of water produced in the reaction greatly influences the solid acid catalyst – HNO₃ system behavior. If water is allowed to accumulate, nitric acid becomes a selective oxidative coupling agent, whereas when it is eliminated efficiently, it behaves as a strong nitrating agent with ability to increase para selectivity as compared to the sulfo-nitric system [23]. The use of solid acid catalysts is potentially attractive because of ease of their separation, simple recycling and the possibility of tailoring their pore size to achieve improved para selectivity. In addition, the solid acids can be easily regenerated by simple thermal treatment [24].

The use of a variety of solid acids and zeolitic materials in the production of aromatics and petrochemicals such as xylene, ethyl benzene, cumene and their alkylbenzenes has been well reported [25]. There are bright prospects for their application in fine chemical and pharmaceutical intermediate synthesis. Super acid catalysts have also been reported by Olah et al. [26].

Table 1.1 Acid strengths of some typical acids

Acid	Hammett acidity (H_o)
Sulfuric acid (100%)	-12
Hydrogen fluoride (anhydrous)	-10
Zeolites, RE-Y/H-ZSM-5/Beta	-12 to -14
Kaolinite clay	+1.2 to -2
Acid washed montmorillonite clay	-5 to -8
Amberlyst-15 resin	-12
Sulfated zirconia	-10 to -14

The solid acid catalysts have been reported to exhibit following unique features:

- a) Ability to be function as Bronsted as well as lewis acids either by donating a proton or accepting an electron pair.
- b) Their acid strength and distribution depends on the method of preparation.
- c) They exhibit higher catalytic activity at high temperatures if they are made resistant to water and alcohols.
- d) Ability to Exhibit shape selectivity.

1.2.2 Classification

Solid acid catalysts can be classified as zeolites, clays and mixed oxides including superacids and also based on their effective pore diameter. Details are given in Tables 1.2 and 1.3.

Table 1.2 Classification of solid acid catalysts

S.No	Solid acid catalyst
1	Natural clay minerals: Kaolinite, bentonite, montmorillonite, zeolites (X, Y, A, H-ZSM-, H-Beta etc)
2	Mounted acids: H ₂ SO ₄ , H ₃ PO ₄ , CH ₂ (COOH) ₂ mounted on silica, quartz sand, alumina or diatomaceous earth
3	Cation exchange resins: Amberlite
4	Metal oxides and sulphides: ZnO, CdO, Al ₂ O ₃ , CeO ₂ , ThO ₂ , TiO ₂ , ZrO ₂ , SnO ₂ , PbO, As ₂ O ₃ , Bi ₂ O ₃ , Sb ₂ O ₅ , V ₂ O ₅ , Cr ₂ O ₃ , MoO ₃ , WO ₃ , CdS, ZnS
5	Metal salts: MgSO ₄ , CaSO ₄ , SrSO ₄ , BaSO ₄ , CuSO ₄ , ZnSO ₄ , CdSO ₄ , Al ₂ (SO ₄) ₃ , FeSO ₄ , Fe ₂ (SO ₄) ₃ , CoSO ₄ , Cr ₂ SO ₄ , KHSO ₄ , K ₂ SO ₄ , (NH ₄) ₂ SO ₄ , AgCl, CuCl ₂ , AlCl ₃ , CaF ₂ , BaF ₂ , Zr ₃ (PO ₄) ₄ , Fe(NO ₃) ₃ , AlPO ₄
6	Mixed oxides: SiO ₂ -Al ₂ O ₃ , SiO ₂ -TiO ₂ , SiO ₂ -SnO ₂ , SiO ₂ -ZrO ₂ , SiO ₂ -Y ₂ O ₃ , SiO ₂ -La ₂ O ₃ , Al ₂ O ₃ -B ₂ O ₃ , Al ₂ O ₃ -ZrO ₂ , Al ₂ O ₃ -V ₂ O ₅ , Al ₂ O ₃ -WO ₃ , TiO ₂ -V ₂ O ₅ , TiO ₂ -MoO ₃ , TiO ₂ -WO ₃ , MoO ₃ -NiO-Al ₂ O ₃ -MgO & heteropolyacids

1.2.3 Zeolites

Zeolites are crystalline hydrated alumino-silicates, possessing a rigid framework based on an infinitely extending three dimensional network of SiO₄⁻⁴ and AlO₄⁻⁵ tetrahedra, linked through oxygen atoms. Within this framework are present well defined channels and cavities of specific dimensions rendering them microporous. The excess negative charge on the AlO₄ tetrahedron is compensated by cations, resulting in an electrically neutral framework. The crystallographic unit cell of a zeolite may be represented as **M_{2/n}.Al₂O₃.XSiO₂.YH₂O**, Where **M** represents the exchangeable cations of variety of valency **n** and is used to balance the framework charge, **X** can assume a value equal or greater than 2 as no two Al³⁺ can occupy the adjacent tetrahedral position as per Lowenstien's rule [27] and **Y** is the number of H₂O molecules present in the channel or cavities of the three dimensional network. They are classified as per their morphological

characteristics [28-30], crystal structure [28-29], effective pore diameter (Table 1.3), chemical composition [31] and natural occurrence.

Table 1.3 Classification of Zeolites on the basis of the effective pore diameter [32]

Small Pore (8 Membered ring)	Medium Pore (10 Membered ring)	Large Pore (12 Membered ring)
Li-A	Dachiardite	Linde X, Y, L
MTN	Epstilbite	Gmelinite
NU-1	Ferrierite (FER)	Mazzite
Bikitaite	Heulandite	Offretite
Chabazite	ZSM-5 (MFI)	ZSM-12 (MTW)
Edingtonite	ZSM-11(MEL)	Omega
Erionite	EU-1 (ZSM-50)	Beta (BEA)
Gismondine	ZSM-23	
ZK-5	Theta-1(ZSM-22)	
Levynite	ZSM-48 (EU-2)	
Linde A		
Merilonite		

Table 1.4 Characteristics of the zeolites [33]

Zeolite	Si/Al	BET surface area (m ² /g)	External surface area (m ² /g)	Pore volume (cm ³ /g)	Average mesopore diameter (Å)	Micropore volume (cm ³ /g)
H-beta	11.5	690	199	0.90	102	0.21
H-ZSM-5	16.9	433	64	0.51	98	0.16
H-ZSM-12	47	355	20	0.20	38	0.15
H-mor (4.6)	4.6	544	6	0.27	64	0.22
H-mor (74)	74	512	38	0.31	57	0.20

1.2.4 Special Features of Zeolites

1.2.4.1 Acidity

When the cationic form of any zeolite is converted into its H or proton form, its acidity increases, the extent of which depends on the number of Al^{3+} present in the framework. In other words, zeolites with low silica to alumina ratios are highly acidic and their acidity decreases with increase in their silica to alumina ratios. When the proton (hydrogen) of the zeolite framework exhibits the proton donor property, it is referred to as Bronsted acid [34]. When it is heated to 823K, Si-O-Al bond breaks giving rise to Lewis acid sites and water.

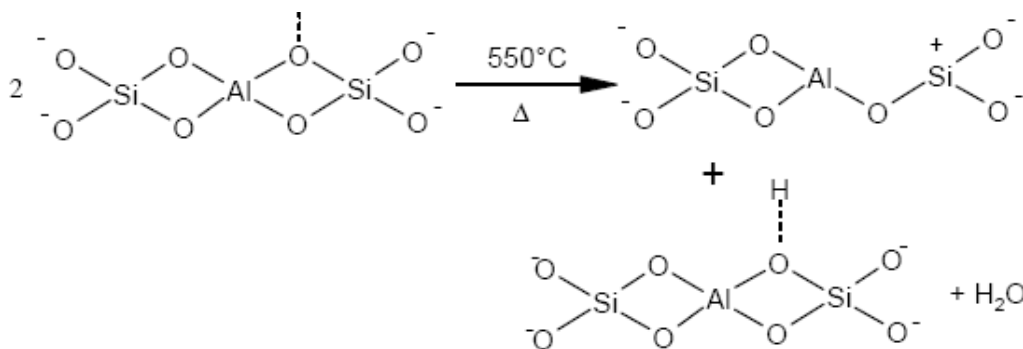


Fig 1.1 Formation of Lewis sites

Generally, in zeolites both Bronsted and Lewis sites exist simultaneously

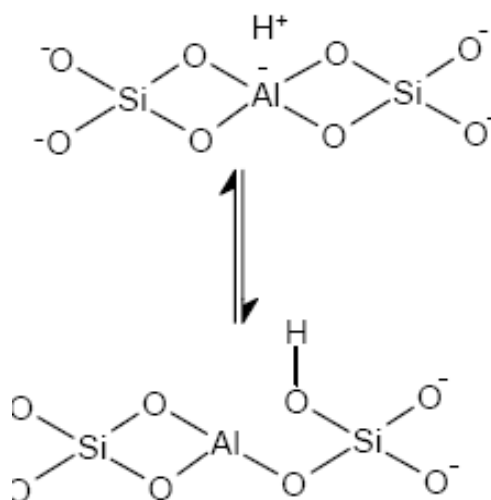


Fig 1.2 Simultaneous existence of Bronsted and Lewis sites

1.2.4.2 Shape selectivity of zeolites

Weisz and Frilette [35] were the first to describe the shape selectivity. The pore size and shape may influence the selectivity of a reaction in three ways viz., reactant, product and transition states. For achieving desired shape selectivity in chemical reactions, the zeolite pore size has to be carefully selected.

Reactant shape selectivity:

Reactant shape selectivity results from limited diffusivity of some of the reactants, which cannot effectively enter and diffuse inside the crystalline structure. The zeolite pore is such that it admits only certain smaller molecules from the reactants and excludes larger molecules and hence in the reaction mixture only the smaller molecules react effectively [Fig. 1.2]

Product shape selectivity:

The product shape selectivity can be achieved by holding certain bulkier compounds produced within the zeolite pores during a reaction and ensure that they cannot diffuse out due to their larger size. These will either be converted to smaller sized products to diffuse out or they may be retained within the catalyst pores which may result in the deactivation of the catalyst. For example in toluene methylation, p-xylene is the major product when modified zeolites are employed as compared to bulky o- and m- isomers due to pore diameter restrictions [Fig. 1.3].

Restricted transition state shape selectivity:

Restricted transition state shape selectivity is observed when certain reactions are prevented because of restrictions in the inner pore space for the corresponding transition state. Diffusion of reactants and products in this situation is neither hindered nor the reactions involving smaller transition state are hindered [Fig. 1.3].

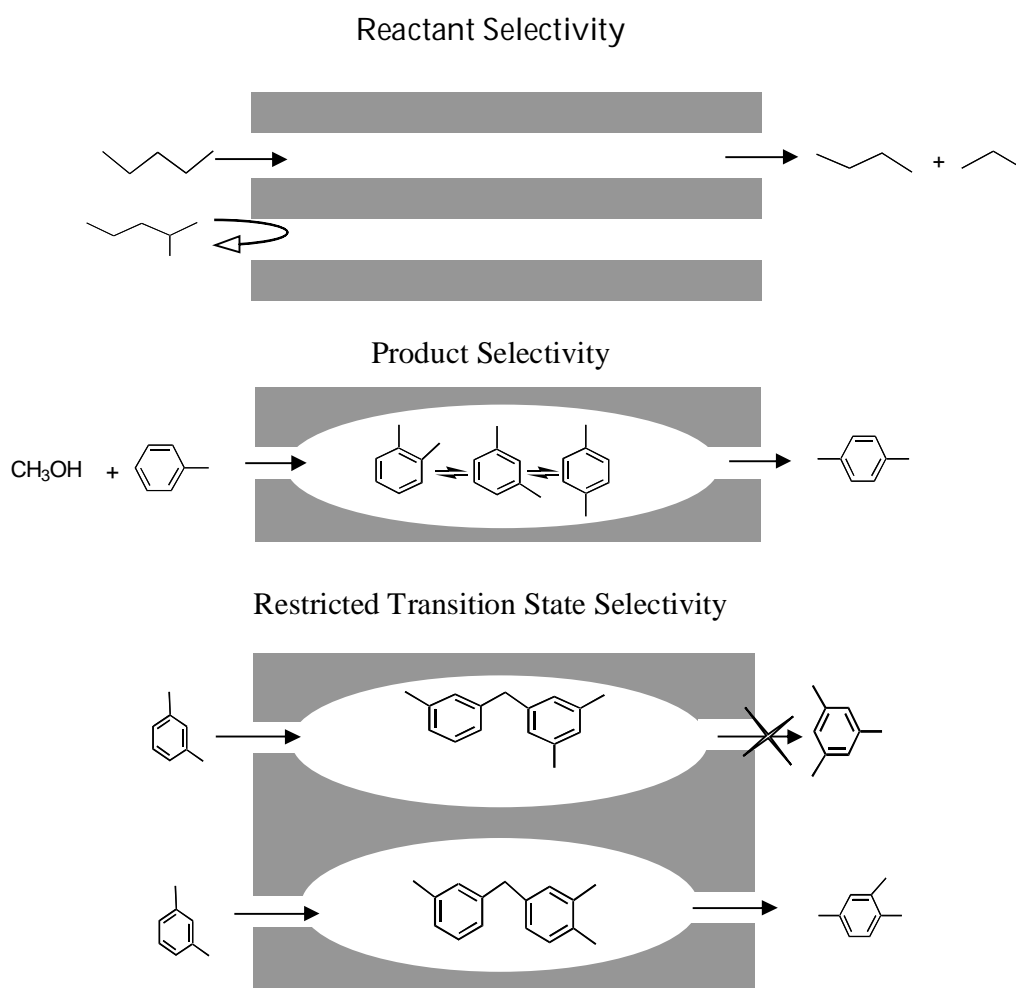


Fig.1.3 Shape selectivity of zeolites

1.2.5 Zeolite Beta

Zeolite beta was synthesized in 1967, by Wadlinger et al. [36]. Its crystal structure was resolved recently [37-38]. Zeolite beta consists of an intergrowth of two distinct structures termed Polymorphs A and B. The polymorphs grow as two-dimensional sheets and the sheets randomly alternate between the two. Both polymorphs have a three dimensional network of 12-ring pores. The intergrowth of the polymorphs does not significantly affect the pores in two of the dimensions, but in the direction of the faulting, the pore becomes tortuous, but not blocked. The two hypothetical polymorphs are depicted in Figs. 1.4 & 1.5 and bond distances in zeolite beta are shown in Table 1.5.

Zeolite beta has several unique and interesting features. It is the only high silica zeolite to have fully three dimensional 12-membered ring pores with two different types of channel systems. It is the only large pore zeolite to possess chiral pore intersections. On account of its rigid three dimensional network of large pores with high framework $\text{SiO}_2/\text{Al}_2\text{O}_3$ ratio, it is a potential catalyst in many hydrocarbon processes of industrial importance [39-44] viz., selectoforming [45], olefin oligomerizations [46], dewaxing [47] and MTG (methane to gasoline) [48]; alkylation and fine chemical synthesis.

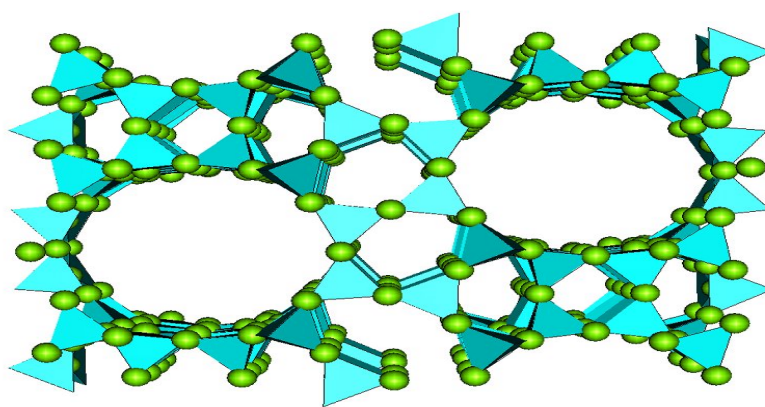


Fig. 1.4 Structure of zeolite beta (poly type A)

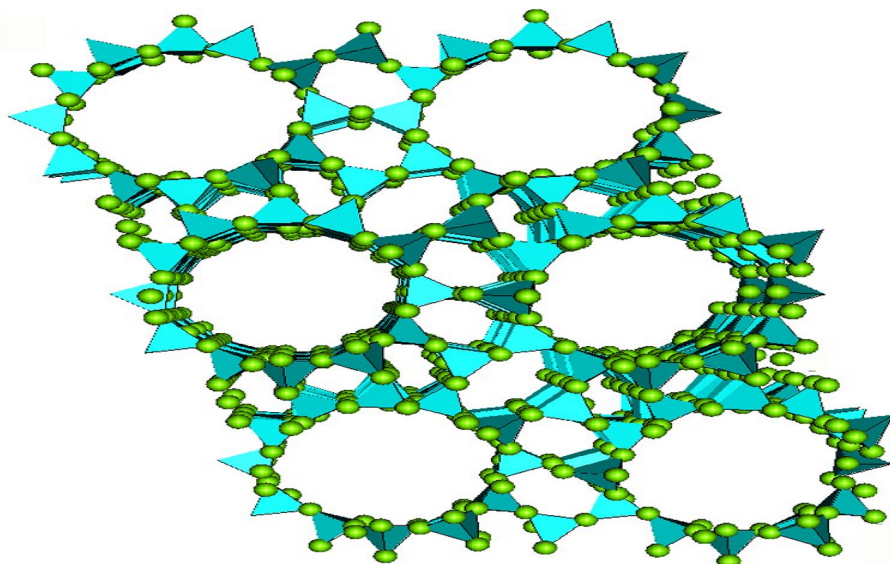


Fig.1.5 Structure of zeolite beta (poly type B)

Table 1.5 Bond distances in zeolite beta

Type	Si – O (Å)	O – Si – O (Å)
Poly type A	1.616	109.47
Poly type B	1.616	109.47

1.2.6. Solid Super Acids

They exhibit an acid strength ($H_0 = -11.9$) exceeding that of 100% sulfuric acid. They have opened new avenues for carrying out chemical reactions needing very strong acid sites under mild process conditions [26]. Recently, four types of solid superacids have been reported viz., (a) metal oxides and mixed oxides containing a small amount of sulfate ion, and those modified with platinum, (b) metal oxides, mixed oxides, metal salts etc treated with antimony fluoride or aluminium chloride, (c) perfluorinated sulphonic acid (Nafion-H) and (d) H-ZSM-5 and heteropolyacids. Superacidity can be measured by the temperature programmed desorption (TPD) method employing ammonia or pyridine, provided that the relative value in TPD is related to the absolute value (H_0) and the interaction of ammonia or pyridine with basic sites on solid surfaces is confirmed to be negligible.

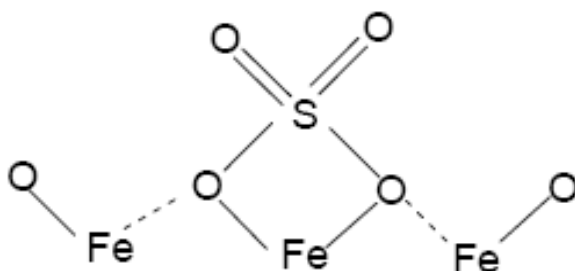


Fig. 1.6 Model structure of a super acid

1.3. RECENT ADVANCES IN GREEN NITRATIONS [49]

Nitrations typically require the use of potent mixtures of concentrated nitric acid and sulfuric acids leading to excessive acid waste and added treatment costs. To avoid this, nitric acid can be used in conjunction with strong Lewis acids such as boron trifluoride at or above the stoichiometric quantity. They have to be destroyed in the aqueous quench liberating large amounts of strongly acidic by-products. The scientists are under increasing pressure to develop processes with high atom economy with minimal or no environmentally hazardous by-products. Development of novel solid catalyst systems that facilitate aromatic nitrations has thus attained highest importance from process greening angle. Recently nitration of aromatic compounds has been successfully carried out by Kun Qiao et al. [50] under solvent free conditions in a biphasic mode in the presence of the Bronsted acidic ionic liquids; the only by-product is water. Ionic liquids are capable of being reused without any separation.

Lanthanides have found increasing use as mild and selective reagents in organic synthesis. In particular, lanthanide(III) triflates have been used to good effect as Lewis acids in Diels-Alder, Friedel-Crafts, Mukaiyama aldol and other reactions. The catalyst can be easily recycled with simple aqueous work up procedure with little detriment to rate or yield. Ytterbium (III) triflate has been reported as a recyclable catalyst for the nitration of arenes where the only side product is water. It represents an efficient and environmentally friendly process. Structural analysis has demonstrated that triflates with charge to size ratios greater than '3' (i.e greater than that of smallest lanthanide: lutetium) are more effective nitration catalysts. Similarly, Hafnium(IV) and Zirconium(IV) triflates in their hydrated forms are found to be more effective in nitrating orthonitrotoluene to dinitrotoluenes than Ytterbium(III) triflates which are required in large quantities. Yamamoto et al. [51] have demonstrated the use of scandium triflamide, $\text{Sc}(\text{NTf}_2)_3$, for acetylation, nitration and acetalisation reactions at an activity level higher than scandium triflate. It was also observed that catalytic quantities of $\text{Yb}(\text{NTf}_2)_3$ and $\text{Sc}(\text{NTf}_2)_3$ are 2-3 times more effective than $\text{Yb}(\text{OTf}_2)_3$ and $\text{Sc}(\text{OTf}_2)_3$. Triflides ($\text{Tf}_3\text{C}-$) were found to be even more stronger and effective nitration catalysts than triflates and triflamide salts [49]. Min Shi et al. [52] have successfully explored the use of a novel

mixed catalyst LiClO_4 (15 % w/w), $\text{Yb}(\text{OPf})_3$ (15%w/w, Pf= perfluorooctanesulfonyl), MoO_3 (15 % w/w) on silica gel for electrophilic aromatic nitration reaction under solvent free conditions. Moreover this mixed catalyst can be easily recovered from the aqueous layer by heating in an oven.

Table 1.6 Physical Properties of various isomers of nitrotoluene [53]

Property	o-nitrotoluene	m-nitrotoluene	p-nitrotoluene
mp ($^{\circ}\text{C}$)	-9.55	16.1	53.5
nbp ($^{\circ}\text{C}$)	221.7	231.9	238.5
ρ , g/ml at 20°C	1.1622	1.1581	1.286
n_D^{20}	1.5474	1.5470	1.5346
σ , (20°C), dyn/cm	44.1	43.5	42.3
μ , (20°C), cP	2.37	2.33	1.2
ΔH_c , MJ/mol	3.75	3.732	3.718
vd	4.72	4.72	4.72
fp, $^{\circ}\text{C}$	106	106	106

Table 1.7 Dimensions of different molecules in their minimum energy configuration [54]

Molecule	Dimensions (A°)		
	<i>a</i>	<i>b</i>	<i>c</i>
Nitronium ion	4.6	3.0	2.7
Toluene	6.9	5.3	2.8
ONT	8.0	6.9	2.9
MNT	8.3	7.0	2.9
PNT	8.8	5.3	2.8
DNT	9.9	7.1	3.0

A variety of solid acids and nitrating agents has been reported for nitration of benzene and toluene. They include zeolites [24, 55-56], partially dealuminated [57] or cationic-exchanged zeolites [58], tributylamine modified zeolites [59] and some Fe, B, and Ti-substituted forms [60] have been investigated. Besides zeolites, other catalysts such as

sulfonated ion-exchange resins (polystyrenesulfonic acid [61], perfluorinated resin sulfonic acid [62]), clay supported metal nitrates [63-64], Fe³⁺ on K10 montmorillonite [65]), modified silica [58] and silica-alumina and supported acids [66-69] have been used. Various liquid nitrating agents such as nitric acid, nitric acid-acetic anhydride, mixed acid, nitrogen dioxide (dinitrogen tetroxide) [70], acyl nitrates (benzoyl nitrate, acetyl nitrate) and alkyl nitrates were tested [6].

Among acidic zeolite catalysts such as H-mordenite, H-beta, H-ZSM-5, H-Y zeolite, H-beta has shown higher conversion and remarkable selectivity for *para* isomer in vapor phase nitration of toluene [55]. Choudary et al. [71] carried out the nitration of toluene in liquid phase employing nitric acid of 60-90% concentration over solid acid catalyst with *in situ* removal of water. Beta zeolite proved to be the best catalyst among the zeolites, in terms of space time yields (STY), *para* selectivity and consistent activity and selectivity even after five cycles without dealumination of the catalyst. Vassena and co-workers [72] investigated the nitration of toluene in the gas phase at 158°C with 65% nitric acid over zeolite catalyst; among the catalysts studied, zeolite H-beta showed promising results. The activity and selectivity decreased over a period of 5 h on stream, due to pore filling/blockage by strongly adsorbed products / byproducts. Nitration of toluene using zeolite H-beta zeolite catalyst to replace sulfuric acid in the conventional process could not be commercialized due to deactivation of catalyst, leading to low space time yields.

Continuous removal of water formed during the nitration from the acidic sites of the catalyst has been a challenge for sulfuric acid free nitration processes. The literature reports four alternatives for water removal viz., (a) vapor phase processing [54, 72], (b) chemical trapping, (c) inert gas passage and (d) azeotropic distillation [62]. The first three options have, so far, not found commercial viability whereas the azeotropic distillation has better chances of succeeding.

1.4 REACTION ENGINEERING ASPECTS

1.4.1 Laboratory reactors for kinetic studies

Stirred, fixed bed and spinning basket reactors with and without reflux and oil-water separation facilities are normally required for laboratory studies of aromatic nitrations. They are operated in batch, semi-batch and continuous modes of operations. Good contact between liquid as well as between liquid and solid phases and the need to remove *insitu* water formed during nitration are important factors for laboratory reactor design. While mixed acid nitration provides challenges of mass transfer in aqueous–aromatic two phase system, the solid catalyzed aromatic nitrations provide much more challenges in view of the complexities of mass transfer in liquid-liquid-solid system.

Liquid-liquid systems

Perego and Peratello [73] presented laboratory catalytic reactors for kinetic investigations. They have classified them based on hydrodynamic behaviour and operational features. For multi-phase reactions, stirred tank, spinning or stationary basket and fixed bed reactors have been recommended. Fixed-bed reactors operate in continuous mode whereas stirred tank reactors are employed for batch, semi-batch and continuous modes of operation. For kinetic studies on hydrotreating reactions, the most used reactors are cocurrent upflow or downflow packed-bed reactors for formed catalyst particles and stirred tank reactors for powdered catalyst [74-76]. The latter are often preferred for their ease of use and low cost. Trickle bed reactors are employed for gas-liquid-solid reactions. Caraviehes et al. [77] demonstrated the use of a centrifugal partition chromatograph (CPC) as a liquid-liquid plug flow catalytic reactor. Compared to STRs, it has definite advantages in its application under non ideal conditions; bifunctionality in terms of reactions and separations and for the determination of liquid-liquid partition isotherms. It suffers drawbacks in terms of complicated construction and good knowledge of liquid/liquid partition parameters. Chamayou et al. [78] employed a continuous loop reactor packed with static mixers to study the kinetics of a liquid-liquid-solid reaction systems for synthesis of Amiodarone. It promotes excellent mixing of the three phases to achieve high heat transfer rates. It behaves as a perfect stirred tank reactor at high recycle

rates. Zaldivar et al. [79-80] studied aromatic nitrations by mixed acid as a heterogeneous liquid-liquid reaction using adiabatic and heat flow calorimetry.

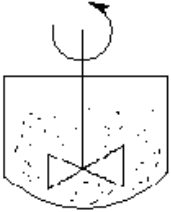
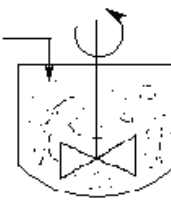
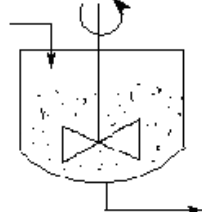
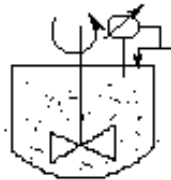
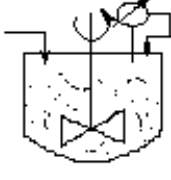
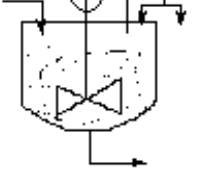
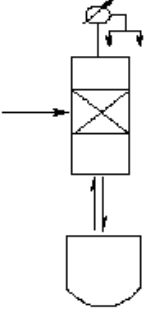
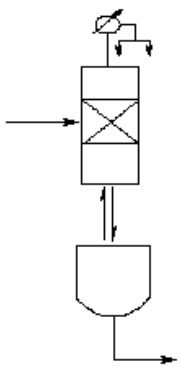
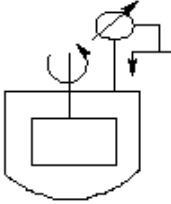
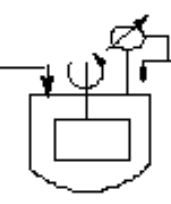
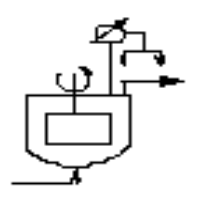
	Batch	Semi-Batch	Continuous	Phases
STR's				<i>L-L</i>
STR's with reflux				<i>V-L-L-S</i>
Fixed bed reactive distillation				<i>V-L-S</i>
Spinning basket				<i>V-L-L-S</i>

Fig. 1.7 Laboratory reactors for aromatic nitrations (L: liquid, V: vapor, S: solid)

Solid-liquid-liquid systems

The developments in this field are more of recent origin. Batch and semi-batch reactors with and without partial reflux are employed for process standardization studies [Fig. 1.7]. There is good scope for employing spinning basket reactor with reflux arrangements for kinetic studies and for process standardization [81]. The reactive distillation concept was employed for toluene nitration to achieve higher levels of conversion and better selectivity since it facilitates effective removal of water from the reaction front and maintenance of appropriate nitric acid concentration locally. The solid acid catalyst can be packed in the distillation column and a liquid-liquid separator can be introduced to recycle toluene after separation from water formed during the reaction. A configuration which will facilitate parallel nitration-water separation processes will have number of positive effects including enhanced mass transfer as well as reaction rates. The chemical reaction and inter and intra diffusion steps will drive each other in a proactive fashion. Incorporation of a distillation column to the reactor will ensure spatial continuity along the axial direction. Both reaction and distillation take place in every slice of reactive distillation section.

1.5. KINETIC AND THERMAL STUDIES FOR MIXED ACID NITRATIONS

Zaldivar et al. [79-80] observed that at low sulphuric acid concentrations (60-62 wt %), the nitration is kinetically controlled whereas at high sulfuric acid concentration (70-80 wt %), the reaction is found to be mass transfer controlled with significant influence exerted by the interfacial area and distribution coefficients. The dynamics of discontinuous nitration process using adiabatic and heat flow calorimetry also received attention. Parametric sensitivity analysis was done to evaluate optimal and safe operating conditions. Chen and Wu [82] conducted thermal hazard and macrokinetics analysis of toluene mononitration using a microcalorimeter. The major thermokinetic parameters evaluated are heat of reaction, specific heat, onset temperature and the heat transfer coefficients of the reactor. They found that the overall order of toluene nitration is 2.5 with 1.2 with reference to toluene and 1.3 for nitric acid. Details are given in Table 1.8

Table 1.8 Reported kinetic parameters [82]

Parameter	15°C	25°C	35°C	45°C
Order of reaction w.r.t toluene	1.2	1.2	1.2	1.2
Order of reaction w.r.t nitric acid	1.3	1.3	1.3	1.3
Frequency coefficient (s ⁻¹)	50	177	186	1082
Activity energy (Ea/R) (J/mol)	1622	2139	2177	2646

Table 1.9 Thermokinetic and safety parameters

Set temperature (°C)	Heat of reaction (kJ/mol)	Specific heat (J/kg.K)	Heat accumulation (%)*	MTSR (°C)*	TMR _{ad} (s)	ΔT_{ad}
15	127.69	1782	55.3	126.5	22	215
25	125.62	1695	47.1	118	30	223
35	121.90	1688	41.8	119	37	237
45	126.86	1690	39.0	123	48	250

* Values measured at 10 min after reaction inception, MTSR – maximal temperature of synthetic reaction; TMR_{ad} – time to maximum rate, ΔT_{ad} – adiabatic temperature rise

Luo and Chang [83] studied the stability of toluene mononitration in a reaction calorimeter as a function of temperature, fractional conversion and physical and kinetic parameters under non-isothermal conditions. It has been found by Deno [84] and Coombes and co-workers [85] that homogeneous nitration follows second order kinetics, the rate coefficient being a strong function of sulfuric acid strength and temperature. The rate of nitration is found to be maximum at around 90 wt% H₂SO₄. Chapman et al. [86] employed a two necked stirred cell (250 ml; 6.6 cm dia) to determine the nitration rate as a function of sulfuric acid strength.

Papayannakos and Petrolekas [87] studied the dependence of reaction velocity constant (k_2) on temperature and mixed acid composition and the dependence of activation energy on the composition of the aqueous medium in a spectrophotometer. The activation energy of toluene nitration at low nitric acid concentrations is found to decrease at a rate of 0.73 kcal/mol for every 1% increase in sulfuric acid concentration between 25.0 and 34.7 mol %.

1.6 FOCUS AND SCOPE OF PRESENT INVESTIGATIONS

The main focus of present investigations is on the solid catalyzed toluene nitration which has tremendous potential for commercial exploitation. The literature survey has shown that it has not been well studied from reaction engineering point of view. The kinetic and mass transfer effects have not received much attention. It is therefore the objective of the present study to cover following:

- Providing a new perspective to solid catalyzed aromatic nitrations by investigating the precise role of acid – aromatic hydrocarbon dispersion morphology on the product distribution and process / catalyst stability.
- Examining the micro reaction environment around the catalyst particle and its influence on heightening the *para*- selectivity.
- Process standardization with particular reference to catalyst characteristics, mode of operation, temperature, agitation speed, catalyst to toluene ratio, nitric acid to toluene ratio, nitric acid dosing rate, boil-up rate and dispersion morphology to achieve high conversion and high *para* selectivity.
- The study of multiphase mass transfer characteristics of liquid-liquid-solid reaction system as applicable to toluene nitration.

An effort is made in Chapter 2 to evaluate thermodynamic, physical and transport parameters relevant to toluene nitration in a solid-liquid-liquid system. They include free energy and entropy changes, heat of reaction, average diameter of bubbles in liquid-liquid dispersions and phase inversion point.

Full details of the experimental facilities and procedures employed in this work are provided in Chapter 3. Solid acid catalyst selection and characterization methodologies employed in this work received attention in Chapter 4. They include XRD, DTA/TGA, FTIR, SEM and solid state NMR studies. The activity of catalyst under different process conditions has been studied to establish its robustness.

Chapter 5 provides value information on process standardization of toluene nitration considering parameters like mixing, HNO₃-toluene dispersion morphology, toluene-HNO₃ proportions and concentration, reaction water removal and catalyst microenvironment characteristics. The latter has been found to have profound influence on *para*-selectivity in addition to shape selectivity capabilities of the catalyst. The importance of semi-batch mode of toluene nitration to study the microenvironment has been well established in this work.

The mass transfer effects of the multiphase reaction system as employed in toluene nitration reaction system in this work have received attention in chapter 6. An attempt has been made to validate the theoretical calculations with experimental data.

Although, the overall goal for aromatic nitration in this work is to make toluene in good yield and high *para*-selectivity, a fresh look has been given to this reaction by investigating new parameters for its optimization. It is a major development for making aromatic nitrations greener.

1.7 LIMITATIONS OF RESEARCH STUDY

The following are the limitations of the research study

- Evaluation of the contribution of non catalytic reaction in the catalytic toluene nitration is found to be difficult with the available experimental tools.

- The mass transfer resistance offered by the liquid-liquid-solid system in toluene nitration is treated as sequential resistances offered by liquid-liquid and liquid-solid systems.
- The kinetic parameters for toluene nitration could not be evaluated in a batch reactor since the process is very fast to obtain measurable time-conversion data. In the present studies, semi-batch experiments are instead conducted for kinetic studies.
- Evaluation of catalyst performance in toluene dispersed in HNO_3 as continuous phase is found to be difficult with the available experimental tools.

THERMODYNAMIC, PHYSICAL AND TRANSPORT PARAMETERS EVALUATION

2.1. THERMODYNAMIC PARAMETERS

Thermodynamically, chemical reactions encompass changes that involve the motion of electrons in the forming and breaking of chemical bonds. Thermochemistry deciphers whether a specific chemical reaction can or cannot occur. Thermodynamics does not attempt to define the process by which a reaction occurs. Chemical kinetics attempts it and also the rate processes involved.

Theoretically, every chemical reaction is reversible but from practicable considerations, some of them can be classified as irreversible if they almost go to completion. According to chemical reaction equilibrium criteria, any closed system will tend to minimize its free energy.

Aromatic nitrations are exothermic in nature. By calculating the amounts of energy required to break all the bonds of reactants and nitration products, the reaction energy difference is evaluated. It is generally referred to as “heat of reaction” and is –ve for toluene nitration. Thermodynamically, an exothermic reaction is more favorable to occur. It also increases the global entropy.

An attempt has been made in this section to evaluate the important parameters for toluene nitration from thermodynamic consideration.

2.1.1. Reaction Chemistry and Product Distribution

The chemistry of toluene nitration can be represented by



Toluene	Nitric Acid	Nitrotoluene	Water
(92)	(63)	(137)	(18)

The typical isomer distribution in the product is

ortho- 60 mol %; *meta*-4 mol %; *para*-36 mol %

ortho and *para* substitutions are preferred in toluene nitration because their resonance structures include one tertiary carbocation while all the resonance structures for the *meta* attack have secondary carbocations only.

2.1.2. Reported Thermodynamic Properties of Reactants and Products

The thermodynamic properties of reactants and products of toluene nitration have been well reported. Details are presented in Table 2.1. They have been used to estimate the thermodynamic parameters of importance to toluene nitration.

Table 2.1 Thermodynamic properties of reactants and products

Chemical	(ΔH_f°) kJ/mol	(ΔG_f°) (kJ/mol)	(S°) (J/mol.K)
Toluene (l)	12.4	113.82	219.4
Nitric Acid (l)	-174.1	-80.7	155.6
o-nitrotoluene (l)	-9.7	168.0	387.0
m-nitrotoluene (l)	--31.5	143.0	387.0
p-nitrotoluene (l)	-48.1	155.0	381.0
Water (l)	-285.8	-237.1	70.0

Ref:

- CRC Handbook of Chemistry & Physics , 74th Edn [88]
- Physical & Chemical Properties of Pure Chemicals [89]

2.1.3. Reaction Feasibility

Under standard conditions, the free energy change of an isothermal reaction is

$$\Delta G^\circ = \Delta H^\circ - T\Delta S^\circ \quad (2.2)$$

If the free energy change is negative, the reaction can occur spontaneously. A negative ΔG corresponds to a downhill direction.

$$\Delta G_{rxn} = \sum \Delta G_{f(\text{products})} - \sum \Delta G_{f(\text{reactants})} \quad (2.3)$$

The value of free energy change of a chemical reaction changes only in sign when the direction of the reaction is reversed. The standard Gibbs free energy change of toluene nitration has been evaluated employing the reported Gibbs free energy of formation of reactants and weighted average standard Gibbs free energy of formation of *o*, *m* and *p* nitrotoluene mixtures.

The Weighted Average of standard Gibbs free energy of formation for the isomer mixture

$$0.6 (168) + 0.04 (143) + 0.36 (155) = 162.32 \text{ kJ/mol}$$

The standard Gibbs free energy change of the reaction is evaluated as follows

$$\begin{aligned}\Delta G_{rxn} &= [1 (162.32) + 1 (-237)] - [1 (113.82) + 1 (-80.7)] \\ &= -107.8 \text{ kJ/mol} < 0\end{aligned}$$

The toluene nitration reaction is thermodynamically feasible since $\Delta G_{rxn} < 0$

2.1.4. Standard Entropy Change of the Reaction

Occurrence of any chemical reaction, at any speed, is attributed to changes in entropy of substances or compounds involved in the reaction and of the surroundings not otherwise involved in the chemical reaction. The entropy change in a chemical reaction can be calculated from the enthalpy change and the free energy change if both are known. It can also be calculated from the standard entropy of reactants and products in pure form. The standard entropy change of the toluene nitration has been evaluated from the standard entropy values of reactants and products.

Weighted Average of standard entropy for the isomer mixture of nitrotoluene

$$0.6 (387) + 0.04 (387) + 0.36 (381) = 384.8 \text{ kJ/mol}$$

Standard Entropy change of the reaction

$$\begin{aligned}\Delta S_{rxn} &= \sum (S^{\circ})_{products} - \sum (S^{\circ})_{reactants} \tag{2.4} \\ &= [1 (384.8) + 1 (70)] - [1 (219.4) + 1 (155.6)]\end{aligned}$$

$$= + 79.84 \text{ kJ/mol} > 0$$

According to second law of thermodynamics, every process proceeds in such a direction that the total entropy change associated with it is positive, the limiting value of zero being reached only by a reversible process. No process is possible for which the total entropy decreases. Hence the toluene nitration reaction is thermodynamically feasible as $\Delta S_{rxn} > 0$ and irreversible as $\Delta S_{rxn} \neq 0$ [90].

2.1.5. Evaluation of Heat of Reaction from Standard Heats of Formation Data

Isomer distribution in the product (conventional nitration of toluene):

ortho- 60 mol%; *meta*- 4mol%; *para*- 36 mol%

Weighted Average of standard heat of formation for the isomer mixture

$$0.6 (-9.7) + 0.04 (-31.5) + 0.36 (-48.1) = -24.4 \text{ kJ/mol}$$

$$\Delta H_{rxn}^{\circ} = \sum (\Delta H_f^{\circ})_{products} - \sum (\Delta H_f^{\circ})_{reactants} \quad (2.5)$$

$$\begin{aligned} \Delta H_{rxn}^{\circ} &= [1 (-24.4) + 1 (-285.8)] - [1(12.4) + 1 (-174.1)] \\ &= -148.5 \text{ kJ/mol} \end{aligned}$$

2.2. ESTIMATION METHODOLOGIES OF VARIOUS PHYSICAL AND TRANSPORT PARAMETERS

2.2.1. Viscosity of Immiscible Liquid Mixtures

Viscosity of immiscible liquid mixture can be estimated using the Arrhenius equation [91]

$$\mu_m = (\mu_1)^{x_1} (\mu_2)^{x_2} \quad (2.6)$$

where μ_1 is the viscosity of liquid 1

μ_2 is the viscosity of liquid 2

x_1 is the molefraction of liquid 1

x_2 is the molefraction of liquid 2

2.2.2. Estimation of Sauter Mean Diameter

The average drop size and its distribution depends upon conditions of agitation in a liquid-liquid dispersion and also on the physical properties of the two liquids. The sauter mean diameter of the droplets can be estimated by using the correlation by Delichatsios and Probstein [92].

$$d_{32} = Af(\varepsilon_d)We^{-0.6}D_a \quad (2.7)$$

where d_{32} is the sauter mean diameter

A is a constant = 0.321

$$f(\varepsilon_d) = \left[\frac{[\ln(c_2 + c_3)(\varepsilon_d)]}{\ln c_2} \right]^{-3/5}, \text{ where } c_2 \text{ is a constant} = 0.011 \text{ and } c_3 \text{ is}$$

a constant = 0.847

ε_d is the volume fraction of dispersed phase

We is the Weber number given by $We = (\rho_c n_a^2 D_a^3) / \sigma$

Where ρ_c is the density of continuous phase

n_a is the stirrer speed in rotations per sec

D_a is the diameter of the impeller

σ is the interfacial tension

2.2.3. Estimation of Phase Inversion Point

Phase inversion is an important phenomenon in liquid-liquid dispersions. When two immiscible liquids are agitated, a dispersion is formed by virtue of the continuous supply of energy by the stirrer. When the external supply of energy is stopped, the dispersion may disengage into two phases. After a transition period, a dynamic equilibrium between break-up and coalescence is attained and a spectrum of drop sizes results. One of the phases becomes dispersed into the other viz., continuous phase. The nature of dispersion depends on the volume fractions of the two liquids, their physical properties and the dynamic characteristics of the mixing process.

If more and more dispersed material is added to the continuous phase as in a semi-batch nitration process, a point is reached when the addition of more dispersed phase causes an inversion i.e the continuous phase suddenly becomes the dispersed one and vice versa.

The Arashmid and Jeffrey [93] proposed that the phase inversion will occur when the ratio of collision and coalescence frequencies (T) is one, where T is given by

$$T = \frac{C}{\varepsilon_d d_{32}^2 n_a^\alpha} \quad (2.8)$$

Where C is a constant = 2.26 exp (-4) for water-toluene system and 1.42 exp (-4) for toluene-water system

ε_d is the volume fraction of dispersed phase

d_{32} is the sauter mean diameter estimated by the equation

n_a is the impeller speed in rotations per second

α is a constant = 2.7

Employing the above correlation, phase inversion point has been estimated for the toluene nitration at an agitation speed of 200 rpm to be **0.55** for toluene in nitric acid / water system and **0.53** for nitric acid / water in toluene system. These calculations indicate that the phase inversion point is almost unique whether it is reached from water-oil to oil-water or vice versa.

2.2.4. Estimation of Interfacial Area

The interfacial area per unit volume is calculated from the equation

$$a = \frac{6\varepsilon_d}{d_{32}} \quad (2.9)$$

sauter mean diameters and interfacial areas at various volume fractions of organic phase are estimated and the results are shown in Table 5.4 a and b in chapter 5

2.2.5. Estimation of Diffusivity

Diffusivity of toluene in HNO₃ is estimated by the following correlation proposed by Perkins and Gaenkoplis [94]

$$D = \frac{FT}{\mu^{0.8}} \quad (2.10)$$

Where F is given by :

$$F = \frac{4.67 \exp(-16)(\Phi M)^{0.5}}{V_b^{0.6}} \quad (2.11)$$

Where V_b is the molar volume in liters per mole at normal boiling point and

$$\Phi M = 2.6x_w M_w + 2.0x_s M_s + 1.05x_N M_N \quad (2.12)$$

according to Cox and Strachan [95]

where x_w , x_s and x_N are mole fractions of water, sulfuric and nitric acids

and M_w , M_s and M_N are molecular weights of water, sulfuric and nitric acids

T is the absolute temperature in K

μ is the viscosity in kg / m.s

The molar volume can be estimated by Benson's method i.e

$$\frac{V_c}{V_b} = 0.42 \log P_c + 1.98 \quad (2.13)$$

where V_c is critical volume and P_c is critical pressure in atmosphere

The diffusivity of toluene in nitric acid is estimated as $6.7 \exp(-10) \text{ m}^2 / \text{s}$ using the above methodology.

EXPERIMENTAL FACILITIES AND PROCEDURES

3.1 EXPERIMENTAL

3.1.1 Materials and Methods

Toluene (99%, commercial grade) and nitric acid (40 mole %, Merck) are used for preparing various feed compositions. The various catalysts used for the experimental study viz., H-Beta zeolite ($\text{SiO}_2 / \text{Al}_2\text{O}_3 = 22$ and 30), H-ZSM-5 (80), H-ZSM-5 (480) are procured from Sud-Chemie India Ltd. The catalysts in powdered form are calcined at 450 °C for 6 h before using in the nitration reactions.

3.1.2. Experimental Set-up and Procedure

The experimental set-up consists of a four necked Borosil-glass reactor of one litre capacity (diameter, 108 mm and height, 178 mm) equipped with a glass stirrer provided with a teflon blade and reflux condenser connected to a decanter leg to remove water as and when formed. For semi-batch experiments, a syringe pump is used to dose the reactant at specified rate. The experiments in the glass reactor are performed under batch and semi-batch modes with azeotropic water removal as shown in Fig. 3.1 under reflux conditions (120 °C) at atmospheric pressure.

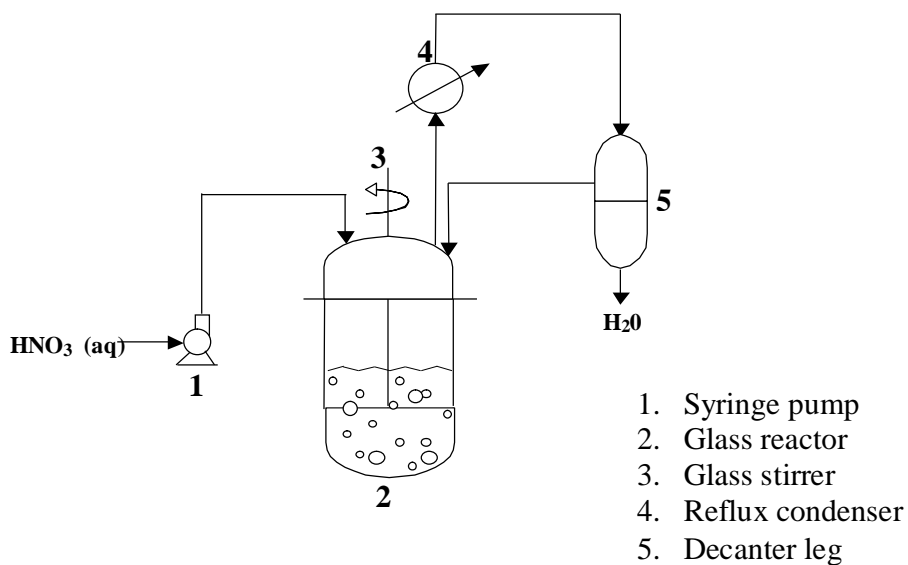


Fig. 3.1. Experimental set-up for batch and semi-batch modes of toluene nitration

3.2. ANALYTICAL FACILITIES AND PROCEDURES ADOPTED

3.2.1. GC Analysis

During the course of the reaction, product samples (about 2 ml) from the organic phase are collected using a sampling syringe. They are immediately quenched in an ice bath to arrest any further reaction. They are then filtered and thoroughly washed with distilled water till they get neutralized. The samples are analyzed for product distribution using a gas chromatograph (GC 17A, Shimatzu) with a column packed with Apizon L (3 m length, 3.2 mm diameter). The conditions employed are FID temperature = 220°C, injection port temperature = 220 °C. The column temperature is maintained at 135 °C for 24 min and then heated upto 190 °C at the rate of 12.5 °C and retained for 5 min. Carrier gas (nitrogen) flow rate has been fixed at 50 ml/min.

Collecting Catalyst Specimen

The catalyst after the reaction is filtered from the reaction mixture and given sufficient washings with acetone and distilled water and then dried in an air oven at around 100°C to remove the moisture. It is subjected to thermal analysis prior to calcination 450 °C for

about 8 h. The sample is now ready for XRD, SEM, NMR, FTIR, TPD and other characterization studies.

3.2.2. X-ray Diffraction

X-ray powder diffraction is the single most important technique used to characterize zeolites. It furnishes vital information regarding phase purity, structure type, isomorphous substitution, degree of crystallinity and also makes possible estimation of unit cell parameters [96-97]. Modern methods have used abinitio calculations and Reitveld analyses to solve zeolite structure using powder X-ray patterns [98-102]. Powder X-ray diffraction is done on SIEMENS / D5000 X-ray diffractometer using Ni-filtered $\text{CuK}\alpha$ radiation (wavelength = 1.506 Å). The operating parameters are 40 kV and 30 milliamp.

3.2.3. Thermal Analysis

This technique provides information regarding the thermal behavior of the catalysts. It is used extensively in the study of kinetics and dehydration of zeolites and also for studying the oxidative combustion of occluded organics in zeolites [103]. DTA curves provide qualitative and quantitative information about the energy of activation and enthalpy of the zeolite systems. Thermal analysis has been done by on METTLER TOLEDO (TGA/SDTA 851° Make), Switzerland. The heating rate is 20 °C / min with inert gas of nitrogen.

3.2.4. Scanning Electron Microscopy (SEM)

The crystalline size and morphology of the catalyst samples are analyzed by a scanning electron microscope equipped with energy dispersive X-ray analysis. A thin film (0.1mm) of the catalyst sample on an alumina carrier is coated with gold film to prevent surface charging and thermal damage by the electron beam [104]. The scanning electron microscopic analysis of the catalyst samples for changes in Si/Al ratio is done using Hitachi S-520 instrument at an accumulation voltage of 10kV with system resolution of 98 eV. The EDX is done on LINK ISIS 300 (Oxford, UK).

3.2.5. Fourier Transform Infrared Spectroscopy

This is one of the most sensitive tools for the investigation of the structural features of the zeolites, the isomorphous substitution in them, their acidity and the nature of zeolite-adsorbate interactions [105-107]. Zeolites may be characterized by infrared spectroscopy yielding valuable information in the vibrational mode region ($400\text{-}1300\text{cm}^{-1}$). IR spectroscopy can also distinguish large pore zeolites from small and medium pore ones on the basis of OH stretching vibrations [34a]. This technique is also used to estimate the acid sites of solid acid catalysts by the adsorption of various basic probe molecules like ammonia, pyridine and benzene and to measure the acidity qualitatively and quantitatively. FT-IR analysis (KBr) is recorded on “Perkin Elmer Spectrum Gx” instrument. 5 mg of catalyst sample is mixed with 500 mg of IR grade KBr and finely ground in mortar and pellets are made with KBr press instrument.

3.2.6. Solid State Nuclear Magnetic Resonance Spectroscopy

High resolution solid state NMR spectroscopy using magic angle spinning (MAS) is a powerful method to characterize zeolite materials [108-111]. Till now twenty different NMR active nuclei have been studied. Much attention has been given to ^{29}Si and ^{27}Al MAS NMR in order to investigate the changes of Si and Al configuration in the zeolite framework [112], as well as the crystallographically equivalent and nonequivalent Si [113] and Al [114] ions in various sites. In the present work, ^1H MAS NMR has been used to study zeolite acidity [115-116], arising out of the various types of protons. The solid state MAS-NMR analysis has been done by employing Varian (PALO ALTO, CA (USA); UNITY INOVA model) with a frequency of 400 MHz. $\text{Al}_2(\text{SO}_4)_3 \cdot 6\text{H}_2\text{O}$ is used as a standard for ^{27}Al .

3.2.7. Temperature Programmed Desorption (TPD) of Ammonia

The estimation of acid strength distribution in solid acid catalysts is carried out by this technique. It is used to characterize weak, medium and strong acid sites. The amount of ammonia released above 753K is normally considered to represent very strong acid sites. The presence of different types of acid sites have been reported by several workers using TPD method [110, 117]. TPD studies are carried out in a AutoChem 2910

(Micromeritics, USA) instrument. The catalyst sample is pretreated at 473 K for 1h by passing pure Helium (99.99%, 50 ml/min) and saturated with anhydrous ammonia from NH₃ and 90% Helium mixture at 80°C at a flow rate of 75 ml/min. It is subsequently flushed at 105°C for 2 h to remove physisorbed ammonia. TPD analysis is carried out by taking 500 mg of sample (dried at 110 °C in oven for 12 h) in a U-shaped quartz sample tube and subjecting it to thermal treatment for ambient temperature to 750°C at a heating rate of 10 °C /min. The amount of NH₃ desorbed is calculated using GRAMS / 32 software.

3.2.8. Surface Area Measurement

The Braunauer-Emmett-Teller (BET) volumetric gas adsorption technique using nitrogen or argon is a well established method for the determination of the surface area and pore size distribution of porous materials [108]. The surface area of the sample is calculated employing following correlation

$$\frac{1}{V_{ads}}(P - P_o) = \frac{1}{V_m C} + \left[\frac{(C-1)}{V_m C} \right] \frac{P}{P_o} \quad (3.1)$$

Where V_{ads} is the volume of gas adsorbed at pressure P , P_o is the standard vapor pressure, V_m is the Volume of the gas adsorbed for monolayer coverage, C is the BET constant.

By plotting the left hand side of the equation (1) against P/P_o , a straight line is obtained with a slope $(C-1)/V_m C$ and an intercept $1/V_m C$. The BET surface area was calculated using the formula

$$S_{BET} = X_m N A_m, \quad (3.2)$$

Where N is the Avogadro number, A_m is the surface area of the adsorbate molecule [for N₂, $A_m = 0.162 \text{ nm}^2$] and X_m is the moles of nitrogen adsorbed.

3.2.9. Reaction Calorimetry for Thermochemical Investigations

The METTLER TOLEDO Reaction calorimeter (RC) is a computer controlled, electronically safeguarded lab reactor used for assessing the thermal performance of isothermal and adiabatic reaction systems. It is a useful tool for process development, optimization, scale up and safety analysis. The RC comprises of a calorimeter equipped with thermostat, stirrer and electronic cabinet, a chemical reactor (glass or metal) and a software support. For control of the auxiliary facilities like pumps or valves, PC with necessary instrumentation is provided.

The computer controlled batch reactor (1.5-2 liters capacity) is well equipped to monitor the course of a chemical or physical transformation at pre-identified process conditions. Both batch and semi-batch modes of operation can be executed with RC. Important process variables such as temperature, pressure, feed dosing rates, extent of mixing, system viscosity, thermal inputs and outputs, heat transfer coefficients are measured and / or controlled. The reaction system is well designed to simulate the commercial process conditions on a bench scale to assess their process and thermal responses.

For conducting nitration reaction, the glass reactor is initially filled with the required amounts of toluene (340 ml) and the catalyst (20 g). The reaction mixture is stirred at 100 rpm and is heated to the desired temperature of 50 °C. On reaching the steady state temperature, 48 ml of 60% nitric acid at 50 °C is charged into the reaction vessel. The time profiles of temperature and heat liberated are recorded during the progress of the reaction. The experiment is terminated after 3 h run and then evaluated for the required parameters.

CATALYST SELECTION AND CHARACTERIZATION

4.1 SELECTION OF A SOLID ACID CATALYST

4.1.1 Reported Studies

4.1.1.1 Aromatic Nitrations

The nitration of toluene is most important route to obtain substituted aromatic intermediates viz., nitrotoluenes and dinitrotoluenes for the production of speciality chemicals mainly after reduction of the nitro group. In the conventional nitration, however, the production of the *ortho* isomer exceeds that of the *para* isomer. To overcome this limitation, nitrations using solid acids as catalysts are receiving increased attention.

Olah et al. proposed [118] that aromatic nitrations could be carried out using nitronium tetrafluoroborate under anhydrous conditions to obtain yields of 80-100%, alkyl nitrates / acetone cyanohydrin nitrate in the presence of BF₃ accounted for yields of 75-80% and silver nitrate in the presence of Lewis acids provided an yield of 60%. Solid superacid catalysts like polystyrene sulfonic acid, perfluorinated sulfonic acid (Nafion H) with HNO₃ or its metal salts, mixed anhydrides or nitrate esters catalyzed by H₂SO₄ and nitrations under essentially neutral conditions using N-nitropyridinium, N-nitroquinolium salts, nitro and nitrite onium salts have been reported to enhance the reactivity of the nitrating agent.

Smith and Fry [119] reported *para*-selective mononitration of alkylbenzenes under mild conditions using benzoyl nitrate in the presence of aluminium or proton exchanged large pore mordenite. A maximum *para*-selectivity of 64 % was achieved employing tetrachloromethane as solvent. It was also reported that catalysts like silica, alumina, K10 clay could not give high *para*-selectivity. Choudary et al. [71] reported higher *para*-selectivities (upto 2) and attractive space time yields in aromatic nitrations employing

various solid acid catalysts like Fe³⁺ montmorillonite, K10 montmorillonite, zeolite Beta, ZSM-5, mordenite, HY and TS-1 employing 60-90% nitric acid and azeotropic water removal.

4.1.1.2 Nitration of Toluene

Vassena et al. [33] have demonstrated that sulfuric acid supported on preshaped silica to be a good recyclable catalyst for the nitration of toluene to dinitrotoluene using 65 wt% nitric acid. Dagade et al. [54] reported vapor phase nitration of toluene at 120 °C using dilute nitric acid (20 %) and Beta zeolite and achieved maximum conversion of 55%, *para*-selectivity of 70% and catalyst life of 75 h. It was also observed by them that the Beta zeolite is highly stable and that the shape selective nitration of toluene takes place inside the pores. The production of dinitrotoluene by nitrating toluene and nitrotoluene in vapor phase mode and in liquid phase with simultaneous distillation were reported by Vassena et al. [33]. They found that zeolite Beta exhibited high stability and gave high *para*-selectivity compared to zeolites like ZSM-5, ZSM-12 and mordenite though its activity was slightly low. It was also observed that liquid phase reaction with simultaneous distillation is preferable to vapor phase reaction for the formation of dinitrotoluene. Nitration of toluene and 2-nitrotoluene was reported by Bernasconi et al. [120] using acetyl nitrate and zeolite Beta of different Si/Al ratios and different crystallite sizes. They observed that the number of bronsted acid sites and diffusion play a major role in determining the catalyst performance. It was found that zeolite Beta gave maximum *para*-selectivity in the nitration of toluene and 2-nitrotoluene due to the fact that heterogeneously catalyzed reaction compete successfully with the homogeneous nitration in the liquid phase. The Table 4.1 indicates the product distribution in the nitration of toluene with acetyl nitrate using different catalysts [121]. The reported data as presented in Table 4.1 clearly shows the superiority of zeolite catalysts in general and H-Beta-24 in particular for achieving higher *para*-selectivity and nitrotoluene yields exceeding 80 %.

Table 4.1 Reported comparative performance of various catalysts for toluene nitration

Catalyst	NT yield (mol%)	DNT yield (mol%)	<i>Para</i> selectivity <i>S4-NT/S2-NT</i>
Blank	76	0.0	0.64
Blank ^a	91	0.0	0.62
Blank ^b	82	0.0	0.62
Amberlyst-15	74	3.8	0.76
Nafion-SAC25	84	0.0	0.69
H-ZSM-5	81	0.04	0.61
H-ZSM-12	78	0.01	0.61
USY	77	0.0	0.64
H-MOR (4.6)	78	0.0	0.67
H-MOR (7.4)	82	0.04	0.75
H-BETA-24	81	1.1	2.13

^a Toluene/HNO₃ = 0.1

^b Double molar amount of acetic acid anhydride was used; 90 wt% HNO₃, AC₂O; toluene / HNO₃ = 1; 30 min

4.1.2. Selection of Catalyst

The activity of H-Beta and ZSM-5 type zeolites is ascribed to their Bronsted acidity whereas the improved *para*-selectivity to their pore size and shape selectivity. Haouas et al. [122] ascribed the higher *para*-selectivity of H-Beta to the lattice aluminium transformations during the reaction. In the present work, H-Beta and H-ZSM-5 catalysts are employed for liquid phase nitration in view of their stated advantages in conversion levels and selectivity. The lower *para*-selectivity of HZSM-5 may be due to its hydrophobic pores that resist the diffusion of aqueous nitric acid resulting in fewer acidic sites available to generate required nitronium ions. The reported molecular modeling studies [54] revealed that *para*-nitrotoluene encountered least resistance for vapor diffusion in H-Beta catalyst and diffusivities decrease in the order *para* > *ortho* > *meta* nitrotoluenes. The role of SiO₂ / Al₂O₃ ratio (hereinafter called S/A) of catalyst on the product distribution is experimentally investigated in the present work. Fig. 4.1 shows the conversion and *para*-selectivity achieved by using four catalyst samples with different S/A ratios in the batch nitration experiments conducted under reflux. It shows H-Beta

zeolite with S/A of 22 has provided better conversions and *para*-selectivity. It is interesting to note that the same catalyst was reported to be highly *para*-selective in liquid phase nitration with acetyl nitrate Smith et al. [123] and in vapor phase nitration of toluene [54] and fluoro benzene [56] and reactive distillation of toluene [71].

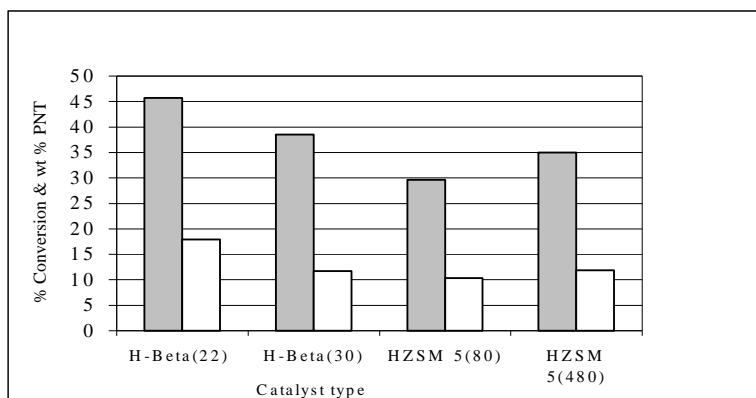


Fig. 4.1 Effect of catalyst on toluene conversion (■) and wt.% *para*-nitrotoluene formation (□). Toluene: nitric acid (molar ratio) = 2.2 : 1.4; catalyst= 10 g; temperature= 110 °C; time= 3 h; agitation speed= 200 rpm; S/A ratio in parenthesis

Our experimental results and these reported advantages have reinforced our decision to select H-Beta catalyst. H-Beta has also superior structural characteristics as shown in Table 4.2. The other advantages are its regenerability through a simple thermal treatment and its facilitated separation from the reaction products. Its limitations viz., the necessity to maintain higher concentration of acid sites for sustaining its activity and the need to remove the water formed during nitration effectively from its acid sites have been given due consideration in this work. After examining the various options of water removal viz., separation as vapor at high temperature, chemical trapping and azeotropic distillation, the latter was favored in the present work in view of its advantages of integrating it with the reaction system in making efficient use of available reaction enthalpy and enabling excellent control of the reaction temperature. Batch and semi-batch nitrations have accordingly been conducted with a reflux bridge with Dean- stark separation leg attached to it. This has enabled the evaporated water-nitric acid –toluene mixture to be condensed in the reflux condenser and collected in the Dean-stark leg for

separation of aqueous and organic phases. Titration of the collected aqueous phase is carried out to determine the nitric acid content.

Table 4.2 Reported* structural characteristics of H-Beta

Catalyst	Si/Al	BET surface area (m ² /g)	External surface area, m ² /g	Pore volume cm ³ /g	Mesopore diameter (Å)
H-Beta [@]	11.5	690	199	0.9	1.2
H-ZSM-5	16.9	433	64	0.51	98
H-ZSM-12	47	355	20	0.2	38
H-Mor (4.6)	4.6	544	6	0.27	64
H-Mor (74)	74	512	38	0.31	57

* Ref: D. Vassena, A. Kogelbauer and R. Prins, *Catalysis Today*. 60, 275, (2000)

@: Average pore dimensions 7.6X 6.4 Å

4.2 CATALYST CHARACTERIZATION

H-Beta catalyst was characterized before and after toluene nitration for its structural, physical and chemical properties using various techniques such as XRD, FTIR, SEM, GC, DTA, TGA, MAS-NMR and others.

4.2.1 X-Ray Diffraction Studies (XRD)

The catalyst crystallinity determination by XRD measurements, involves the division of sum of several specific peak intensities by the respective sum found for a well crystallined sample measured under the same conditions. X-ray diffraction has been used in the present studies to investigate not only the structural stability of the catalyst used in this work but also zeolite phase characteristics. Powder X-ray diffraction studies are carried out with SIEMENS / D5000 X-ray diffractometer using Ni-filtered CuK_α radiation ($\lambda = 1.506\text{Å}$). The operating parameters are 40 kV and 30 milliamp. The Fig. 4.2. shows the XRD pattern of fresh zeolite H-Beta catalyst (S/A = 22). The XRD pattern of zeolite H-Beta catalyst shows that the catalyst has high phase purity and crystallinity.

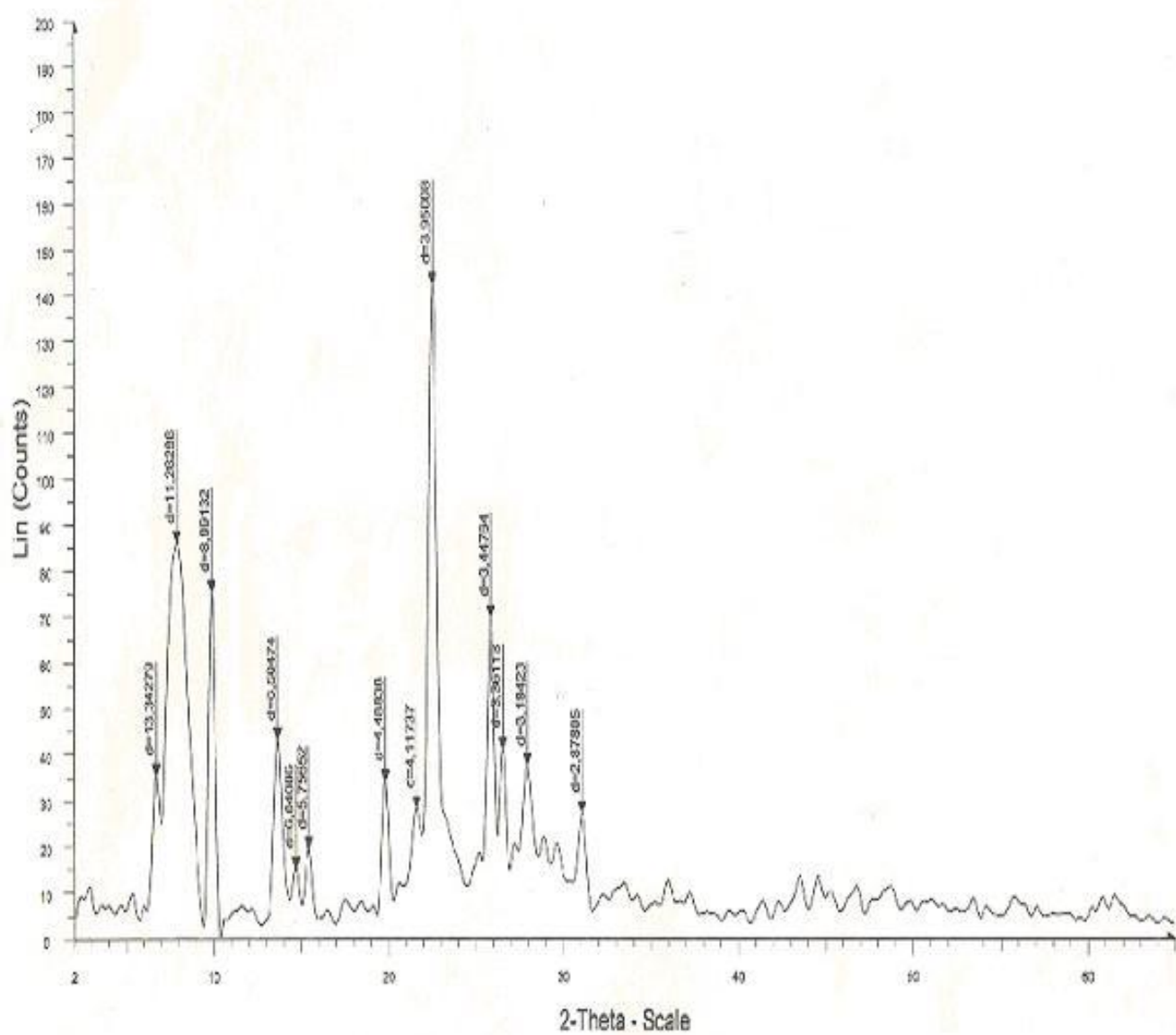


Fig. 4.2 XRD pattern of fresh zeolite H-Beta (S/A=22)

4.2.2. FTIR Studies

In the present work, FTIR studies have been conducted to assess the structural status, acidity levels and adsorbate interactions of H-Beta catalyst under different process conditions. FTIR spectroscopy measures the energy of the radiation transmitted through the catalyst sample as a function of the IR frequency (wave number or length). Apart from assessing the framework vibrations of zeolites, IR has been used to determine the Bronsted and Lewis acid sites and zeolite adsorbate system. FTIR spectrometer of Nexus 670 model (USA) has been used in this work in the frequency range of 400-4000 cm^{-1} . Spectra are recorded using a mixture of dry KBr wafers. The spectrum of dry KBr has been used for background correction. The Fig. 4.3 shows the FTIR spectra of fresh zeolite H-Beta catalyst (S/A = 22). The bands around 3600 cm^{-1} indicate the hydroxyl groups attached to tetrahedrally coordinated aluminium and the region around 1400 to 1700 cm^{-1} correspond to Bronsted and Lewis acidity.

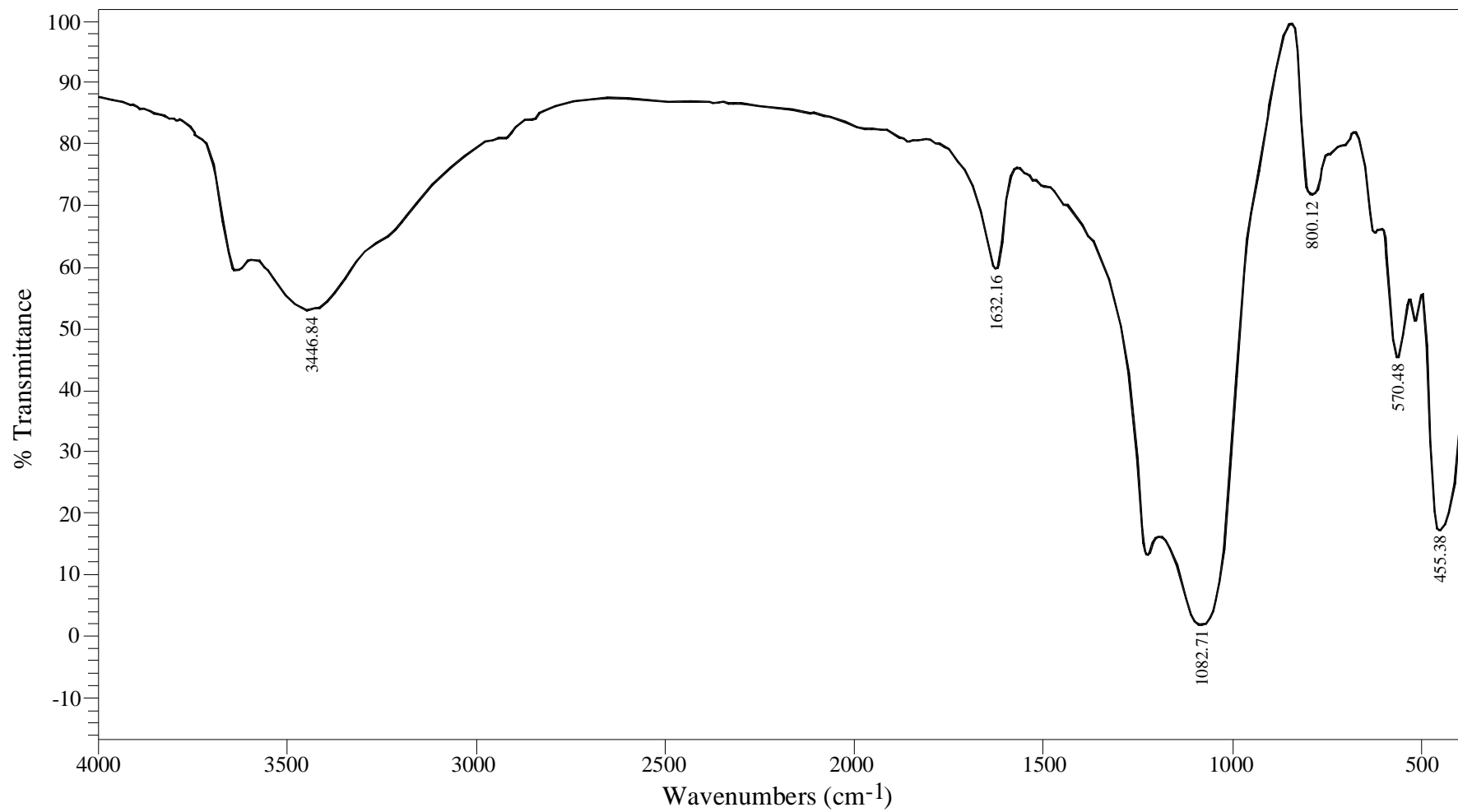


Fig. 4.3 FTIR plot of freshly prepared zeolite H-Beta (S/A=22)

4.2.3 Scanning Electron Microscopy

Scanning electron microscopy (SEM-EDX) has been used in this work to provide an insight into the structure and morphology of H-Beta catalyst. Atomic scale structural details of the catalyst can be mapped along with the local elemental composition and chemical state. SEM is carried out on a Hitachi S-520 instrument at an accumulation voltage of 10 kV with 2.5 k magnification. The EDX is done on LINK ISIS 300 (Oxford, UK). The elemental analysis of freshly prepared H-Beta catalyst is obtained as O, 69.89%; Al, 2.5% and Si, 27.62%.

4.2.4 Thermal analysis

DTA/TGA analysis has been carried out in the present work to understand the thermal behavior of the catalyst and its dehydration characteristics. The Differential thermal analysis (DTA) has provided qualitative and quantitative information about the energy of activation and enthalpy of the catalyst system. Thermal analysis has been done by employing METTLER TOLEDO (TGA / DTA 851 Make), Switzerland. A heating rate of 20 °C / min is employed with inert gas (nitrogen). Fig. 4.4. shows the DTA and TGA plots of freshly prepared H-Beta (S/A = 22) catalyst. The weight loss observed upto 200 °C is due to evaporation of moisture as indicated by the DTA. No further weight loss has been observed till 1000 °C.

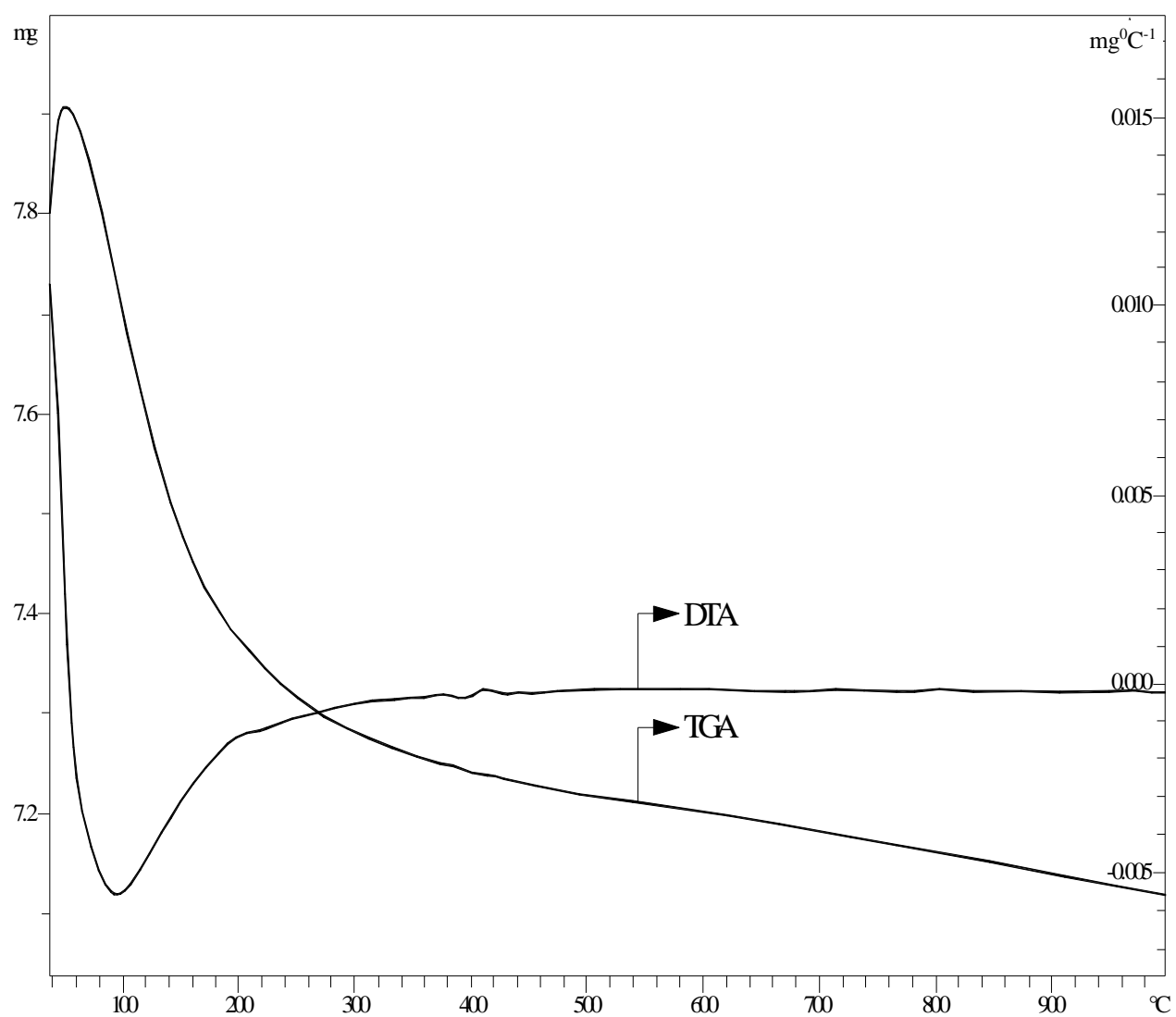


Fig. 4.4 DTA/TGA plot of freshly prepared H-Beta (S/A = 22)

4.2.5 Solid State NMR spectroscopy

Solid state MAS-NMR spectroscopy has been employed in this work to study the behaviour of lattice aluminium in H-Beta catalyst during the nitration of toluene. MAS-NMR minimizes the interference of water that would be detrimental to IR spectroscopic investigations and furthermore allows the handling of the corrosive reaction medium by using inert zirconia rotors. The solid state MAS-NMR analysis has been done using Varian (PALO ALTO, CA (USA); UNITY INOVA Model) with a frequency of 400 MHz. $\text{Al}_2(\text{SO}_4)_3 \cdot 6\text{H}_2\text{O}$ is used as standard for ^{27}Al . The ^{27}Al MAS-NMR spectrum of the freshly prepared H-Beta zeolite (Fig. 4.5) showed two signals centred at 54.0 ppm (tetrahedrally coordinated aluminium) and 0.0 ppm (octahedrally coordinated aluminium) respectively. In the present investigations, MAS-NMR analysis has been effectively used to study the effect of nitric acid concentration on the lattice aluminium transformation in the zeolite catalyst.

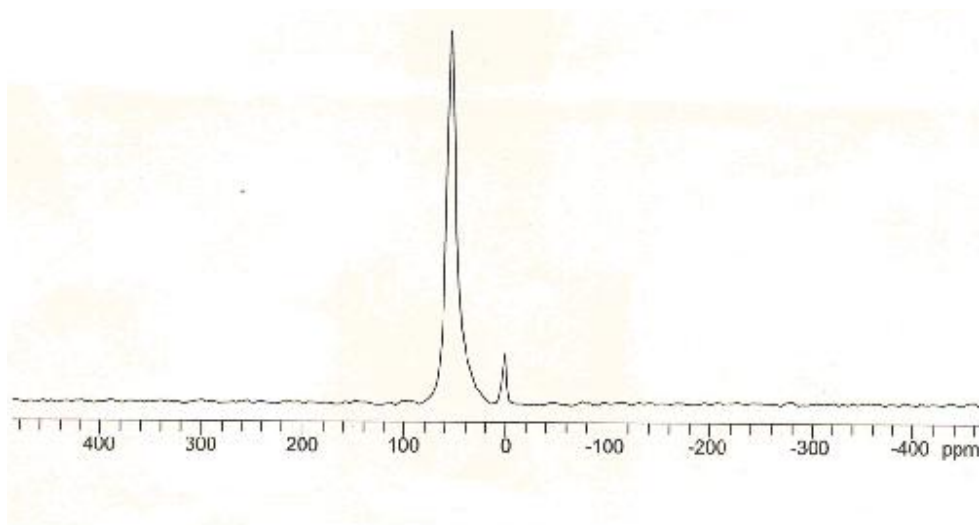


Fig. 4.5 ^{27}Al MAS NMR spectrum of freshly prepared zeolite H-Beta catalyst.

4.2.6 Catalyst Stability and Regenerability

4.2.6.1 Catalyst Stability

XRD investigations have been done prior to and after nitration reaction to study the structural changes experienced by H-Beta catalyst. In our present studies, batch nitration of toluene in the presence of catalyst has been conducted using various mole ratios of toluene and nitric acid. Fig 4.6 shows the XRD patterns of the freshly prepared catalyst and that used under different process conditions. It has been established that the structural integrity of the catalyst is maintained in all cases. To demonstrate the longevity of the catalyst, batch nitration of toluene has been conducted for 24 h under high (0.9) and low (0.2) volume fractions of toluene in the reaction mixture. The basic objective of these studies is to assess the structural and performance stability of H-Beta catalyst employed in this work after exposing it to specific process conditions for longer duration viz., 24 h. Figures 4.7 to 4.9 provide XRD, TGA and FTIR profiles of H-Beta catalyst after long duration exposure (24 h). The XRD profiles show that the structural integrity of the catalyst is maintained even after long exposure time at high volume fractions of toluene. This observation reinforces the stability of zeolite H-Beta in highly acidic dispersed phase conditions. The crystalline nature of the catalyst is found to be very little affected by the volume fraction of toluene. The TGA profiles, however, show the vulnerability of H-Beta catalyst under low toluene volume fraction viz., nitric acid as a continuous phase and toluene as dispersed phase. The FTIR profiles demonstrate that the bands at about 3600 cm^{-1} and 1600 cm^{-1} (ascribed to hydroxyl groups attached to lattice aluminium and Bronsted acidity respectively) got significantly reduced under the conditions prevailing at low volume fraction of toluene. This indicates the reduction in total and Bronsted acidity under high concentrations of the acid as continuous phase. Hence nitric acid dispersed in toluene is preferable to toluene dispersed in nitric acid as far as catalyst stability is concerned.

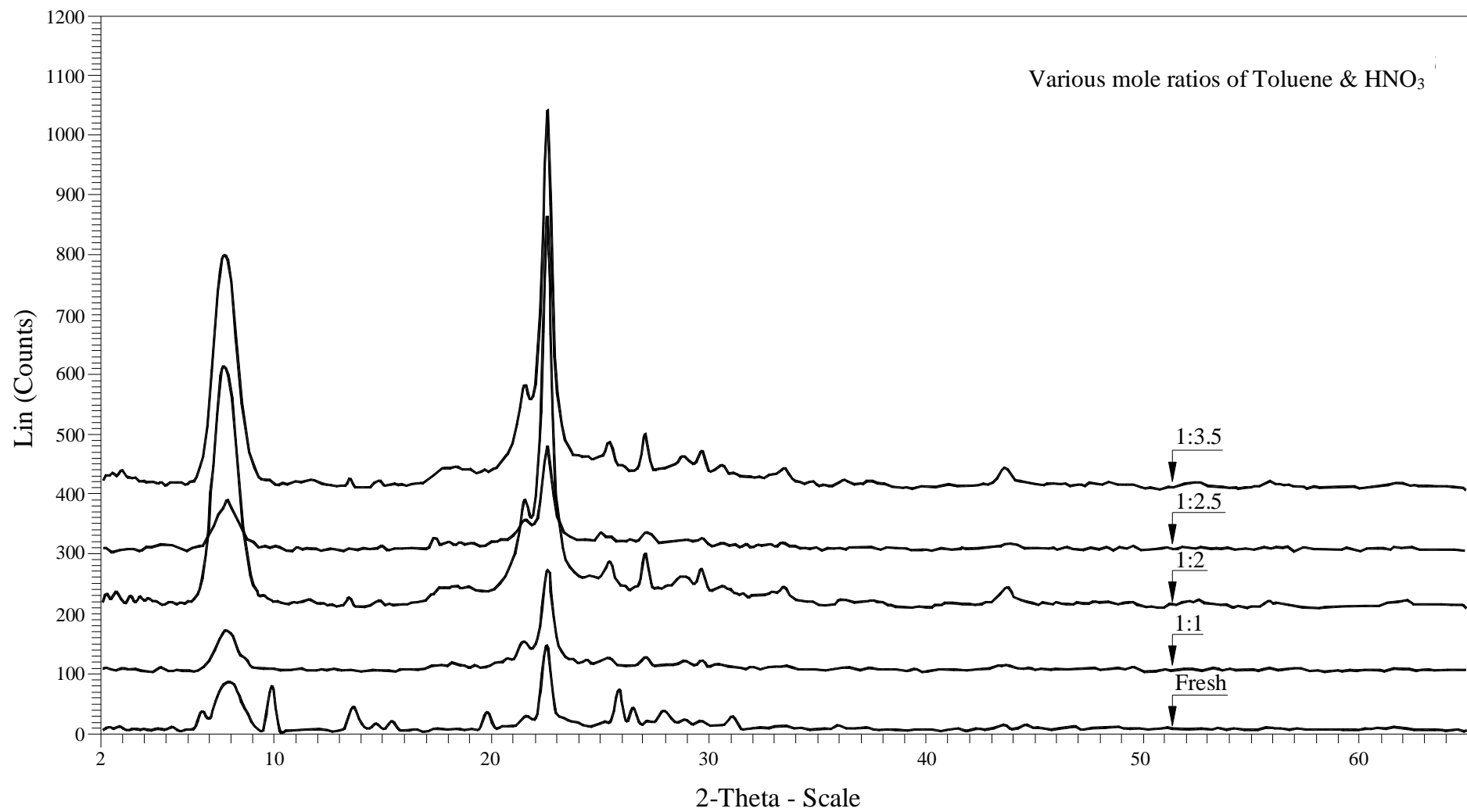


Fig. 4.6 XRD patterns at various mole ratios of toluene and nitric acid-batch nitration; F, fresh catalyst; 1:1; 1:2; 1:2.5; 1:3.5 = mole ratios of toluene nitric acid.

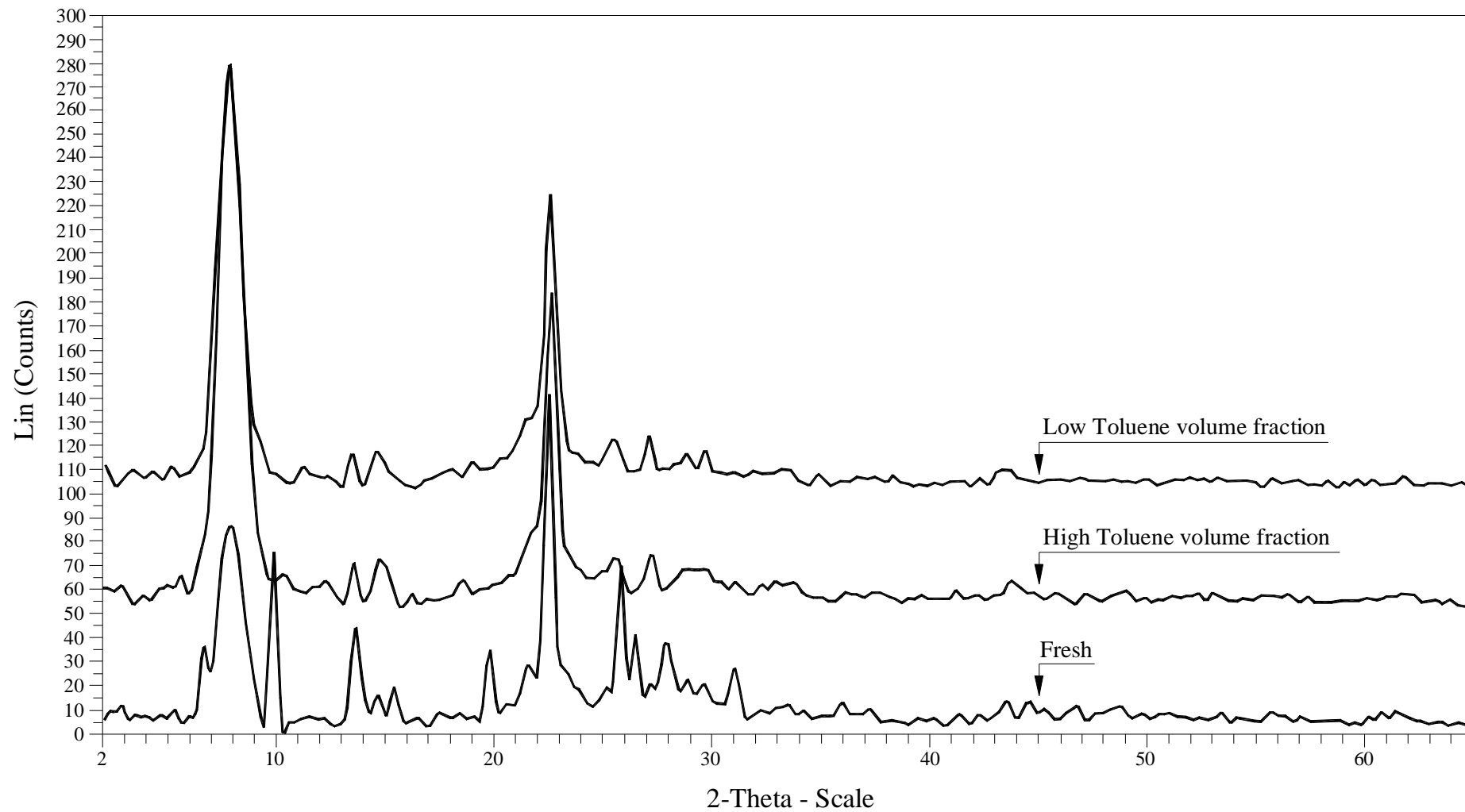


Fig. 4.7 XRD patterns of H-Beta catalyst after batch nitration continued for 24 h under low (N24) and high (T24) volume fractions of toluene; F: fresh catalyst.

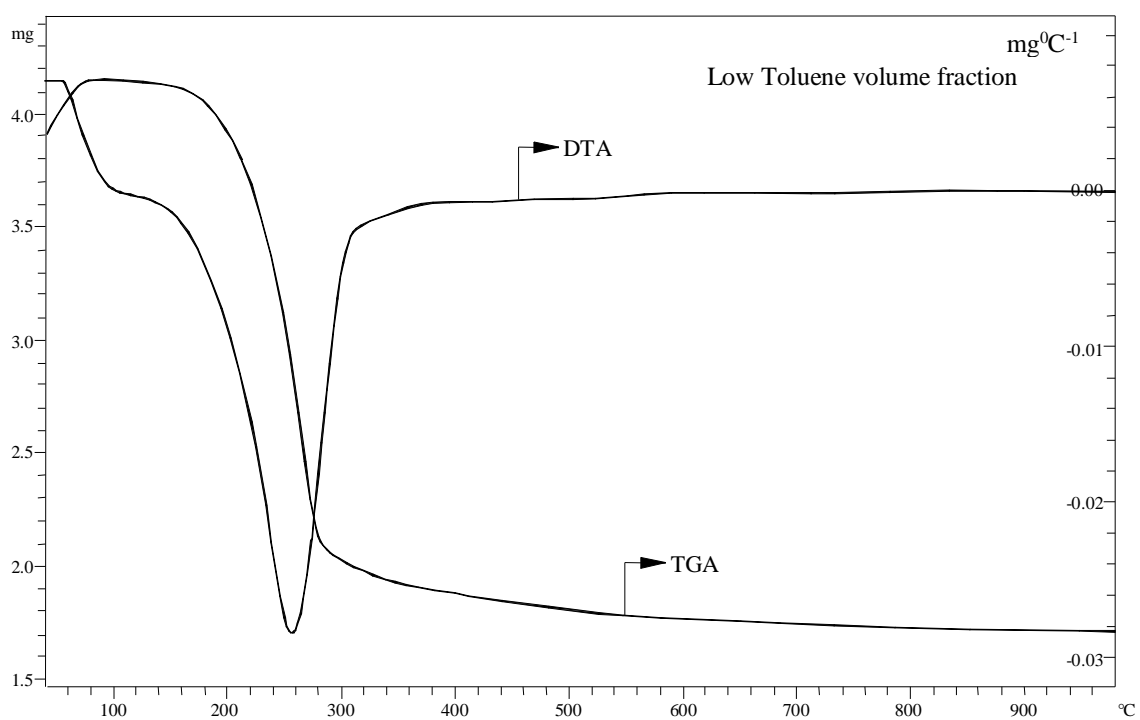
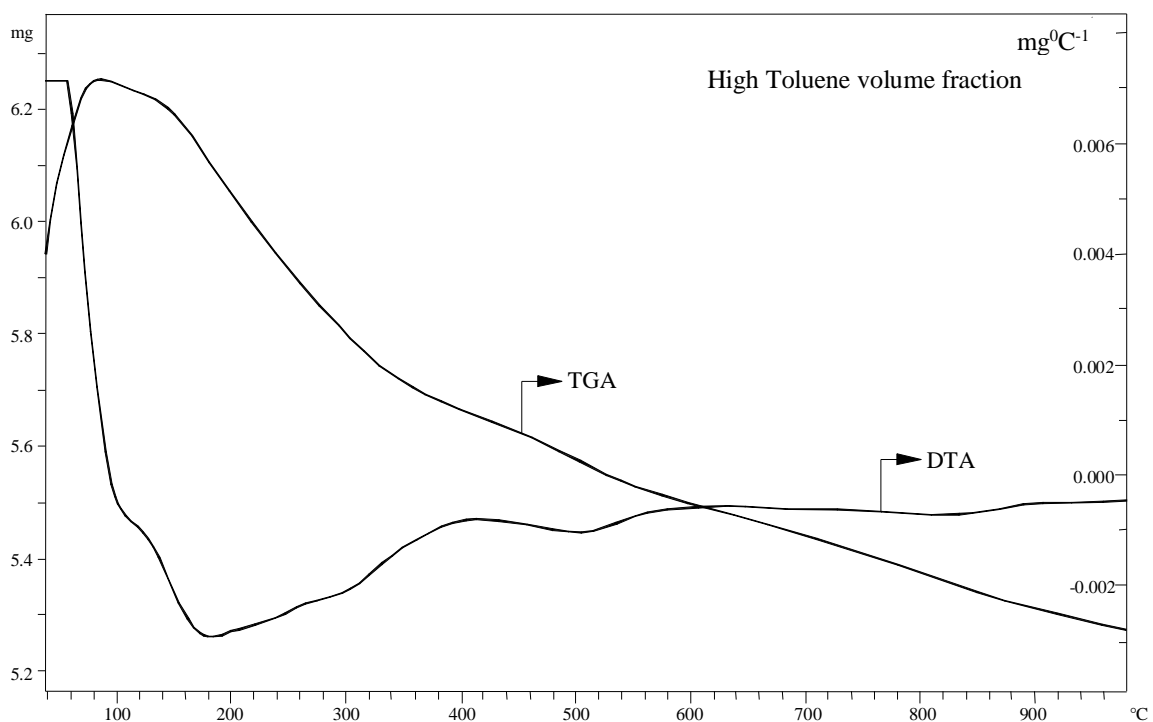


Fig. 4.8 DTA / TGA profiles of H-Beta catalyst after batch nitration of toluene continued 24 h under low and high volume fraction of toluene.

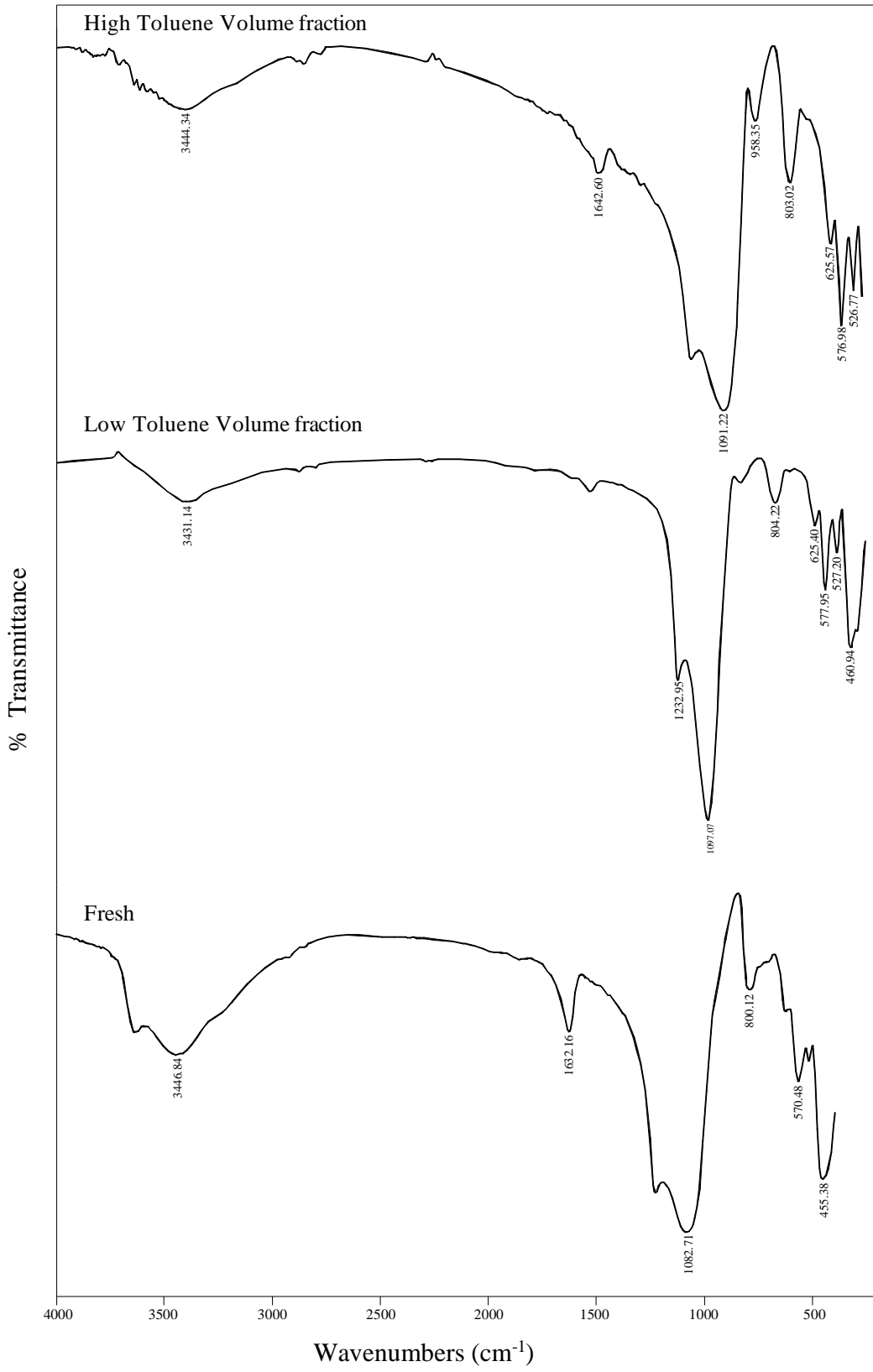


Fig. 4.9 FTIR plot after batch toluene nitration continued for 24 h under low and high toluene volume fraction.

4.2.6.2 Catalyst Regenerability

With reference to the regenerability and reuse of H-Beta zeolite catalyst for toluene nitration, there are no reports to confirm its behavior when recycled. An attempt has, therefore, been made in this work to assess the catalyst characteristics during and after three regenerations and recycles. The catalyst after the reaction has been filtered and thoroughly washed with water and acetone till the filtrate is neutralized. It is then dried in an oven to remove the moisture for about 2 h and then calcined at a temperature of 450 °C for 6-8 h.

Semi-Batch mode of nitration is employed for regeneration and recycle studies. Two nitric acid dosing rates viz., 30 and 60 ml/h at high toluene volume fraction have been employed to assess the catalyst behavior at two levels of *para*-selectivity. The results are presented in Table 4.3 for 3 catalyst recycles. They clearly establish that the toluene conversions and *para*-selectivity are practically unaffected by the catalyst regeneration and recycle.

The XRD patterns as shown in Figs. 4.10 and 4.11 show that they remained unchanged after the reaction even after three cycles except for the marginal decrease in the relative peak intensities. This indicates that the catalyst crystalline structure remained intact after the reaction. This also confirms the efficacy of simple thermal treatment for catalyst regeneration. Figs. 4.10 and 4.11 also show that HNO₃ dosing rate has a marginal influence on the structural integrity of the catalyst even in highly acidic environment. Similar observation was made by Dagade et al. [54] in vapor phase nitration of toluene, Breck et al. [124] for hydration and He and co-workers [125] for methylation reaction. The TGA profiles presented in Fig 4.12 reinforce the uniformity and consistency in catalyst behavior even after three regenerations. They indicate that upto 200 °C (region 1) there is an endothermic weight loss of adsorbed water or toluene from the catalyst and above 200-400°C (region 2) the weight loss is due to the evaporation of volatile oxidation products deposited on the catalyst. The final exothermic weight loss below 690 °C

(region 3) is due to the combustion of high boiling species suggesting the formation of coke precursors. It can also be observed from these plots that acid dosing rate has marginal influence on the percent weight loss which is less than 10%. The FTIR spectrum presented in Fig. 4.13 show that with an increase in acid dosing rate, there is a reduction in the total and Bronsted acidity. This observation again reinforces our selection of lower dosing rate for achieving higher conversions and *para*-selectivity.

Table 4.3 Influence of catalyst regeneration and recycle on toluene conversion and *para*-selectivity

Nitric acid dosing rate (ml/h)	Cycle no	Dosing time (h)	Tol Conversion	ONT	MNT	PNT	Others	<i>Para/Ortho</i>
30	I	1	18.5	8.97	0.7	8.3	0.5	0.93
		2	23.2	9.3	0.8	11.7	1.4	1.25
		4.5	33.0	11.8	1.2	17.6	2.4	1.50
30	II	1	16.5	8.17	0.5	7.5	0.3	0.92
		2	21.7	8.8	0.5	11.2	1.2	1.27
		4.5	31.5	11.3	0.9	17.1	2.2	1.51
30	III	1	16	7.92	0.5	7.25	0.3	0.92
		2	21.5	8.8	0.5	11.4	1.2	1.30
		4.5	31	11	0.9	16.9	2.2	1.54
60	I	1	22.5	11.7	0.6	9.7	0.5	0.83
		2	40.7	20.1	1.8	17.7	1.1	0.88
		4.5	55.0	27.4	2.3	23.9	1.4	0.87
60	II	1	21.0	11.2	0.3	9.2	0.3	0.82
		2	39.5	19.6	1.7	17.2	1.0	0.88
		4.5	53.0	26.6	2.1	23.0	1.3	0.86
60	III	1	20.5	11.0	0.2	9.0	0.3	0.82
		2	39.2	19.4	1.6	17.2	1.0	0.89
		4.5	52.5	26.4	2.0	22.9	1.2	0.87

Toluene= 2.2 moles; catalyst (H Beta S/A, 22)= 10 g; agitation speed= 200 rpm; temperature= 130°C.

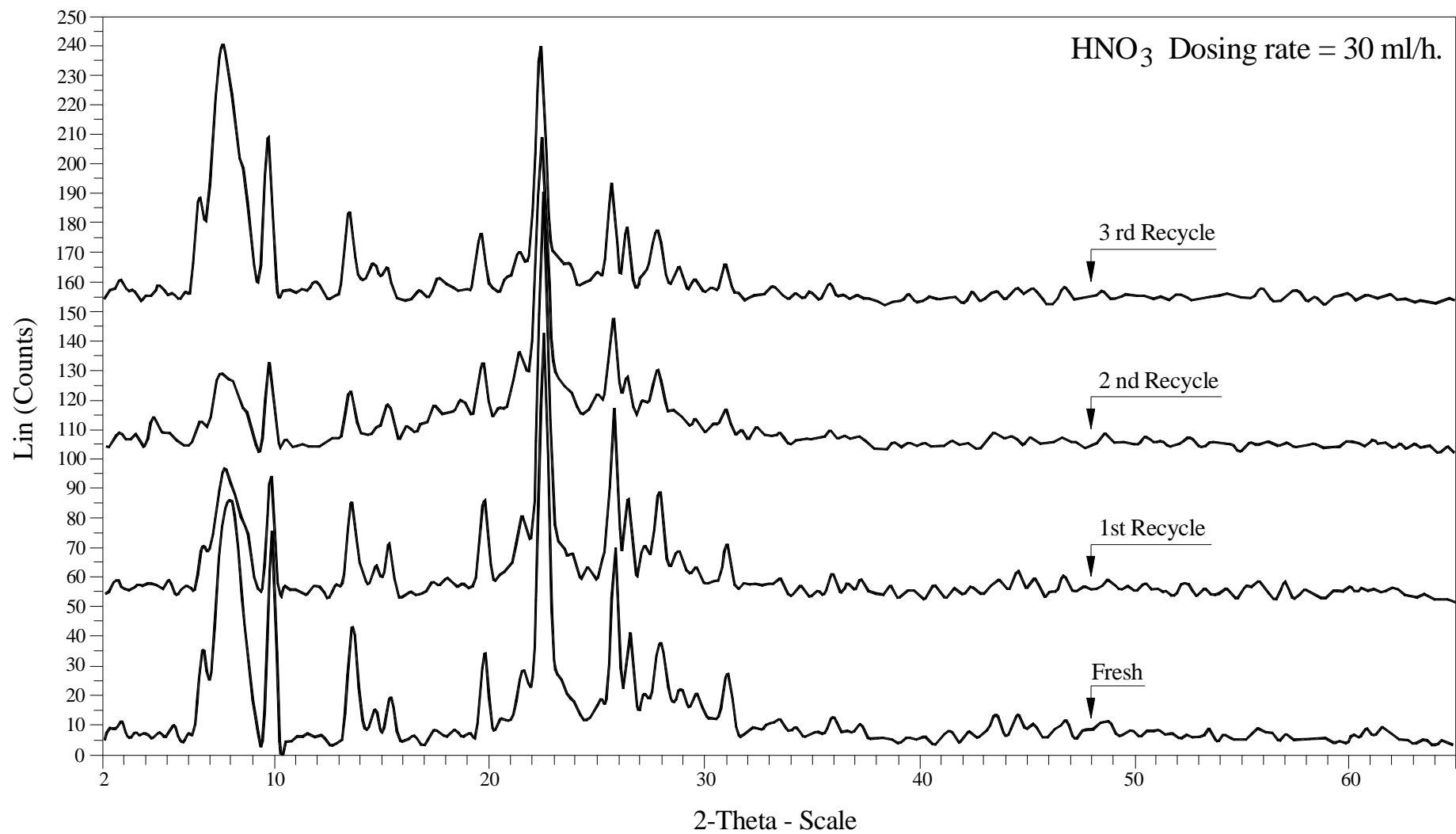


Fig. 4.10. XRD patterns of H-Beta catalyst in semi-batch nitration with nitric acid dosing rate 30 ml/h upto 3 cycles.

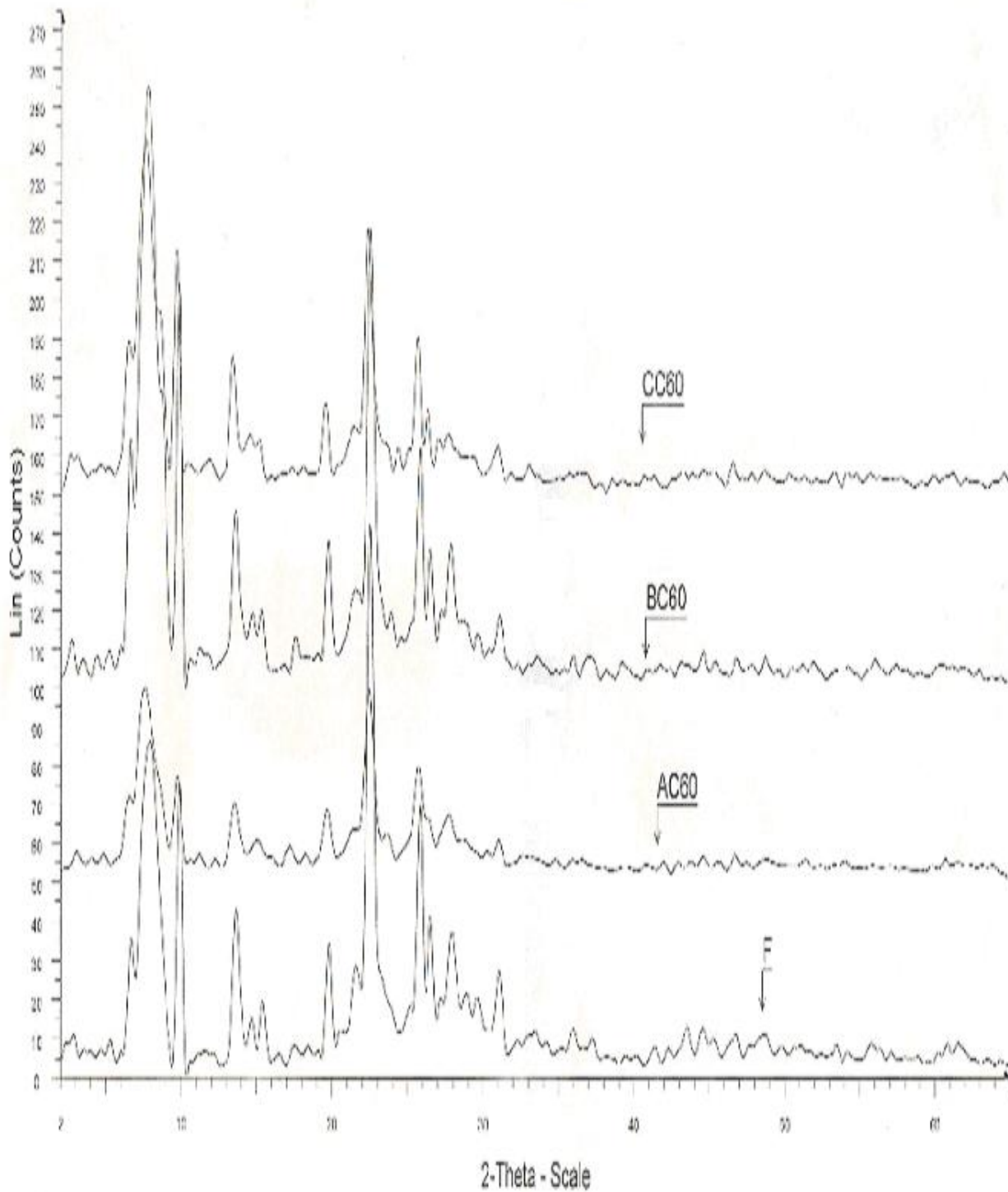


Fig. 4.11. XRD patterns of H-Beta catalyst in semi-batch nitration with nitric acid dosing rate 60 ml/h upto 3 recycles; F, fresh catalyst; AC60, after 1st recycle at an acid dosing rate 60 ml/h; BC60, after 2nd recycle at acid dosing rate 60 ml/h; CC60, after 3rd recycle at acid dosing rate 60 ml/h.

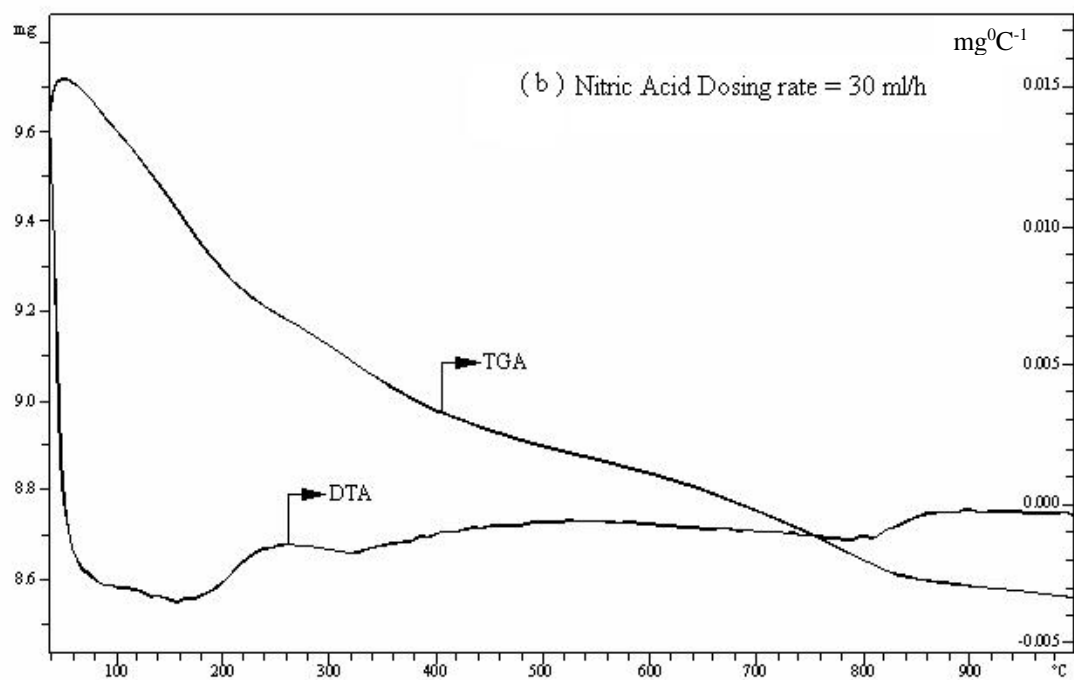
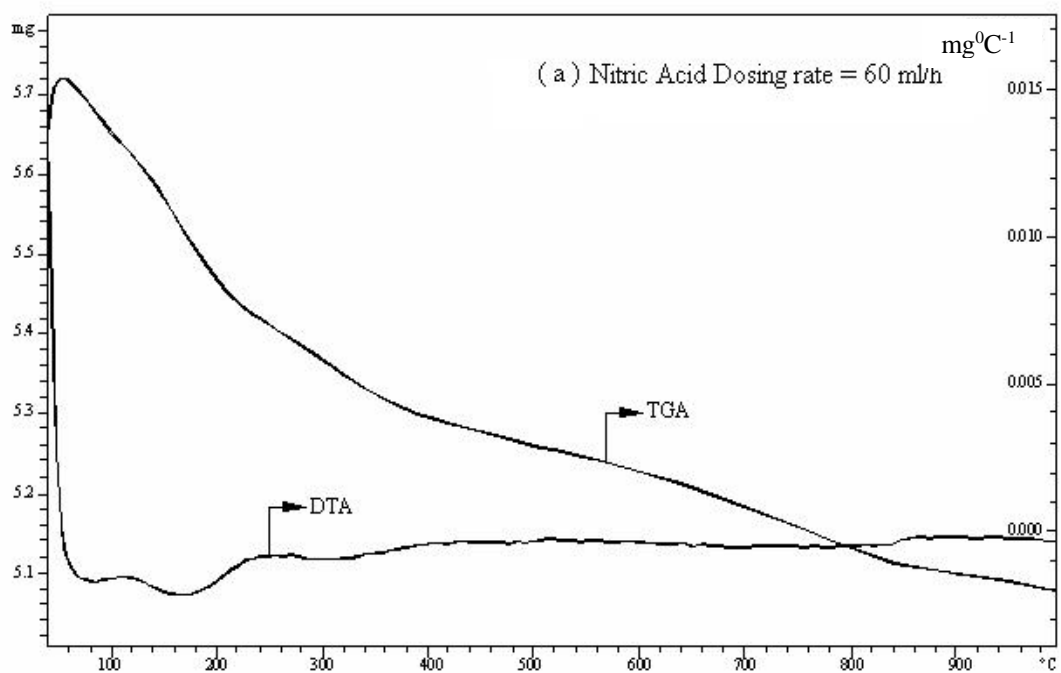


Fig. 4.12 TGA analysis after 3 cycles of semi-batch nitration at acid dosing rate of (a) 60 ml/h. and (b) 30 ml/h.

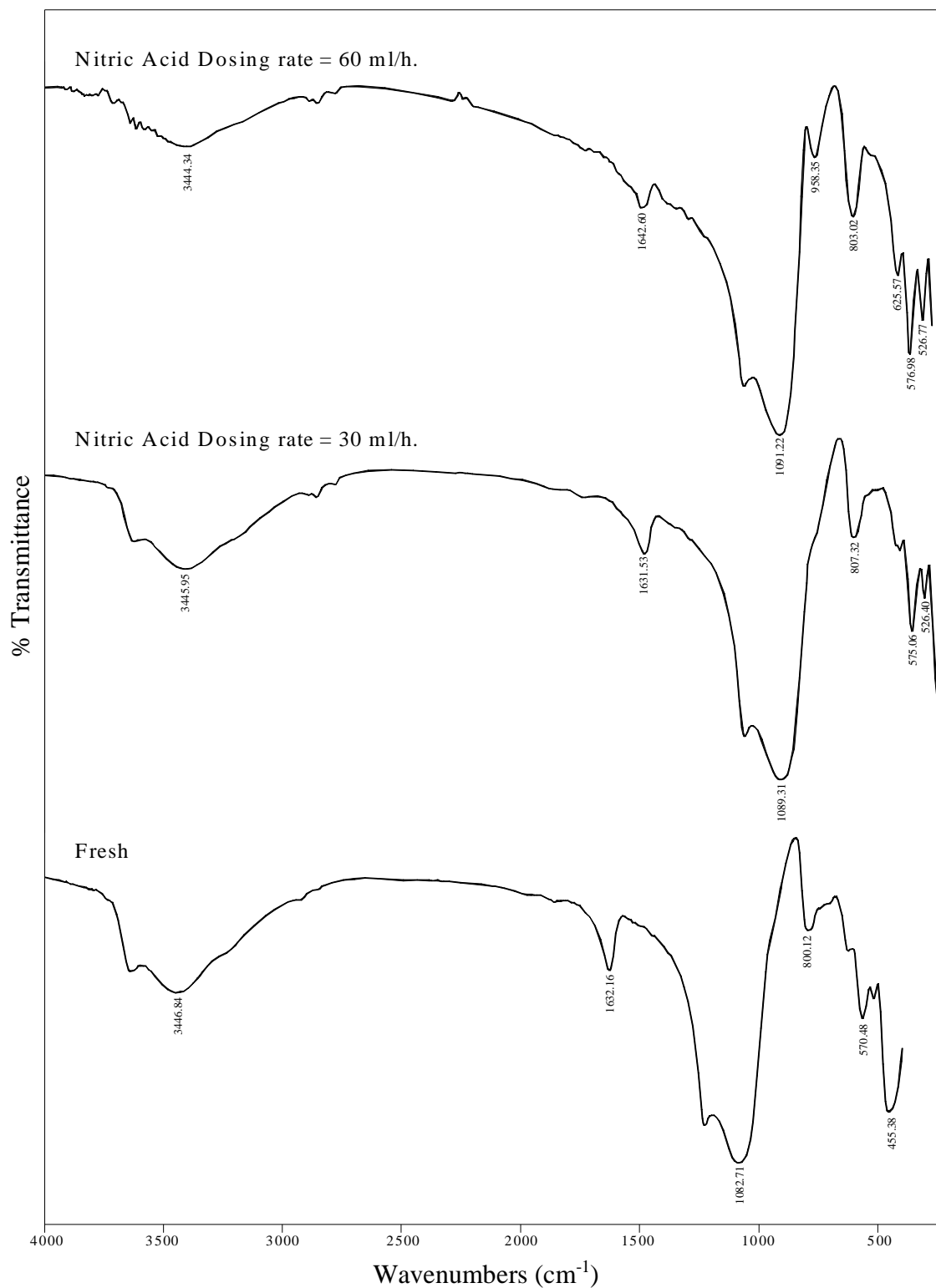


Fig. 4.13. FTIR plot after 3 cycles of semi-batch nitration with nitric acid dosing rate of 30 and 60 ml/h.

4.3 DEALUMINATION OF CATALYST

Dealumination of aluminosilicate catalysts has been reported in literature. The extent of dealumination depends on the aluminium content of the precursor and the free acid concentration of reaction environment. A sufficiently high acid concentration can effectively remove non structural Al species. Bertia et al. [57] studied the dealumination of mordenite on leaching with 1N HCl. They found that the extent of dealumination increases with acid concentration. They also established that the higher the alumina content in the mordenite sample, more of it can be removed by thermal and acid treatments at a suitable temperature. Sufficiently high acid concentration can remove the non structural Al species which are formed during thermal treatment.

The dealumination phenomenon in aromatic nitration in the presence of zeolite catalysts has not received much attention. In the present work, an attempt is, therefore, made to study this phenomenon at low and high toluene volume fractions with the objective of assessing the catalyst performance under these conditions. Both batch and semi-batch modes of operation have been employed.

4.3.1 Effect of HNO₃ Concentration

Though high conversions of toluene could be achieved in laboratory nitration at its low volume fractions, the stability of the catalyst need to be investigated since nitric acid, in high concentrations, has been reported to remove extra framework aluminium species from the zeolite catalysts.

Due to practical difficulty in handling toluene nitration under very high HNO₃ concentration, the catalyst performance is evaluated at two volume fractions viz., 0.42 and 0.9. It is interesting to note from Table 4.4 that H-Beta catalyst employed in this work, has undergone very significant level of dealumination and loss of structural strength within 4 h of reaction at lower toluene volume fraction of 0.42. On the other hand, no appreciable dealumination has been noted at higher toluene volume fraction of 0.9. In order to establish the effect of catalyst dealumination on *para*-selectivity, semi-batch nitration is carried out in a laboratory reactor employing a nitric acid dosing rate of 30 ml/h for a specific duration maintaining toluene

volume fraction at 0.42 and other conditions as specified in Table 4.4. The dealuminated catalyst is regenerated and recycled two times and in each cycle, toluene conversion and selectivity are measured. It is found that the *para* selectivity has dropped by 25% in first recycle and by 40% in second recycle. These results show that toluene dispersed in nitric acid does not provide a viable option. On the other hand nitric acid dispersed in toluene as the continuous phase is more preferred for achieving consistent catalyst activity for toluene nitration. Toluene nitration in semi-batch mode has also been conducted at two different acid dosing rates of 30 and 60 ml/h upto three cycles at a toluene volume fraction of 0.42. The elemental analysis of catalyst has been conducted at the end of each cycle and the results are shown in Tables 4.5. It shows the level of dealumination experienced by the catalyst on its recycle. The deterioration is faster at higher HNO₃ dosing rates.

Table 4.4 Dealumination of catalyst

Element	Fresh catalyst	Toluene volume fraction ($V_T=0.9$)	Toluene volume fraction ($V_T=0.42$)
O	61.43	64.14	62.13
Al	2.86	2.80	1.15
Si	35.72	33.06	36.72
Total	100.00	100.00	100.00

Semi-Batch experiments under reflux; toluene = 1.2 moles; nitric acid dosing rate= 30 ml/h, temperature= 120°C; catalyst (H -Beta zeolite S/A, 22) = 10 g.

Table 4.5 Effect of catalyst recycle on dealumination at lower toluene volume fractions (0.42)

Element %	Freshly prepared catalyst	1 st Cycle 30ml/h	1 st Cycle 60ml/h	2 nd cycle 30ml/h	2 nd Cycle 60ml/h	3 rd Cycle 30ml/h	3 rd Cycle 60ml/h
O	69.9	61.5	66.1	64.1	68.42	65.09	76.5
Al	2.4	1.8	0.84	1.51	0.72	1.27	0.6
Si	27.8	36.8	33.0	34.42	30.86	33.64	22.8

Semi-Batch experiments under reflux; toluene = 1.2 moles; nitric acid dosing rate= 30 ml/h and 60 ml/h, temperature= 120°C; catalyst (H -Beta zeolite S/A, 22) = 10 g.

Dealumination phenomenon has also been studied in a batch nitrator and the results corroborate the above findings.

4.3.2 Effect of Prolonged Exposure

Batch nitration studies have been conducted under prolonged exposure (24 h) at 0.42 and 0.9 volume fractions of toluene. The results are presented in Table 4.6. They clearly show the drastic effect of prolonged exposure on H-Beta catalyst at a toluene volume fraction of 0.42 and somewhat moderate effect on it at a toluene volume fraction of 0.9. In the case of latter, there is a need to restrict long exposure of catalyst to reaction mixture. A low residence time continuous process nitration is best suited for achieving high conversion and selectivity.

Table 4.6 Effect of exposure time on dealumination

Element %	Fresh	Toluene volume fraction	
		0.9	0.42
O	69.9	59.51	62.44
Al	2.4	1.38	0.00
Si	27.8	39.1	37.56

Batch experiments under reflux, temperature = 120°C;
catalyst (H -Beta zeolite S/A, 22)=10g; duration 24 h.

4.4 LATTICE ALUMINIUM TRANSFORMATIONS IN H-BETA CATALYST

Haouas et al. [122] found that the transformation of lattice aluminium from tetrahedral to octahedral configuration is mainly responsible for heightening *para* selectivity in toluene nitration. By employing semi-batch mode of nitration in the present study, we are able to confirm this phenomenon by MAS-NMR studies. The details are given in Fig. 4.14.

An attempt has also been made in the present work to check the level of lattice aluminium transformation occurrence when regenerated and recycled catalyst has been employed for nitration. Once, twice and thrice recycled catalysts have been used in semi-batch nitration at a HNO₃ dosing rate of 30 ml/h and the ²⁷Al MAS-NMR spectra of the catalyst samples have been taken after each cycle and the results are presented in Fig. 4.15. They show that the

lattice aluminium transformation continues to occur in recycled catalyst to maintain high *para*-selectivity.

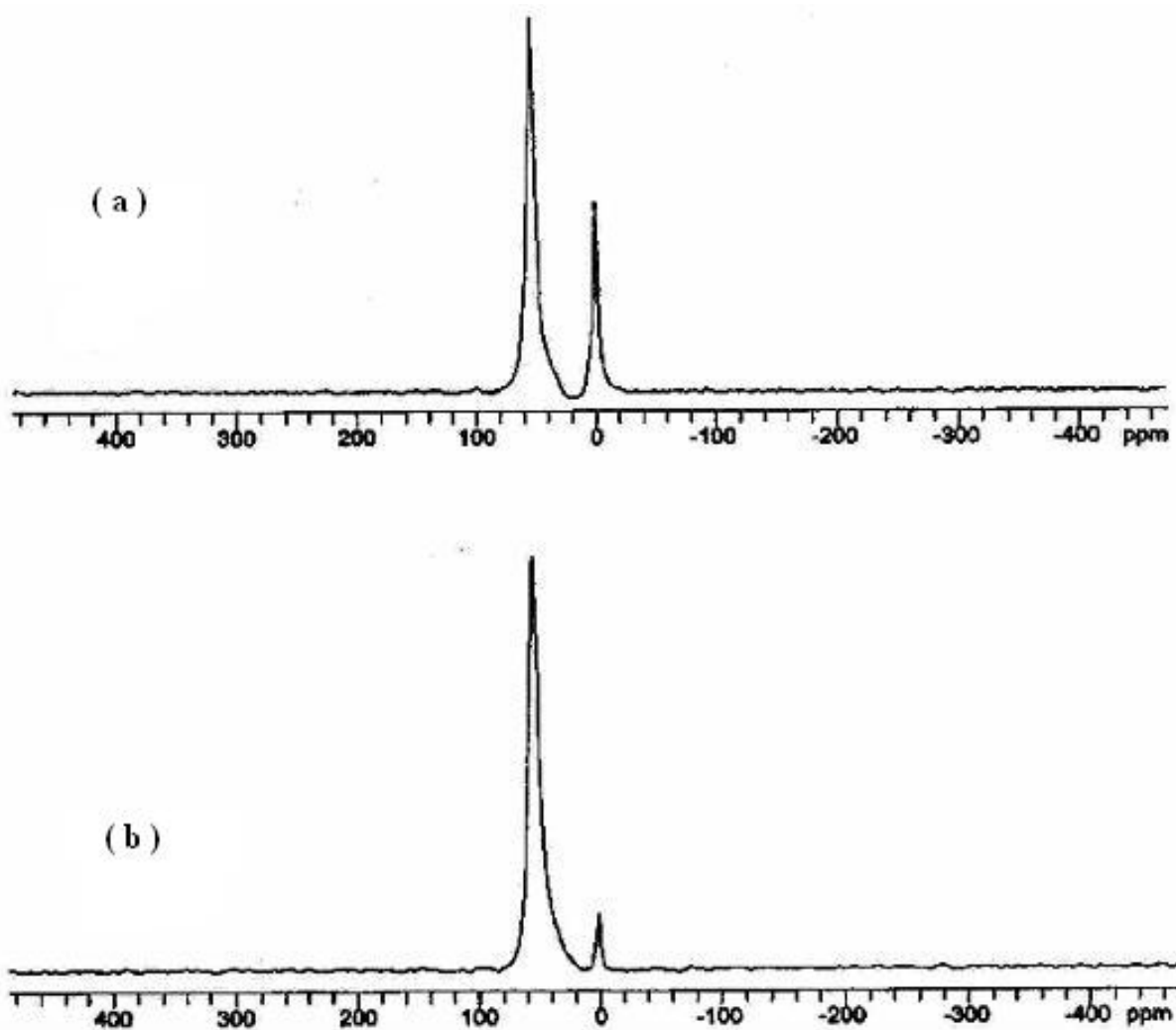


Fig. 4.14 Solid state ^{27}Al MAS-NMR spectra of zeolite H-Beta (a) after semi-batch nitration at 30 ml/h HNO_3 dosing rate for 3h. (b) freshly prepared zeolite.

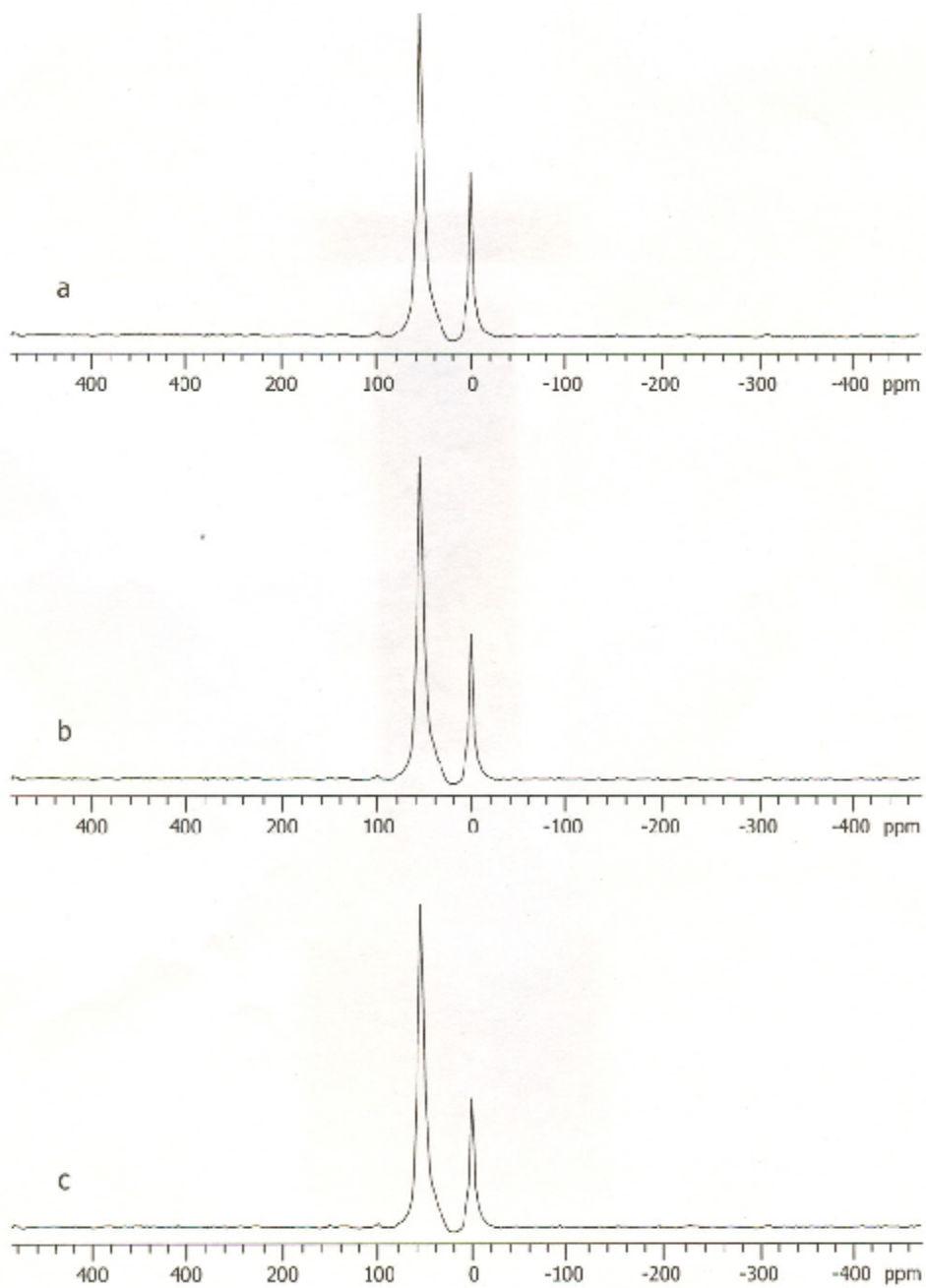


Fig. 4.15 Solid state ^{27}Al MAS-NMR spectra of recycled zeolite H-Beta catalyst in semi-batch nitration at 30 ml/h HNO_3 dosing rate for 3 h ; (a) after 1st cycle (b) after 2nd cycle and (c) after 3rd cycle.

PROCESS STUDIES

With an initial focus on material accountability in batch and semi-batch toluene nitration, this chapter deals with the intricacies of multiprocess parameter rationalization to achieve heightened *para*-selectivity and attractive conversions levels in solid acid catalyzed toluene nitration. The effects of HNO₃-toluene dispersion morphology and mechanical agitation on the nitration process received primary attention.

The water formed during nitration has been reported to have mediating effect on catalyst acidity. We focused our attention to optimize the boil-up rate for the nitrator to minimize its inhibiting effect on the catalyst. The effect of critical process viz., toluene-nitric acid molar ratio, temperature and acid concentration on toluene conversion and *para*-selectivity received adequate attention.

The highlight of this chapter is our successful efforts to heighten the *para*-selectivity in toluene nitration through a two step standardization process which takes advantage of the shape selectivity of H-Beta catalyst and also the acidity level of microenvironment in and around the catalyst particles

5.1 MATERIAL AND ENERGY BALANCES

Sulfuric acid free nitration of toluene in the presence of zeolite catalyst (H-beta, S/A = 22) has been conducted in batch and semi-batch modes under reflux conditions with azeotropic water removal. Material and energy balances have been evaluated and the results are presented in this section.

5.1.1 Material Balances in a Typical Batch Nitration of Toluene

Catalytic nitration of toluene in batch mode has been conducted under reflux conditions with azeotropic removal of water. Fig. 5.1 provides the overall and component wise material balance for toluene nitration and the overall material accountability. The water generated during the reaction and the quantum of HNO₃ consumed match well with nitrotoluene formed and the effectiveness of reflux and liquid – liquid separation system in removing all the water formed as a result of nitration.

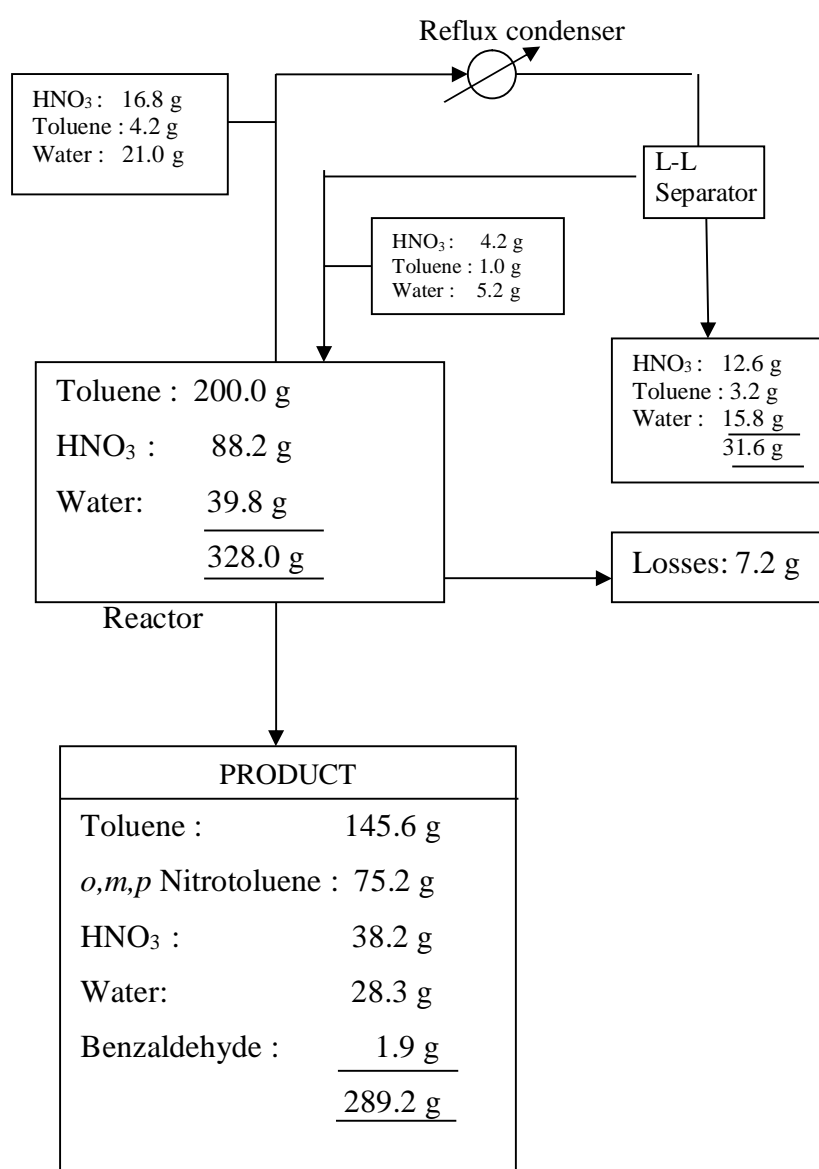


Fig. 5.1 Material balances in a typical batch nitration.

5.1.2 Material Balances in Semi-Batch Nitration of Toluene

Semi-Batch nitration of toluene at various nitric acid dosing rates of 15, 30 and 60 ml/h has been conducted under reflux conditions for various time durations with azeotropic water removal. The Table 5.1 given under shows the material balances for a typical semi-batch nitration at an acid dosing rate of 30 ml/h.

Table 5.1 Semi-Batch nitration at an acid dosing rate of 30 ml/h

Dosing rate (ml/h)	Duration (h)	Feed In	In the Reactor	Aq Phase Out
30	1	Toluene-200g	Toluene-158g	Nitric acid-10.3g
		Nitric acid-29.4g	Nitrotoluene-34.6g	Water-15.0g
		Water-12.6g	Nitric acid-3.2g	Toluene-16.2g
			Water-1.6g	Losses-2.5g
			Benzaldehyde-0.6g	
		Total	242.0 g	198.0 g
30	2	Toluene-200g	Toluene-127.7g	Nitric acid-20.2g
		Nitric acid-58.8g	Nitrotoluene-69.5g	Water-30.8g
		Water-25.2g	Nitric acid-5.6g	Toluene-23.2g
			Water-2.5g	Losses-3.5g
			Benzaldehyde-1.0g	
		Total	284.0 g	206.3 g

Toluene= 2.2 moles; catalyst (H Beta S/A, 22) = 10 g; agitation speed = 200 rpm; temperature= 130 °C

5.1.3 Energy Balance for a Typical Toluene Nitration in Batch mode

Catalytic nitration of toluene conducted in batch mode under reflux conditions with azeotropic removal of water. Fig. 5.2 gives the energy balance for a typical batch nitration.

Table 5.2 Thermodynamic properties of reactants and products

Chemical	Std Heat of formation (kJ/mol)	Std Gibbs free energy of formation (kJ/mol)	Standard entropy (J/mol.K)	Specific heat at constant pressure (J/mol.K)
Toluene (L)	12.4	113.82	219.4	157.3
Nitric Acid (L)	-174.1	-80.7	155.6	109.9
Orthonitrotoluene	-9.7	168.0	387.0	172.3
Metanitrotoluene	--31.5	143.0	387.0	172.3
Paranitrotoluene	-48.1	155.0	381.0	172.3
Water	-285.8	-237.1	70.0	75.3

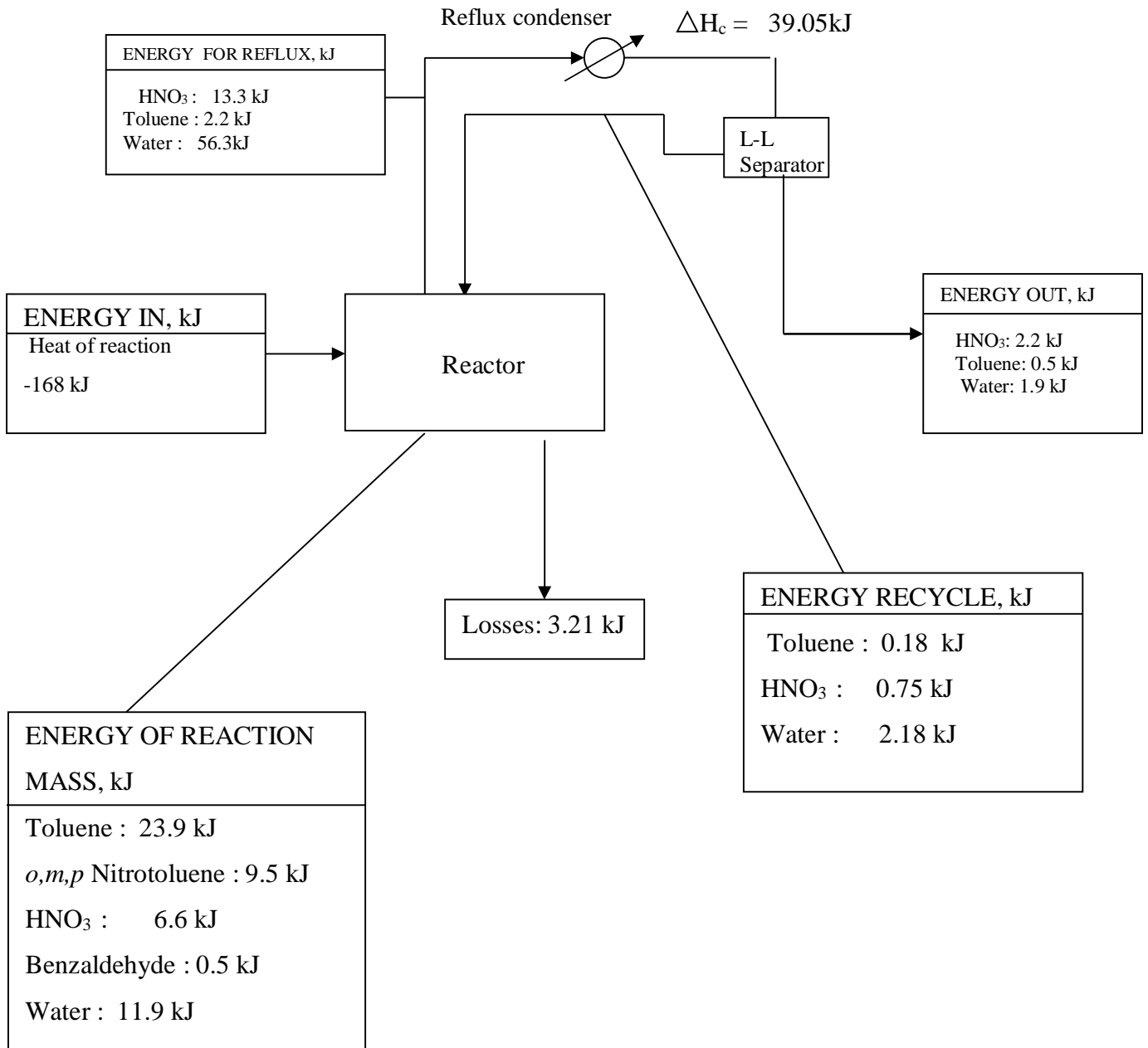


Fig. 5.2 Energy balance for a typical batch nitration.

5.1.4 Evaluation of Thermal Data through Reaction Calorimetry

Intrinsic nature of nitration reaction could be established from the heat generated vs time profiles in a reaction calorimeter. At the time of dosing of nitric acid, a steep heat signal was observed for a very short duration. This is clearly indicative of the exothermic nature of the reaction. The total heat evolved during the reaction is accurately measured by the reaction calorimeter and the heat of reaction determined experimentally is found to be in good agreement with the reported value. Employing the calibration heater that supplies heat at a given rate to the reaction mass and by measuring the resulting temperature difference between the reaction mass and the reactor jacket, the overall heat transfer coefficient (U) and the heat exchange area (A) could be determined. Specific heat of the reaction mass could be determined by using a temperature ramp i.e heating the system to the desired temperature in a given time interval and the heat generation data.

Adiabatic temperature rise (ΔT_{ad}) during the isothermal reaction could be determined from the reaction enthalpy data using the equation

$$\Delta T_{ad} = \frac{\Delta H_r}{m_r C_{pr}} \quad (5.1)$$

- It indicates the safety level of a reaction and should not be too large. If the reaction mass reaches into a temperature range in which it becomes unstable and can decompose in an exothermic fashion, it causes further increase in T_r . The values estimated using the reaction calorimeter are given below.

Table 5.3 Estimation of thermal data

U (W/m ² K)	A (m ²)	C_p (J/kg.K)	ΔH_{rxn} (kJ/mol)	ΔT_{ad} (K)
180	0.021	1960	125	16

5.2 MIXING AND DISPERSION EFFECTS ON TOLUENE NITRATION

5.2.1 Morphology of HNO₃-Toluene Dispersions

HNO₃ – toluene system can have two types of dispersions viz., organic in acid which consists of dispersed toluene in continuous HNO₃ phase or acid in organic containing the acid as dispersed phase. Either type may be formed depending on system parameters viz., phase volume ratio and energy input. Phase inversion occurs in such systems whereby an interchange occurs between the acid and organic phases. The point at which phase inversion occurs in this system corresponds to the hold up of the dispersed phase at which transition occurs after an infinitesimal change is made to the properties of the system. Dispersion characteristics and phase inversion phenomenon provides interesting process optimization options for toluene nitration. Zaldivar et al. [126] studied the phase inversion phenomenon and its influence on interfacial area, heat and mass transfer and other parameters associated with non reactive mixtures of water–toluene. They found that interfacial area increases if the continuous phase changes to aqueous with the accompanying change in density of both phases. Focussing our attention on HNO₃ – toluene dispersion in an agitated vessel, an attempt has been made in this chapter to delineate the three dispersion regimes and study the reaction under these regimes. It is surprising that the effect of HNO₃ – toluene dispersion morphology and phase inversion on conversions and para selectivity of toluene nitration has not received much attention except for the investigations reported by Zaldivar et al. [127] for semi-batch aromatic nitrations with mixed acids.

5.2.2 Delineation of Dispersion Regimes

Quinn and Singloh [128] and Selker and Sleicher [129] found liquid properties, geometry of impeller and reaction vessel, speed of agitation and mode of initiation of dispersion as important factors for achieving stable liquid-liquid dispersions. The latter reported the existence of an ambivalent region in which either component can remain stably dispersed. Kumar [130] proposed a validated model to address the coalescence phenomenon in liquid-liquid dispersions. Norato et al. [131] studied the role of physical and operating parameters

on the phase inversion. In a recent study, Leslie et al. [132] reported a simple tool based on interfacial energy minimization for predicting the limits of ambivalent region of phase inversion process. In the present work, an attempt has been made to study the role of morphology of toluene-nitric acid dispersions on conversion and *para*-selectivity in liquid phase nitration. Selkhar and Sleicher [129] correlated the limits of ambivalence as a function of the ratio of kinematic viscosities of the two phases. The limits of ambivalence for our system have been accordingly estimated and three regimes viz., toluene dispersed in nitric acid, ambivalent and nitric acid dispersed in toluene have been delineated. Fig. 5.3. provides the details.

5.2.3. Phase Inversion in HNO₃-Toluene Dispersions

The ambivalent region is notable for the occurrence of phase inversion(s) since the nature of dispersion in this region mainly depends on history [129]. It has been reported that phase inversion is accompanied by a decrease or increase in the interfacial area and a step change in the dispersion viscosity. The effect of phase inversion on semi-batch aromatic nitrations was studied by Zaldivar et al. [126] with reference to interfacial area, effective heat transfer coefficients and conversion of aromatic compound. Their studies indicated that interfacial area increased on inversion from organic / aqueous to the aqueous / organic configuration and decreased on inversion in the opposite direction.

Employing the correlations reported by the Zaldivar et al. [126], the phase inversion characteristics of HNO₃-Toluene dispersions have been calculated in the present work. Table 5.4a shows the occurrence of phase inversion at a toluene volume fraction of 0.53 at which point a step increase in Weber number, a drop in droplet diameter and a step increase in interfacial area are observed when HNO₃ is added to the toluene (continuous phase). Table 5.4b shows the reverse trend when toluene is added to HNO₃ as continuous phase. Our calculations show that phase inversion occurs almost at the same point as in earlier case.

Table 5.4a Sauter mean diameters and interfacial areas at various volume fractions of organic phase (Starting from organic phase as continuous phase)

S.No	V_A	Continuous phase	Dispersed phase	ϵ_d	We	d_{32} (mm)	A (m^2/m^3)
1	0.0	organic	Aqueous	0.0	112	1.42	0
2	0.2	organic	Aqueous	0.2	112	2.54	472
3	0.4	organic	Aqueous	0.4	112	3.41	704
4	0.53*	aqueous	Organic	0.47*	182	2.80	1007
5	0.6	aqueous	Organic	0.4	182	2.54	945
6	0.8	aqueous	Organic	0.2	182	1.90	632
7	1.0	aqueous	Organic	0.0	182	1.10	0

*phase inversion point; V_A is volume fraction of aqueous phase; ϵ_d is volume fraction of dispersed phase; d_{32} is sauter mean diameter; a is interfacial area

Table 5.4b Sauter mean diameters and interfacial areas at various volume fractions of organic phase (Starting from aqueous phase as continuous phase)

S.No	V_d	Continuous phase	Dispersed phase	ϵ_d	We	d_{32} (mm)	a (m^2/m^3)
1	0.0	aqueous	Organic	0.0	182	1.06	0.0
2	0.2	aqueous	Organic	0.2	182	1.89	635
3	0.4	aqueous	Organic	0.4	182	2.54	945
4	0.55*	organic	aqueous	0.45*	112	3.65	740
5	0.6	organic	aqueous	0.4	112	3.35	716
6	0.8	organic	aqueous	0.2	112	2.50	480
7	1.0	organic	aqueous	0.0	112	1.42	0.0

*phase inversion point; V_d is volume fraction of organic phase; ϵ_d is volume fraction of dispersed phase; d_{32} is sauter mean diameter; a is the interfacial area

5.2.4 Effect of Toluene-HNO₃ Dispersion Morphology on Nitration

It is of interest to note the findings of Zaldivar et al. [126] on the effect of phase inversion on semibatch nitration of benzene, toluene and chlorobenzene employing mixed acids. When the initial continuous phase consists of organic compound, phase inversion increases the reaction rate suddenly when the acid becomes the continuous phase. An increase in interfacial area was also recorded. They also found the possible existence of multiple inversion points.

In the present work, the effect of toluene - nitric acid dispersion morphology on solid acid catalyzed toluene nitration in terms of its conversion and para selectivity has been studied. Batch nitration experiments have been conducted under reflux conditions covering a wide range of toluene volume fractions (0.1 to 0.95) to generate the conversion and *para*-selectivity data covering all the three regions. Details are presented in Fig. 5.3.

The following observations can be made:

- Conversion of limiting reactant exceeds 80% in case of toluene dispersed in nitric acid ('a' region; toluene volume fraction < 0.3).
- The conversion of the limiting reactant dropped to a minimum value (35%) and increased again in ambivalent region ('c' region). Our calculations presented in Chapter 2 have shown that phase inversion occurs at a toluene volume fraction of 0.53 and this behavior looks justified.
- A maximum of 60% conversion of limiting reactant is achieved when nitric acid is dispersed in toluene ('b' region; toluene volume fraction > 0.7).
- The morphology of toluene–nitric acid dispersions has very marginal effect on *para*-selectivity, which remained in the range of 0.7 to 0.8.

Interestingly, Hanson and Ismail [133] found that mass transfer resistances are more important at high sulfuric acid concentrations whereas the conversion at low sulfuric acid concentrations is kinetically controlled in conventional two-phase nitration processes.

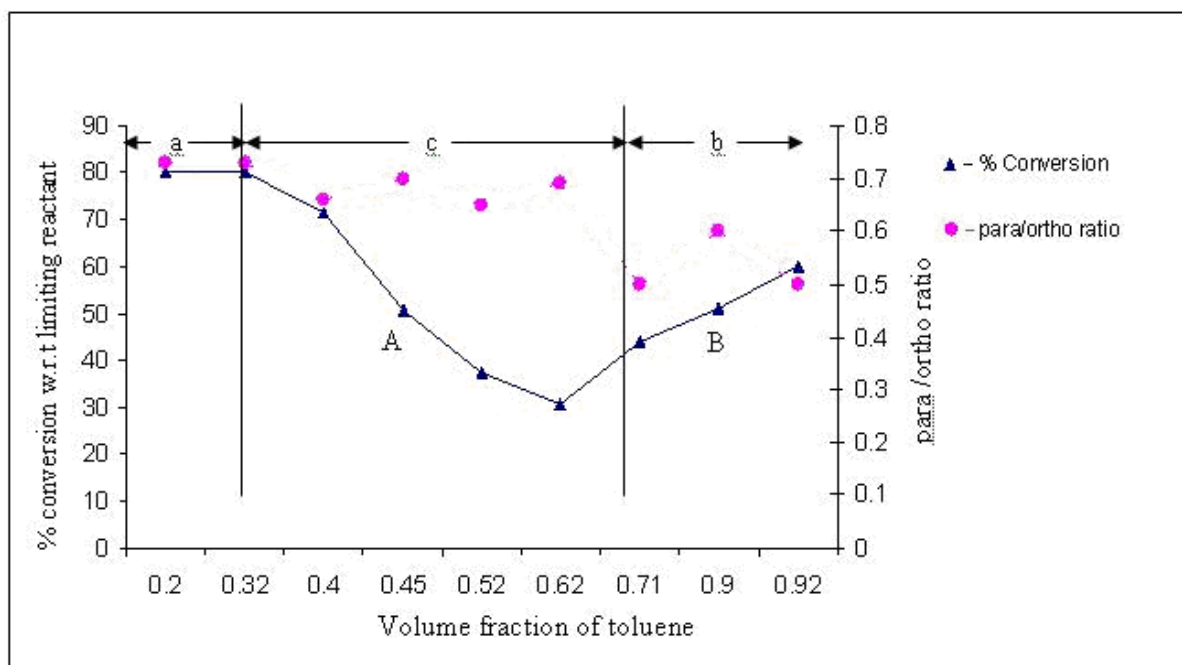


Fig. 5.3. Effect of Dispersion morphology on conversion and selectivity. Batch experiments with azeotropic water removal; catalyst (H-Beta S/A, 22) = 10 g; temperature= 120 °C; agitation speed= 200 rpm; a: toluene dispersed in nitric acid; b: nitric acid dispersed in toluene; c: ambivalent region

5.2.5 Agitation Effects

Apart from promoting a good contact between the phases for enhanced mass transfer rate, the agitation has stabilization effect on liquid-liquid-solid dispersions. Inversion hold-up of intensely agitated liquid-liquid systems was studied by Deshpande and Kumar [134]. In the present work, the agitation effect was studied separately in (a) toluene dispersed in nitric acid and (b) nitric acid dispersed in toluene as the continuous phase. Experiments have been conducted in batch mode with finely powdered catalyst and water removal under reflux conditions at four different stirrer speeds (Table 5.5). While the radial and longitudinal velocity components created by the agitation have been reported to make positive contribution to the mixing action, the tangential component contributes to the vortex

formation, which tends to outwardly throw the catalyst particles by centrifugal action contributing to their concentration rather than distribution. The tip velocity ‘u’ and impeller Reynolds number ‘ N_{ReI} ’ and Weber numbers (We_I) have been evaluated at four agitation speeds employing Olney-Carlson methodology [91] and are presented in Table 5.5. The vortex depths at various agitation speeds have been calculated employing the correlations proposed by Rieger et al. [135] for mixed unbaffled vessels. It has been found that there is a steep increase in the vortex formation at rpm > 200. The influence of agitation speed on conversions can now be explained more effectively in (a) and (b) dispersions. The intensity of agitation has no influence on conversion of limiting reactant as well as on *para*-selectivity in dispersion ‘a’. However, in dispersion ‘b’, agitation speed, vortex depth and turbulence have significant effect on conversion of limiting reactant. The best limiting reactant conversion is obtained at a stirrer speed of 200 rpm for the given geometric configuration of vessel and propeller agitator employed in this work. Impeller Reynolds number beyond 20,000 and vortex depth beyond 2 cm have negative influence on conversion of limiting reactant.

Table 5.5 Contrasting effects of agitation speed on nitric acid –toluene dispersions

N (rpm)	u (m/s)	Vortex depth (cm)		$N_{Re,I}$		We_I		% Conv of limiting reactant		Para/ Ortho ratio	
		a	b	a	b	a	b	A	b	a	b
100	0.39	0.52	0.55	9,380	11,270	46	28	85.00	21.4	0.65	0.63
200	0.78	2.06	2.15	18,750	22,540	182	112	85.00	47.2	0.65	0.50
400	1.58	7.80	8.00	37,500	45,080	730	450	85.00	38.5	0.62	0.68
600	2.37	17.00	17.40	56,250	67,620	1640	1010	85.00	24.1	0.67	0.68

a: Toluene : nitric acid (molar ratio)= 0.85 : 3.66; catalyst (zeolite H-Beta S/A, 30) = 10 g; temperature under reflux= 120 °C, limiting reactant: toluene
 b: Toluene : nitric acid (molar ratio)= 2.2: 1.4; catalyst (zeolite H -Beta S/A, 30) = 10 g; temperature under reflux= 120°C; limiting reactant: nitric acid; batch Experiments with azeotropic water removal.

5.3 EFFECT OF CRITICAL PROCESS PARAMETERS

There are several parameters which need to be optimized for achieving high conversions and high *para*-selectivity in toluene nitration. An attempt has been made in this section to address the subject of their effect on nitration process.

5.3.1 Effect of Toluene-Nitric Acid Molar Ratio

Batch experiments are carried out (Table 5.6) under reflux employing nine different ratios of toluene to nitric acid. It is found that a nitric acid to toluene ratio of 1: 3.5 gave maximum conversion and *para* selectivity. A similar trend has been reported by Diego Vassena et al. [72] who achieved yields higher than 75% of mono nitrotoluene at a nitric acid to toluene molar ratio of 2 as compared to 1 for solid acid catalyzed vapor phase nitration of toluene

Table 5.6 Effect of toluene to nitric acid molar ratio on product distribution

Toluene:Nitric Acid (mol:mol)	V_T	X	ONT	MNT	PNT	Others	Para/Ortho ratio
1:6.5	0.2	80.3	53.5	5.1	38.9	2.1	0.73
1:3.5	0.32	80.3	53.5	5.1	38.9	2.1	0.73
1:2.5	0.40	71.7	49.3	4.5	32.7	2.8	0.66
1:2.0	0.45	50.7	37.1	3.6	24.3	0.9	0.70
1:1.50	0.52	37.5	27.20	2.70	17.60	1.00	0.65
1:1	0.62	30.5	21.95	2.00	15.13	1.74	0.69
1:0.67	0.71	44.0	23.19	1.49	11.70	2.17	0.50
1:0.19	0.90	51.0	6.66	0.43	3.97	1.46	0.60
1:0.14	0.92	60.0	6.35	0.41	3.18	1.56	0.50

10g catalyst (zeolite H beta S/A=30), Agitation speed 200rpm, Temp under reflux=383K, X : percent conversion with respect to limiting reactant, V_T : volume fraction of toluene, Batch Experiment with azeotropic water removal for 3 hrs

5.3.2 Effect of Reaction Water Removal

Olah et al. [62] reported that nitration of alkyl benzenes in the presence of Nafion-H catalyst slows down with time due to H₂O molecule produced in the reaction. It dilutes nitric acid and

demands excess of the same. By refluxing the reaction mixture and azeotropically distilling off H₂O-aromatic mixture until no remaining HNO₃ could be detected. They obtained nitrotoluene yields upto 80% with a product distribution of *o*, *m*, *p* at 56, 4, 40. They found that H₂O molecules get strongly adsorbed on the catalyst acid sites leading to mediating effect on its acidity. The other secondary effect is the loss of HNO₃ on account of (a) ternary azeotrope formation with water and aromatic compound and (b) decomposition into nitrous gases at the reaction conditions. Both of these have to be minimized.

Continuous removal of water formed during the nitration from the acidic sites of the catalyst has been a challenge for sulfuric acid free nitration processes. The literature reports four alternatives for water removal viz., (a) vapor phase processing [72, 54], (b) chemical trapping, (c) inert gas passage and (d) azeotropic distillation [62]. The first three options have, so far, not found commercial viability whereas the azeotropic distillation has better chances of succeeding. In the present work, the effect of water on toluene nitration has been studied with and without reflux to study the boil-up rate effect on the product distribution.

5.3.3 Effect of Temperature

Batch nitrations have been conducted at a constant atmospheric pressure and three different temperatures including the reflux temperature (110 °C). It is observed (Table 5.7) that conversions are maximum at reflux temperature since the inhibiting effect of water on the catalyst activity is minimal due to its speedier removal.

Table 5.7. Temperature effect on product distribution

Temperature (°C)	%Tol Conversion	ONT	MNT	PNT	Others	Para / ortho ratio
45	11.4	6.12	0.80	4.00	0.48	0.65
65	14.9	7.91	1.22	4.66	1.10	0.59
Reflux (110)	38.5	23.19	1.49	11.70	2.17	0.50
-do-*	45.7	22.96	2.40	17.90	2.44	0.78

Toluene: nitric acid (molar ratio) = 2.2 : 1.4; catalyst (zeolite H-Beta S/A, 30)= 10 g; agitation speed= 200 rpm; time= 3 h; batch experiments with azeotropic water removal; catalyst (zeolite H-Beta S/A, 22).

5.3.4 Effect of Concentration of Nitric Acid

Experiments have also been conducted employing 19 mole % and 40 mole % nitric acid at 65°C maintaining the same nitric acid content in each case. There is practically no conversion in case of 19 mole % nitric acid whereas nearly 15% conversion has been achieved with 40 mole % nitric acid.

5.3.5 Effect of Boil-Up Rate

The boil-up rate effect on toluene conversion and selectivity has been studied under reflux conditions in semi-batch mode. The intensity of boil-up rate (BR) is measured in terms of the difference between the oil bath (t_b) and the reaction mixture (t_r) temperatures. The results are presented in Fig. 5.4. The nitric acid is dosed at 30ml/h for three hours employing 2.2 moles of toluene and 10 g of H-Beta catalyst (S/A, 30). The results show that at a boil-up rate as represented by $t_r - t_b = 20$, high toluene conversion is achievable. The drop in conversion at higher boil-up rates is due to the offset of water removal by greater loss of nitric acid. The effect of boil-up rate on *para*-selectivity is, however, minimal.

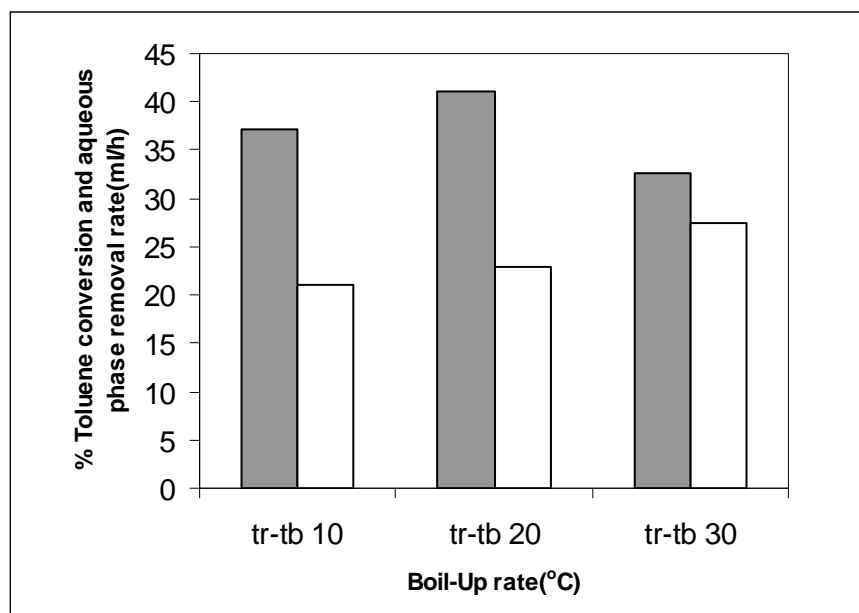


Figure 5.4 Effect of boil-up rate on % toluene conversion (■) and aqueous phase removal rate (□); Semi-Batch experiments with azeotropic water removal; catalyst (zeolite H-Beta S/A, 30) = 10 g; nitric acid dosing rate= 30 ml/h; dosing time= 3 h; toluene= 2.2 moles

5.4. A TWO PRONGED APPROACH TO HEIGHTEN PARASELECTIVITY

5.4.1 Reported Approaches

Until recently, the *ortho* isomer of nitrotoluene represented a commercially less valued product. Clearly, there was a need for more regioselective control of electrophilic aromatic substituents. Microporous solids such as aluminosilicates have been reported to offer a wide range of active sites for regioselective conversions. The geometric consequence of anchoring onto such solid systems is to restrict the angles of attack i.e., to enhance selectivity. Zeolites have also been reported to increase the shape selectivity through molecular sieving inside their pores having smooth inner walls with potential for high diffusivities.

The nitronium ion was believed to possess greater activity and selectivity and several researchers sought its incorporation in an ion pair having a highly stabilized anions like acetyl or benzoyl nitrates. Nagy et al. [136] compared the reactivities and isomer distribution of benzene, chlorobenzene, toluene and o-xylene nitration with mixed acids, benzoyl nitrate in the presence of aluminosilicates such as H-Y and H-ZSM-11 zeolites. Their results of benzene and toluene nitrations are summarized in Table 5.8. They show the pronounced para preference of substituted H-ZSM -11.

Table 5.8 Comparison of reactivities and isomer distribution using various nitrating agents and catalysts

S.No	Catalyst	Nitrating agent	Relative rates (II) and (I) and K_{II}/K_I	Isomer distribution		
				<i>o</i>	<i>m</i>	<i>p</i>
1	H ₂ SO ₄	HNO ₃	17	34.6	3.4	62.0
2	H ₂ SO ₄	Benzoyl nitrate	35.3	34.5	3.4	62.1
3	Aluminosilicate	--do--	7	55.0	1.0	44.0
4	Pentasil zeolite	HNO ₃	4	NA		
5	H-ZSM-11	Benzoyl nitrate	7	75.0	1.0	24.0
				98.0*	< 1.0	2.0
6	H-Y	--do--	11	64.0	1.0	25.0

*catalyst treated with NBCl₃; II: Toluene; I: Benzene

Laszlo and Vondorneal [64] had shown that dilution with highly polarizable solvents like carbon tetrachloride has a profound influence on regioselectivity. They found that these solvents stabilize the charged NO₂⁺ electrophile through electrostatic interaction which competes with the polarizable methyl group of toluene. The latter's own interaction with the electrophile tend to bring the substituent into the *ortho* position [137].

5.4.2 A Two Level Standardization Process for Heightening Para Selectivity

A two level standardization process has been adopted in the present work to heighten the para selectivity. Semi-Batch mode of reactor operation has been chosen to minimize side product formation and to keep the HNO₃ concentration at sufficiently low level. The first level standardization process has been designed to allow macro level process parameter adjustments to take advantage of the catalyst shape selectivity to the fullest extent. The second level standardization process attempts to tailor the acidic microenvironment in and around the catalyst particles to investigate the role of undefined or unexplored parameters other than the shape selectivity of catalyst.

5.4.2.1 Level I Standardization

Semi-Batch mode of nitration has been employed to assess the effect of HNO₃ dosing rate on conversion and *para*-selectivity (Table 5.9a). A dosing rate of 30 ml/h is found to provide the best selectivity at 40 % toluene conversion level. Experiments are then conducted in the presence and absence of the catalyst covering a toluene volume fraction in the range of 0.16 to 0.43. The results are presented in Table 5.9b. The *para* selectivity has been enhanced by 2.5 times when H-beta catalyst is employed for nitration. These results also show the possibility of significant level of non catalytic nitration occurring along with catalytic nitration under reflux conditions and the indicated isomer distribution may be net result of these two parallel processes.

Table 5.9a Effect of acid dosing rate

Dosing rate (ml/h)	Dosing time (h)	%Tol Conversion	ONT	MNT	PNT	Others	Para/Ortho ratio
15	6	70.7	43.60	1.83	24.13	1.18	0.55
30	2.5	41.1	19.60	0.84	19.31	1.32	0.99
70	1.3	18.6	9.09	0.53	8.14	0.84	0.90

2.2moles toluene,1.4moles nitric acid,10g catalyst(H-beta Si/Al=15);Agitation speed 200rpm,Temp under reflux =383K

*semi-batch experiment with 1.4 moles or 90 ml of 70% nitric acid is dosed at different rates

Table 5.9b Effect of catalyst on para selectivity in semi-batch nitration of toluene

Non Catalytic nitration							Catalytic nitration						
Dosing time, h	X_A (%)	X_B (%)	Para / Ortho	o	m	p	Dosing time, h	X_A	X_B	Para/Ortho	o	m	p
1.5 (0.16)	40*	12.7	0.59	16.4	1.22	9.7	1 (0.11)	59.8*	18.5	0.93	8.97	0.7	8.3
3.5 (0.31)	25.7*	19.3	0.64	20.1	2.0	13.0	2 (0.22)	41.1*	23.2	1.25	9.3	0.8	11.7
6.0 (0.43)	41.3**	32.2	0.60	33.0	3.4	21.9	4.5 (0.37)	27.7*	33.0	1.50	11.8	1.2	17.6

Nitric acid (40 mole %) dosed; figures in parantheses refer to toluene volume fraction; toluene= 235ml; *: limiting reactant: nitric acid; **: limiting reactant: toluene; X_A = % Conversion w.r.t nitric acid; X_B = % Conversion w.r.t toluene, acid dosing rate = 30 ml/h

5.4.2.2 *Level II Standardization*

An attempt has been made in these investigations, to explore the possibility of further heightening of para selectivity in H-beta catalyzed toluene nitration by changing the acidity (HNO_3) levels of microenvironment in and around catalyst particles to bring in transformation in their lattice aluminium. The multiphase reaction system with HNO_3 finely dispersed in the continuous phase of toluene provided the right backdrop for tailoring the microenvironment.

From mass transfer view point, solid acid catalyzed toluene nitration can be considered as liquid-liquid-solid system. Toluene provides the continuous phase for dispersion of HNO_3 . The reactants viz., diluted HNO_3 and toluene are part of aqueous and organic phases respectively. The catalyst being hydrophilic in nature, exhibits affinity for the aqueous phase. The reaction products are formed in toluene which is the continuous phase. During nitration, the acidity of aqueous phase varies as the reaction proceeds due to the formation of nitrotoluenes and water and depletion of nitric acid.

During nitration, toluene diffuses through the organic phase to the interphase and then into the aqueous phase. Finally the reaction mixture in aqueous phase enters the pores of the catalyst. The rate of reaction can be limited by the mass transfer processes between the phases which in turn will be governed by the distribution of phase fractions, partitioning of reactants and products and fluid dynamics of both liquid phases including the coalescence phenomenon. In view of catalyst hydrophilicity, catalyst particles are likely to be surrounded by aqueous phase which in turn is surrounded by organic phase. This situation provides a distinct microenvironment in and around the catalyst particles which may influence the process conversion and para selectivity.

As stated earlier, this is on the premise that there could be hidden or undefined parameters other than shape selectivity of the catalyst that could heighten *para*-selectivity. Viewed from this angle, the findings of Haouas et al. [122] on the transformation of flexible lattice aluminium configuration assumes high credibility.

5.4.2.3 Semi-Batch Experimentation

A semi-batch reactor presents lot of advantages for making above studies. The progressive addition of HNO₃ during the reaction enables to keep its concentration at a sufficient level to ensure good dispersion in toluene, the continuous phase. It will ensure its minimum accumulation which is governed by the competition between HNO₃ input and toluene conversion. In the present studies, maximum accumulation is reached at the instant when the stoicheometric amount of HNO₃ has been added. It may also be possible to detect phase inversion if it occurs during reaction.

Experiments have been carefully planned to vary HNO₃ concentration in dispersed aqueous phase from 55% to 85%. This could be achieved through the variation of HNO₃ dosing rate and the removal rate of water formed during the reaction. The details are presented in Table 5.9c. Three dosing rates have been employed. The dosing process is continued in each case for sufficient time to obtain a stabilized value of para selectivity.

Table 5.9c Effect of nitric acid dosing rate-time interactions

Acid dosing rate (ml/h)	Reaction Time (h)	X _A	X _B	ONT	MNT	PNT	Para-selectivity	% HNO ₃ in aq phase	H ₂ O removed/ H ₂ O formed g/g
15	1	57.0	9.0	5.3	0.2	3.0	0.57	63	1.88
	2	38.8	12.2	7.2	0.3	4.2	0.58	69	2.78
	2.5	33.4	14.6	8.3	0.4	5.1	0.61	69	2.78
30	1	59.8	18.5	8.97	0.7	8.3	0.93	74	2.44
	2	41.1	23.2	9.30	0.8	11.7	1.25	81.7	1.44
	4.5	27.7	33.0	11.8	1.2	17.6	1.50	84.6	5.88
	6	25.7	38.6	13.9	1.5	20.8	1.50	78.4	3.70
60	1	40.2	22.5	11.7	0.6	9.7	0.83	71.1	2.02
	2	37.9	40.7	20.1	1.8	17.7	0.88	55.5	3.85
	4.5	48.0	55.0	27.4	2.3	23.9	0.87	70.6	3.57

Toluene= 2.2 moles; catalyst (H Beta S/A, 22)= 10 g; agitation speed= 200 rpm; temperature= 130, X_A : % Conversion of HNO₃ X_B : % Conversion of toluene; acid dosing terminated at 6 h

The effect of time after HNO₃ dosing on its conversion and *para*-selectivity has been studied (Table 5.9d) in semi-batch toluene nitration under reflux conditions.

Table 5.9d Effect of time after dosing on *para*-selectivity

Acid doing rate (ml/h)	Time after dosing termination (h)	ONT	MNT	PNT	Others	para/ortho ratio
30	0	13.9	1.5	20.8	2.4	1.5
	2	12.5	1.5	25.6	3.2	2.0
	4	21.6	2.7	42.3	1.7	2.0

Toluene= 2.2 moles; catalyst (H-Beta S/A, 22) = 10 g; agitation speed = 200 rpm; temperature = 130 °C

The data presented in Table 5.8d show the need to provide at least 2 h time after dosing to complete the reaction and to achieve further heightening of *para*-selectivity.

The two level standardization as presented in this section has enabled the *para*-selectivity to be increased nearly four fold employing the same catalyst.

5.4.2.4 Solid State NMR Studies

The catalyst samples before and after the reaction are subjected to solid state NMR spectroscopy. The ²⁷Al MAS-NMR spectra of the parent H-beta zeolite showed two signals centred at 54.0 ppm (tetrahedrally coordinated aluminium) and 0.0 ppm (octahedrally coordinated aluminium). It is observed that the intensity of the signal corresponding to the octahedral aluminium has increased after the reaction indicating the transformation of framework aluminium from tetrahedral into octahedral configuration resulting in enhanced *para*-selectivity (Fig. 5.5).

To check the consistency of the phenomenon of transformation of flexible lattice aluminium from tetrahedral to octahedral configuration, the catalyst has been reused up to 3 cycles and the ^{27}Al MAS-NMR spectra of the catalyst is taken after each cycle. The catalyst after each recycle is filtered and washed thoroughly with water and acetone till the filtrate is neutralized. It is then dried in the oven at 100°C for 2-3 h to remove the moisture and then calcined at a temperature of 450°C for 6-8 h. It is evident from the data in Fig. 4.4 presented in section 4.4 of chapter 4, that there is consistency in transformation of aluminium framework from tetrahedral to octahedral configuration even after 3 cycles. This could be the cause of consistent *para* selectivity even after 3 cycles by zeolite H-beta catalyst.

An overall analysis of the above process leads to following conclusions:

- (i) Process optimization to achieve higher *para*-selectivity is closely linked to creating a favorable micro environment around the catalyst particle with focus on creating necessary acidity level to achieve lattice aluminium transformation.
- (ii) Nitration process has to be properly controlled through water removal to maintain high HNO_3 concentration (>85%) conducive for high *para*-selectivity
- (iii) The lower the non catalytic reaction, the better for achieving high *para*-selectivity

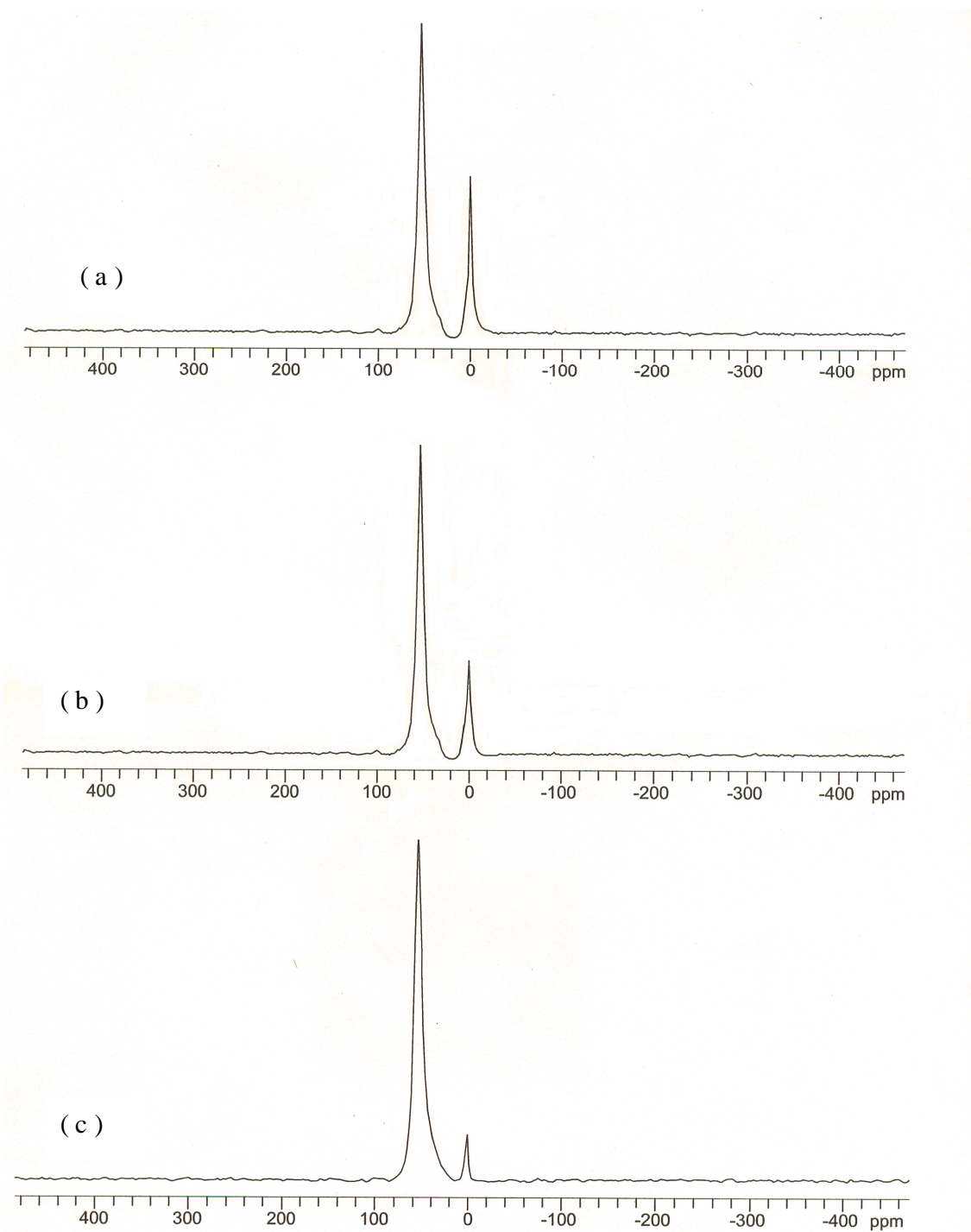


Fig. 5.5 Solid state ^{27}Al MAS-NMR spectra of zeolite H-beta (a) after semi-batch nitration at 30 ml/h HNO_3 dosing rate for 3h; (b) after semi-batch nitration at 60 ml/h HNO_3 dosing rate for 3h ; (c) fresh zeolite

5.5 BEST COMBINATION OF PROCESS PARAMETERS

Experiments have been conducted extensively in the present investigations in batch and semi-batch modes to standardize the process. The effect of various parameters like catalyst to toluene ratio, toluene to nitric acid ratio, dispersion morphology, agitation speed, temperature, boil-up rate, acid dosing rate, dosing rate-time interactions on conversion and para selectivity have been studied.

It has been observed that an agitation speed of around 200 rpm, catalyst to toluene ratio of about 4.5 g /mol, boil-up rate of nearly 20°C, reflux temperature, acid dosing rate of about 30 ml/h for about 8 h, dispersion morphology of nitric acid dispersed in toluene are favorable set of conditions to achieve higher conversions and para selectivity in the range of 1 to 2.

MASS TRANSFER AND KINETICS

Introduction

Multiphase processes involve very critical reaction engineering issues covering process chemistry complex governing kinetics and mass transport processes, mixture of fluid phases and dispersion morphology. In this chapter, kinetics and mass transport issues are dealt with. Solid acid catalyzed aromatic nitrations provide tremendous challenges in terms of evaluating kinetics and mass transfer rates. Basically they are two phase aqueous-organic systems in which catalyst particles are dispersed in organic phase. The hydrophilic nature of catalyst particles provides the necessary affinity for them to be drawn towards the dispersed aqueous phase. The reaction product viz., a mixture of *o*, *m*, and *p*-nitrotoluenes are found in organic phase (continuous).

From mechanistic viewpoint, macrokinetics continuous and dispersed phase mass transfer, intraparticle diffusion and rate controlling factors are important to be studied for toluene nitration. It is to be noted that in such agitated liquid-liquid dispersions, the chemical reactions and multiphase mass transfer occur simultaneously. Our studies reported in Chapter 5 have shown that apart from the shape selectivity of the catalyst, its lattice aluminium transformation from tetrahedral to octahedral configuration is responsible for achieving high *para*-selectivity. This has brought a new dimension of microenvironment engineering for such processes.

6.1. REPORTED LITERATURE ON MULTIPHASE TRANSPORT PROCESSES

During 1940 to 1970, macrokinetics of toluene nitration received attention of several researchers from kinetics and reaction engineering points of view [95, 138-140]. They broadly concluded that the nitration of toluene in liquid-liquid system is mass transfer controlled under the conditions investigated by them. Engel and Hougen [141] studied the mass transfer and efficiency of a stirred liquid-liquid-solid contactor considering the mass transfer resistances offered by liquid surrounding the solid and by the porous structure of the solid itself. They developed a correlation for a liquid-solid reaction in a stirred vessel. Particle-liquid mass transfer in mechanically agitated contactors received attention in recent past [142]. The effects of particle diameter, liquid viscosity, impeller characteristics and speed and vessel diameter were studied. Subsequent investigations have brought new dimensions to the understanding of mass transfer and kinetic mechanisms of aromatic nitrations in general and toluene nitration in particular.

Zaldivar et al. [79-80] studied toluene nitration by mixed acids under slow and fast liquid-liquid regimes. In the case of former regime, low sulfuric acid strength was employed. They found that the rate of mass transfer was not enhanced by the reaction which proceeds in the bulk of the reaction phase and not in the boundary layer. In the case of latter, high sulfuric acid strength (70-80 wt%) was employed and the nitration occur in the acid phase. The overall toluene conversion was shown to be affected by the interfacial area, distribution coefficients and Hatta number.

Molga and Cherbanski [143] studied liquid catalyzed liquid-liquid batch and semi-batch reaction systems. The organic compound was reported to possess limited solubility in aqueous phase when the reaction took place. They considered mass transfer with chemical reaction for expressing the overall conversion rate. The effect of parameters such as liquid-liquid contact surface area and the effect of solubility of the reaction product in aqueous phases on mass transfer was assessed.

Dispersed phase mass transfer in agitated liquid-liquid systems was studied by [144] by employing photographic techniques to measure the mean drop size as a function of time

in a batch operation. The mass transfer coefficient was formulated in terms of drop breakage and changes in their size as a function of time. Liquid-liquid-Solid reaction systems received attention by Chamayou et al. [78] in case of fine chemical synthesis. They developed a mathematical model with the reaction taking place in the organic phase. Pangarkar et al. [145] evaluated particle-liquid mass transfer coefficient for the rational design of a solid-liquid and solid-liquid-gas stirred tank reactors.

6.2. SCOPE OF PRESENT WORK

An attempt has been made in the present work to experimentally determine the apparent or macrokinetic rate of toluene nitration in a semi-batch mode of operation. The rate so obtained is compared with the rates of external mass transfer as applicable to agitated liquid-liquid-solid systems considering the following resistances in series

- (i) Transfer of toluene from continuous phase to aqueous phase surrounding the catalyst particle.
- (ii) Liquid-solid mass transfer
- (iii) Diffusion of reactants into the catalyst particle and simultaneous nitration

6.3. MECHANISTIC ASPECTS OF TOLUENE NITRATION

Despite the fact that solid catalyzed aromatic nitrations have received environmental acceptance, there still exist a considerable knowledge gap for predicting their dynamic behavior even in batch and semi-batch reactors. This is mainly due to the complexities of simultaneous chemical reaction and mass transfer phenomena in a heterogeneous system. Aspects like distribution of reactants between two nearly immiscible liquid phases, droplet sizes and phase inversion. Some of these aspects have received attention in previous chapters.

Batch or semi-batch nitration of toluene under reflux mode in vapor-liquid-solid system can be visualized to possess vapor-liquid, liquid-liquid, liquid-solid and pore diffusional

resistances to mass transfer. The schematic details are given in Fig. 6.1. For simplifying the model, following assumptions have been made for evaluating the rates of various mass transfer events occurring in a semi-batch stirrer reactor for toluene nitration with H-beta catalyst:

- (i) The liquid and vapor phases in the top section of the reactor are well back mixed under the influence of mechanical agitation.
- (ii) Dispersed phase mass transfer rates are applicable to liquid-liquid mass transfer involving dil HNO_3 and toluene
- (iii) The resistance to mass transfer at the outer surface of the catalyst particle is offered by the liquid film (aqueous phase) surrounding to it.
- (iv) The mass transfer resistances inside the catalyst particles are controlled by intraparticle pore characteristics.
- (v) The catalyst particles are completely wetted and the reaction proceeds inside the pores.

An attempt is made in this chapter to evaluate the rates of (ii) to (iv) mass transfer processes.

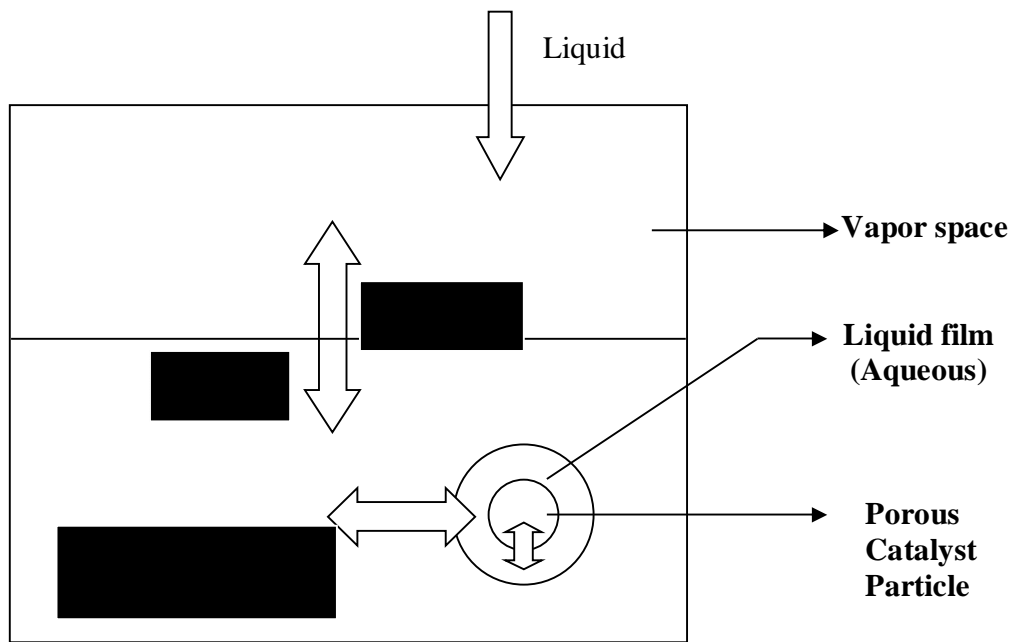


Fig. 6.1. Model representing multiphase mass transfer in toluene nitration

6.4. MASS TRANSFER PROCESS IN AGITATED LIQUID-LIQUID SYSTEMS

The rate of mass transfer of toluene at the interphase between it and HNO_3 (aqueous phase) depends on the concentration difference, interfacial area between the two liquids and the mass transfer coefficient. The mass transfer coefficient can be estimated using the following empirical correlation developed by Calderbank and Moo-Young [146] which was experimentally validated under a wide range of systems and operating conditions

$$k = 0.13 \left[\frac{P \mu_c}{V_d \rho_c^2} \right]^{1/4} \left[\frac{\mu_c}{\rho_c D_{ArH}} \right]^{2/3} \quad (6.1)$$

where P is the power dissipated by the stirrer and is given by

$$P = \phi' \rho_m n_a^3 D_a^5 \quad (6.2)$$

where ϕ' is a constant =2.2

ρ_m is density of the mixture = $\sum_{i=1}^n \rho_i v_i$ where ρ_i and v_i are the density and volume fractions of the individual constituents, kg / m³

n_a is the stirrer speed (rev/s)

D_a is the impeller diameter, m

μ_c is the viscosity of the continuous phase, kg / m.s

V_d is the volume of the dispersed phase, m³

ρ_c is the density of the continuous phase, kg / m³

D_{ArH} is the diffusion coefficient (m² / s) of the aromatic compound estimated using the modified Perkins and Geankoplis correlation [94]

The mass transfer coefficient for dispersed phase has been evaluated employing above correlation at various volume fractions of the organic phase. The details are given in the Table 6.1. The presented data shows that at inversion point, mass transfer coefficient registered significant increase and it improved further at high toluene volume fractions. This trend reinforces our earlier recommendation that solid acid catalyzed toluene nitration to be preferably toluene continuous.

Table 6.1 Calculated mass transfer coefficients at various volume fractions of organic phase

S.No	X_A	Continuous phase	Dispersed phase	k_{L2} in continuous phase (m / s)
1	0.2	aqueous	organic	3.96 exp (-5)
2	0.4	aqueous	organic	3.28 exp (-5)
3	0.53*	organic	aqueous	4.22 exp (-5)
4	0.6	organic	aqueous	4.37 exp (-5)
5	0.8	organic	aqueous	5.13 exp (-5)

*phase inversion point; ref: Zaldivar et al. [126]

6.5. MASS TRANSFER CHARACTERISTICS OF LIQUID-SOLID SYSTEMS

Knowledge of particle-liquid mass transfer coefficient (k_{SL}) is vital for a rational design of solid catalyzed aromatic nitrators. Mechanical agitation is provided to ensure the maximum utilization of available surface area. The particle-liquid mass transfer coefficient in two and three phase STRs depends on the degree of suspension of the particles which in turn is a function of the ratio of actual speed of rotation (N) and that required to achieve the condition of just complete suspension i.e. critical suspension speed (N_s).

Four approaches have been reported in the literature to correlate particle-liquid mass transfer coefficient (k_{SL}) viz., Dimensional analysis, Kolmogoroff's theory of isotropic turbulence, Slip velocity theory and Momentum and mass transfer analogy based approaches [145]. The latter exploits the analogy to correlate speed of agitation, critical suspension speed of particles and solid-liquid mass transfer coefficient k_{SL} .

In the present work, solid-liquid mass transfer coefficient has been estimated using the following correlation proposed by Jadhav and Pangarkar [142]

$$K_{SL} = 1.72 \exp(-3) \left[\frac{N}{N_s} \right]^{1.16} (Sc)^{-0.53} \quad (6.3)$$

Where k_{SL} = solid-liquid mass transfer coefficient, m / s

N = speed of agitation, rev / s

N_s = critical suspension speed of particles, rev / s

Sc = Schmidt number

The critical suspension speed can be estimated by Zwietering correlation which is given as

$$N_s = \frac{Sv^{0.1} D_p^{0.2} \left(g \frac{\Delta\rho}{\rho} \right)^{0.45} B^{0.13}}{D_a^{0.85}} \quad (6.4)$$

Where S is a constant and is a function of impeller type

v is the kinematic viscosity of a liquid

D_p is the particle diameter

g is the acceleration due to gravity

$\Delta\rho$ is the density difference between particle and liquid

ρ is the density of the liquid

B is the weight percent of solids

D_a is the impeller diameter

The particle liquid mass transfer coefficient has been estimated for two specific cases viz., nitric acid dispersed in toluene and toluene dispersed in nitric acid. The values obtained for these cases are $6.75 \exp(-5) \text{ m/s}$ and $7.3 \exp(-5) \text{ m/s}$ respectively.

6.6. EVALUATION OF APPARENT REACTION KINETICS UNDER SEMI-BATCH MODE OF OPERATION

The chemistry of semi-batch nitration of toluene in the presence of finely powdered H-Beta catalyst ($D_p = 400 \exp(-9) \text{ m}$) can be represented as



in which A (HNO_3) is slowly fed to B (toluene)

Overall mole balance on A is

$$F_{AO} - F_A + r_A V(t) = \frac{dN_A}{dt} \quad (6.6)$$

Where F_{AO} is the input molar flow rate

F_A is the output molar flow rate

r_A is the rate of reaction with respect to A

V is the volume of variable volume reactor

dN_A/dt is the rate of accumulation of A

The above equation can be written in terms of the concentrations as

$$v_o C_{AO} - v_o C_{AE} + r_A V = V \frac{dC_A}{dt} + C_A \frac{dV}{dt} \quad (6.7)$$

where v_o is the volumetric flow rate (here boil-up rate is so adjusted that input rates and output rates are equal)

C_{AO} is the initial concentration of A

C_{AE} is the concentration of A at exit which is constant at steady state

C_A is the concentration of A at time t

Using $dV/dt = v_o$ and $dC_A/dt = dC_A/d\tau$ where τ is the space time given by V/v_o

Assuming pseudo first order reaction with reference to HNO_3 since toluene is very much in excess, the above equation can be rewritten as

$$\frac{dC_A}{d\tau} + \left(\frac{1 + \tau k}{\tau} \right) C_A = \frac{C_{AO} - C_{AE}}{\tau} \quad (6.8)$$

Solving the differential equation using the boundary conditions of at $t = 0$, $\tau = \tau_o = V/v_o$ and $C_A = C_{Ai} = 0$, the concentration profile is obtained as

$$C_A = \frac{C_{AO} - C_{AE}}{(t + \tau_o)k} - \left(\frac{C_{AO} - C_{AE}}{\tau_o k} - C_{Ai} \right) \frac{\tau_o e^{-tk}}{\tau_o + t} \quad (6.9)$$

The apparent rate constant is calculated as $2 \exp (-3) \text{ s}^{-1}$ from the known concentration profile. The apparent rate of reaction is $2.6 \exp (-4) \text{ mol/lit.s}$

6.7. ASSESSMENT OF RELATIVE CONTRIBUTION OF MASS TRANSFER AND KINETIC EFFECTS

The first order apparent reaction rate constant, $k_{r,app}$, which was determined experimentally in section 6.6 of this chapter, is influenced by both external mass transfer and pore diffusional resistances. Its relationship with external and internal mass transfer resistances can be expressed by the following relationship

$$\frac{1}{k_{r,app}} = \frac{1}{k_{L2}a} + \frac{1}{k_{SL}a_p\rho_p} + \frac{1}{\eta k_1} \quad (6.10)$$

Where $k_{r,app}$ = apparent reaction rate constant, s^{-1}

k_{L2} = liquid-liquid mass transfer coefficient, m / s

a = interfacial area, m^2 / m^3

k_{SL} = solid-liquid mass transfer coefficient, m / s

a_p = external surface area of catalyst, m^2 / kg

ρ_p = particle density, kg / m^3

η = Effectiveness factor

k_1 = Intrinsic 1st order rate constant, s^{-1}

The first term on the R.H.S of equation (6.10) represents the external liquid-liquid mass transfer contribution and the second term represents solid-liquid mass transfer resistance. The third term represents the intrinsic kinetics combined with pore diffusion.

The contributions of external mass transfer resistances on the R.H.S of equation (6.10) have been evaluated and presented in Table 6.3.

Table 6.2 Computed kinetic and mass transfer

Tol Vol fraction	$(K_{r,app})^{-1}$	$(K_{L2,a})^{-1}$	$(k_{SL}a_p\rho_p)^{-1}$	$a,$ m^2 / m^3	$a_p,$ m^2 / kg	$\rho_p,$ kg / m^3
0.9	500	42	0.03	400	199 exp (3)	2.5 exp (3)

The results clearly show that the contribution of solid-liquid mass transfer on reaction kinetics is very negligible. This is rechecked by employing Mears criterion [147] which states that solid-liquid mass transfer is negligible if following inequality is satisfied

$$\frac{r_{A,app}(d_p/2)n}{k_{SL}C_{AS}} < 0.15 \quad (6.11)$$

Where $r_{A,app}$ = apparent reaction rate, mol / lit.s

d_p = diameter of the particle, m

n = reaction order

C_{AS} = saturated concentration of A, mol /lit

Our calculations show that the RHS of the expression is $9.7 \exp (-6)$ and is accordingly less than 0.15 ie., external solid-liquid mass transfer is negligible. Equation (6.1) now reduces to

$$\frac{1}{k_{r,app}} = \frac{1}{k_{L2}a} + \frac{1}{\eta k_1} \quad (6.12)$$

since external liquid-liquid mass transfer has some effect on the apparent kinetics, its contribution is accordingly subtracted from the apparent constant

$$k_1 = \frac{1}{\eta} \left(\frac{1}{k_{r,app}} - \frac{1}{k_{L2}a} \right)^{-1} \quad (6.13)$$

The extent of pore diffusion effect can be estimated from the particle effectiveness factor and thiele modulus [147]

$$\phi_s = \left(\frac{d_p}{2} \right) \frac{k_1^{1/2}}{D_{A,eff}} \quad (6.14)$$

$$\eta = \left(\frac{3}{\phi_s} \right) \left(\frac{\phi_s \cot \phi_s - 1}{\phi_s} \right) \quad (6.15)$$

Equation (6.13) is substituted in equation (6.14) and η value is evaluated by solving equations (6.14) and (6.15) simultaneously.

Our calculations show that $\eta \approx 1$ i.e., pore diffusional resistance can be neglected. This can be cross checked by Weisz-Prater criterion which states that when the following inequality holds, pore diffusion is not important.

$$\frac{r_{A,app} (d_p / 2)^2}{D_{A,eff} C_{AS}} \ll 1.0 \quad (6.16)$$

Our calculations show that the Weisz –Prater criterion holds good in the above case and pore diffusion is not important.

The above studies indicate that the measured apparent reaction rate is nearly the intrinsic rate.

It has also been reported by Zaldivar et al. [79] that a liquid-liquid reaction is kinetically controlled if the Hatta number is < 0.3 where the Hatta number is given as

$$\frac{[k_2 D_{ArH} C_{HNO_3}^{L2}]^{0.5}}{k_{L2}} \quad (6.17)$$

Where

k_2 = second order rate constant, lit /mol.s

D_{ArH} = diffusivity of aromatic compound, toluene, m^2 / s

$C_{HNO_3}^{L2}$ = concentration of HNO₃ in organic phase, mol / lit

$L2$ = organic phase

k_{L2} = liquid-liquid mass transfer coefficient, m / s

Our calculation of Hatta number is much less than 0.3 and hence the reaction can be treated as kinetically controlled with the reaction velocity constant **$k_1 = 2.18 \exp (-3) s^{-1}$** .

6.8 EVALUATION OF THERMAL CONSTANTS

Since the system is kinetically controlled, an attempt has been made to evaluate the reaction velocity constant at three more temperatures viz., 45°C, 55°C and 65°C to estimate the activation energy and other kinetic parameters. The conversion and temperature levels have been kept low for this experimentation to minimize the adverse effect of water not removed during the nitration.

The values of reaction velocity constants determined experimentally as a function of temperature are given in Table 6.3. From the Arrhenius plot of $\ln k$ vs $1/T$, the values of activation energy and arrhenius constant have been determined to be **28.5 kJ** and **12.7 s⁻¹** respectively.

Table 6.3 Effect of temperature on the rate constant

T (K)	318	328	338	393
k (s^{-1})	$2.67 \exp(-4)$	$3.64 \exp(-4)$	$5.00 \exp(-4)$	$2.1 \exp(-3)$

The value of the rate constant at 120 °C determined experimentally ($2.1 \exp(-3) s^{-1}$) is found to agree with that determined from the arrhenius plot ($2.2 \exp(-3) s^{-1}$).

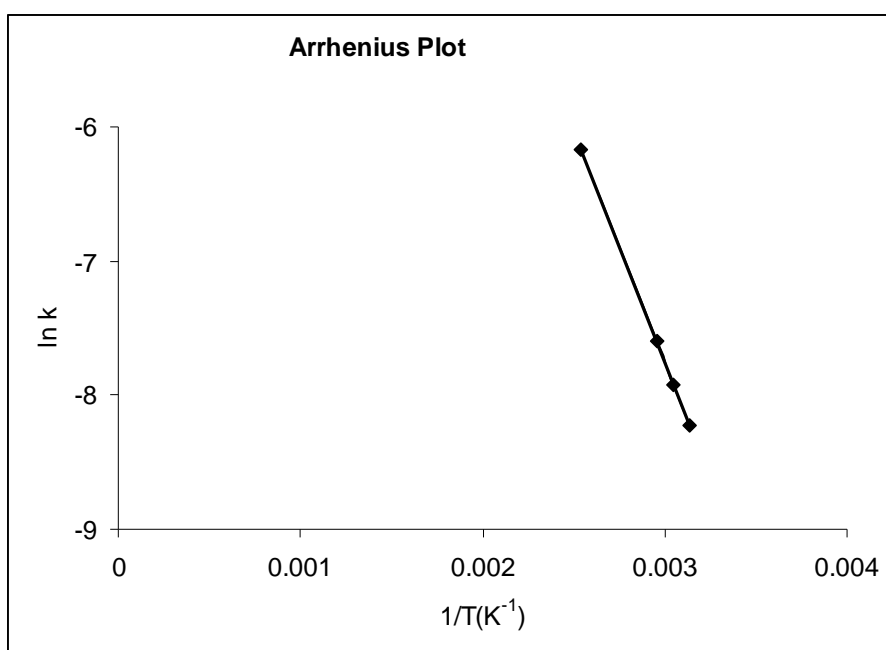


Fig. 6.2 Arrhenius plot

Hence the Arrhenius equation can be represented as $\ln k = 2.55 - 3430.6/T$

CHAPTER 7

SUMMARY AND CONCLUSIONS

In the current study, the desirability of sulfuric acid free nitration of toluene in the presence of solid acid catalyst has been established. The present investigations include process standardization, dispersion morphology of toluene-nitric acid system, study of microenvironment around the catalyst particle, catalyst characterization studies to demonstrate the suitability and stability of the catalyst and mass transfer effects.

The catalytic nitration of toluene using solid acid catalyst has been standardized with reference to many parameters viz., agitation speed, nature of catalyst, catalyst-toluene ratio, toluene-nitric acid molar ratio, temperature, boil-up rate, mode of operation batch vs semi-batch, dosing rate and dosing period. It has been found that an agitation speed of 200 rpm, catalyst –toluene ratio of 4.5 g/mol, lower ratio of toluene to nitric acid, reflux temperature of 120°C, a boil-up rate of 20°C, semi-batch mode of operation at a lower dosing rate of 30 ml/h for about 8 h gave relatively higher conversion and better para selectivity. Employing a commercial catalyst like zeolite H-beta, para selectivity has been nearly quadrupled from 0.5 to 2.0 by proper maneuvering of the process parameters and microenvironment in and around catalyst particles. Our study has clearly established the importance of process standardization in the catalytic nitration of toluene.

Nitration of toluene in the presence of solid acid catalyst has been visualized in terms of catalyst dispersed in agitated liquid-liquid dispersions. Nitration of toluene has been conducted using various volume fractions of toluene and nitric acid. Dispersion morphology of the reaction system has been studied and three regions have been

demarcated viz., toluene dispersed in nitric acid (toluene volume fraction < 0.3), ambivalent region (volume fraction of toluene from 0.3 to 0.7) and nitric acid dispersed in toluene (toluene volume fraction > 0.7). It has been found that latter type of dispersion is more preferable in view of catalyst dealumination observed at lower volume fractions of toluene or higher volume fractions of nitric acid. Phase inversion point has been estimated to be around 0.53 (toluene volume fraction) at which the ratio of collision and coalescence frequencies is unity and toluene dispersed in nitric acid is just converted to nitric acid dispersed in toluene. It has also been found from the estimations that there is a significant increase in the interfacial area at this point.

As our investigations established that *para*-selectivity could be greatly enhanced using the rational combination of process parameters, it was assumed that factor other than shape selectivity should be responsible for improvement in the selectivity. It has been found from solid state NMR investigations that the transformation of flexible lattice aluminium configuration from tetrahedral to octahedral form is responsible for the enhanced *para*-selectivity. This transformation has been found to be consistent even after three recycles explaining the probable cause of consistent *para*-selectivity exhibited by zeolite H-beta catalyst.

Catalyst characterization studies have been conducted to establish the suitability and the stability of the catalyst. XRD studies under various process conditions viz., different mole ratios of toluene and nitric acid, semi-batch nitration at two dosing rates of nitric acid upto three recycles demonstrated the structural integrity of the catalyst. Thermal analyses of the catalyst post reaction indicate that upto 200 °C (region 1) there is an endothermic weight loss of adsorbed water or toluene from the catalyst and above 200-400 °C (region 2) the weight loss is due to evaporation of volatile oxidation products deposited on the catalyst. The final exothermic weight loss below 690 °C (region 3) is due to the combustion of high boiler species suggesting the formation of coke precursors. It was also observed that under excess nitric acid conditions, the major weight loss is restricted to regions 1 and 2 suggesting the minimum adsorption of high boiler species and under excess toluene conditions, the weight loss is not restricted to any one region.

From EDX studies, it was found that there the catalyst was getting dealuminated under excess nitric acid conditions which led to the conclusion that the dispersion of nitric acid in toluene is preferable to toluene dispersed in nitric acid. FTIR studies also indicated that under the conditions of low volume fraction of toluene, there is a significant reduction in the overall and Bronsted acidity.

Mass transfer parameters like sauter mean diameter, interfacial area, diffusion and mass transfer coefficients have been estimated for liquid-liquid systems and liquid-liquid-solid systems at various volume fractions of organic phase. Mass transfer rate has been estimated. Reaction kinetics have been studied for semi-batch nitration under standardized conditions using excess toluene conditions (pseudo 1st order with respect to nitric acid is assumed). After a detailed analysis of external and internal mass transfer resistances, the toluene nitration is found to be kinetically controlled for the conditions employed in the semi-batch nitration studies. The kinetic constants have been estimated by studying the effect of temperature on the reaction velocity constant.

CONTRIBUTIONS FROM THE STUDY

1. Sulfuric acid free nitration of toluene in the presence of zeolite H-beta catalyst has been standardized with respect to various process parameters.
2. A simple methodology based on semi batch investigations has been developed to indirectly assess the effect of microenvironment in and around the catalyst particles in toluene to heighten the *para*-selectivity.
3. Morphology of nitric acid –toluene dispersions has been studied and analysed.
4. Effect of the microenvironment around the catalyst particle has been studied with respect to changes in lattice aluminium configuration to explain the probable cause of consistent *para* selectivity exhibited by the catalyst.
5. Stability and Suitability of zeolite H-beta catalyst in toluene nitration have been established with elaborate analytical studies.
6. Mass transfer effects have been estimated for liquid-liquid noncatalytic and liquid-liquid-solid catalytic reaction systems.
7. Kinetic control over toluene nitration in a reaction medium in which HNO₃ is dispersed in toluene as continuous phase has been decisively established after proving the negligible role of mass transfer resistance offered by liquid-liquid-solid system.

SCOPE OF FUTURE WORK

The present work has opened up new R&D avenues in solid acid catalyzed aromatic nitrations. The notable amongst them are:

- (a) The solid acid catalyzed aromatic nitration requires more extensive reactor studies to facilitate its commercial utilization on larger scale. Our investigations have established the desirability of employing reactive distillation concept for toluene nitration to achieve higher levels of conversion and *para*-selectivity with minimum catalyst dealumination since it facilitates effective removal of water from the reaction front and maintenance of desired nitric acid concentration locally. The solid acid catalyst can be conveniently packed in the distillation column and a liquid-liquid separator can be incorporated after condenser to recycle toluene after separation from water formed during the reaction. Such a configuration which facilitates effective nitration-water separation processes will have a positive effect on catalyst acidity and enhanced mass transfer as well as reaction rates. The chemical reaction and inter and intraphase diffusion steps will drive each other in a proactive fashion. Incorporation of distillation column to the reactor will ensure spatial continuity along the axial direction. Both reaction and separation will take place in all sections of the packed distillation column. Reaction engineering studies on a reactive distillation system will be more complex and there will be a definite need to evaluate kinetic and mass transfer parameters relevant to a gas-liquid-solid system. There is tremendous scope and academic challenges to model such a system to simulate the reactor operation.

- (b) Application of reaction calorimetry to assess intrinsic reaction rates and catalyst life through the measurement of microthermal responses will be a challenging task in standardizing the continuous process based on solid catalyzed aromatic nitrations in general and toluene nitration in particular.
- (c) The aromatic nitrations being highly exothermic, the accumulation of unreacted HNO_3 in high concentration can be hazardous if accompanied by a phase inversion under mass transfer controlled reaction rate. This aspect needs attention to ensure safe operation of solid catalyzed aromatic nitrations.

REFERENCES

1. K. Winnacker and L. Kuchler, in *Chemische Technologie*, Band 6, Organische Technologie II (4th edition), Edited by H. Harnisch, R. Steiner, K. Winnacker (Carl Hanser Verlag, Munchen, 1982) p. 169.
2. Ullmann's, *Encyclopedia of Industrial Chemistry.*, VCH, Weinheim, Vol.A17, 411 (1991).
3. T. Travis, *Early Intermediates for the Synthetic Dyestuffs Industry.*, *Chem.Ind.*, London 508-514 (1988).
4. L. Bretherick, *Handbook of reactive Chemical Hazards.*, 3rd ed., Butterworths, London (1985).
5. C. K. Ingold, *Structure and Mechanism in Organic Chemistry.*, Cornell University Press, Ithaca, NY, (1969).
6. G. A. Olah, R. Malhotra and S. C. Narang, *Nitration: Methods and Mechanisms.*, VCH Publishers, (1989).
7. K. L. Nelson and H. C. Brown, "Distribution of isomers in the mononitration of t-butylbenzene; properties of the pure mononitro-t-butylbenzenes.", *JACS.*, **73**, 5605 (1951).
8. E. Berliner, *Progr. Phys. Org. Chem.*, **2**, 253 (1964).
9. G. S. Hammond, "A correlation of reaction rates.", *JACS.*, **77**, 334 (1955).
- 10 a) C. K. Ingold, D. J. Millen and H. G. Poole, "Vibrational spectra of ionic forms of oxides and oxy-acids of nitrogen. Part I. Raman-spectral evidence of the ionization of nitric acid by perchloric, sulfuric and selenic acids. Spectroscopic identification of the nitronium ion, NO_2^+ .", *J. Chem. Soc.*, 2576 (1950)
- b) R. J. Gillespie, E. D. Hughes, C. K. Ingold and E. R. A. Peeling, "Cryoscopic measurements in sulfuric acid. Part III. The solutes nitric acid, dinitrogen pentoxide, dinitrogen tetroxide. Cryoscopic proof of the formation of the nitronium ion, NO_2^+ .", *J. Chem. Soc.*, 2504 (1950)

- c) E.D. Hughes, C. K. Ingold and R. I. Reed, "Kinetics and mechanism of aromatic nitration. Part II. Nitration by the nitronium ion, NO_2^+ , derived from nitric acid.", *J. Chem. Soc.*, 2400 (1950).
11. a) G. A. Olah, "Mechanism of Electrophilic aromatic substitutions.", *Acc. Chem. Res.*, **4**, 240 (1971). & b) J. H. Ridd, "Mechanism of aromatic nitration.", *Acc. Chem. Res.*, **4**, 248 (1971). & c) L. M. Stock and H. C. Brown, "A quantitative treatment of directive effects in aromatic substitution.", *Adv. Phys. Org. Chem.*, **1**, 35 (1963).
12. a) N. C. Marziano, A. Tomasin, C. Tortato and J. M. Zaldivar, "Thermodynamic nitration rates of aromatic compounds. Part 4. Temperature dependence in sulfuric acid of $\text{HNO}_3 \rightarrow \text{NO}_2^+$ equilibrium, nitration rates and acidic properties of the solvent.", *J. Chem. Soc. Perkin Trans.*, **2**, 1973 (1998).
- b) M. Sampoli, A. DeSantis, N. C. Marziano, F. Pinna and A. Zingales, "Equilibria of nitric acid in sulfuric and perchloric acid at 25°C by Raman and UV spectroscopy.", *J. Phys. Chem.*, **89**, 2864 (1985).
- c) N.C. Marziano, A. Tomasin and M. Sampoli, "Nitric acid equilibrium in concentrated trifluoromethanesulfonic acid studied by Raman spectroscopy.", *J. Chem. Soc. Perkin Trans.*, **2**, 1995 (1991).
13. J. Kenner, *Nature* (London), **156**, 369 (1945).
14. S. Nagakura and J. Tanaka, "On the relation between the chemical reactivity and energy levels of the chemical.", *J. Chem. Phys.*, **22**, 563 (1954).
15. a) C. Yang and Q. Xu, *Zeolites*, "States of aluminium in zeolite beta and influence of acidic or basic medium.", **19**, 404 (1997).
- b) G. A. Olah, S. J. Kuhn and S. H. Flood, "Aromatic substitution VIII. Mechanism of the nitronium tetrafluoroborate nitration of alkylbenzenes in tetramethylene sulfone solution. Remarks on certain aspects of electrophilic aromatic substitution.", *J. Am. Chem. Soc.*, **83**, 4571 (1961).
16. V. A. Koptjug, *Arenonium Ions: Structure and Reaction Ability.*, Nauka, Novosibirsk, (1983).
17. J. Feng, X. Zheng and M. Zerner, "Theoretical study of Ipso attack in aromatic nitration.", *J. Org. Chem.*, **51**, 4531-4536 (1986).
18. K. Schofield, *Aromatic Nitration*, Cambridge University Press, London, (1980).

19. L. Ebersson, M. Hartshorn and F. Radner, "Ingolds nitration mechanism.", *Acta Chemica Scandinavica*, **48**, 937-950 (1994).
20. R. J. Gillespie and D. J. Millen, "Aromatic nitration.", *Rev. Chem. Soc.*, **2**, 277 (1948).
21. H. Suzuki, T. Murashima, K. Shimizu and K. Tsukamoto, "A non-acid methodology for polynitration of arenes at low temperatures.", *J. Chem. Soc. Commun.*, 1049 (1991).
22. A. V. Ramaswamy, "Clays, zeolites and solid acid catalysts.", *Chim. Ind. (Milan)*, **82(6)**, E/1-E/9 (Italian) (2000).
23. M. H. Gubelmann, C. Doussain, P.J. Tirel and J. M. Popa, "Heterogeneous catalysis and fine chemicals –II.", *Stud. Surf. Sci.Catal.*, **59**, 471 (1991).
24. L.V. Malysheva, E.A. Paukshtis and K.G. Ione, *Catal. Rev. Sci. & Eng.*, **37**, 179 (1995).
25. K. Tanabe and W. F. Holderich, "Industrial applications of solid acid-base catalysts.", *Appl. Catal. A: General.*, **181**, 399 (1999).
26. G. A. Olah, G. K. S. Prakash and J. Sommer, *Superacids*, Wiley, New York, (1985).
27. D. W. Breck, *Zeolite Molecular Sieves*, Wiley Pub. New York, (1974).
28. E. P. Parry, "An infrared study of pyridine adsorbed on acidic solids. Characterization of surface acidity.", *J. Catal.*, **2**, 371 (1963).
29. R. M. Barrer, *Hydrothermal Chemistry of Zeolites*, Acad. Press, New York, (1982).
30. T. R. Hughes and H. M. White, "A study of the surface structure of decationized Y-zeolite by quantitative infrared spectroscopy.", *J. Phys. Chem.*, **71**, 2192 (1967).
31. W. M. Meier and D. H. Olson, *Atlas of Zeolite Structure Types*, 2nd Edn. Butterworths, London, (1987).
32. E. M. Flanigen, in "*Proceedings of the Fifth International Zeolite Conference*", Ed. L. V. C. Rees, Heydon, London, 760 (1980).
33. D. Vassena, A. Kogelbauer and R. Prins, "Potential routes for the nitration of toluene and nitrotoluene with solid acids.", *Catal.Today.*, **60**, 275 (2000).
- 34 a) J. W. Ward, *Zeolite Chemistry and Catalysis*, [C. Rabo, J.A. Eds.], ACS monograph. Chp. 2, **171**, 118 (1976)
- b) D. W. Breck, *Zeolite Molecular Sieves*, John Wiley and Sons, New York, 449 (1974).

35. P. B. Weisz and V. S. Frilette, "Intracrystalline and molecular shape-selective catalysis by zeolite salts.", *J. Phys. Chem.*, **64**, 382 (1960).
36. R. L. Wadlinger, G. T. Kerr and E. J. Rosinski, "Catalytic composition of a crystalline zeolite.", U.S. Pat. 3, 308, 069 (1967).
37. J. M. Newsam, M. M. J. Treacy, W. T. Koetsier, and C. B. De Gruyter, "*Proc. Royal. Soc. Lond.*" **A420**, 375- 405 (1988).
38. J. B. Higgins, R. B. La Pierre, J. L. Schlenker, A. C. Rohrman, J. D. Wood, G. T. Kerr and W. J. Rohrbaugh, "The framework topology of zeolite Beta.", *Zeolites*, **8**, 446 (1988).
39. L. B. Young, *Eur. Pat. Appl.*, 30, 084 (1981).
40. M. A. Tobias, "Conversion of polar compounds using highly siliceous zeolite-type catalysts.", *U.S. Pat* 3, 728, 408 (1973).
41. R. B. La Pierre and R. D. Patridge, *Eur. Pat. Appl.*, 94, 827 (1983).
42. R. B. La Pierre, R. D. Patridge, N. Y. Chen and S. S. Wong, "Catalytic dewaxing process using zeolite Beta.", *US. Patent* 4,501,926 (1986).
43. J. A. Martens, J. Perez-Pariente, E. Sastre, A. Corma and P. A. Jacobs, "Isomerization and disproportionation of m-xylene selectivities induced by the void structure of the zeolite framework.", *Appl.Catal.*, **45**, 85 (1988).
44. L. J. Leu, L. Y. Hou, B. C. Kang, C. C. Li, S. T. Wu and J. C. Wu, "Synthesis of zeolite Beta and catalytic isomerization of n-hexane over Pt/H-beta catalysts.", *Appl. Catal.*, **69**, 49 (1991).
45. Y. Chen, J. Mazink, A.B. Schwartz and P.B. Weisz, "Selectoforming, a new process to improve octane and quality (of gasoline).", *Oil Gas J.*, **78**, 154 (1968).
46. W. E. Garwood, "Conversion of C₂-C10 to higher olefins over synthetic zeolite ZSM-5.", *ACS Symp. Ser.*, **218**, 383 (1983).
47. S. C. Meisel, J. P. Mc Cullough, C. J. Lechthaler and P. B. Weisz, "Gasoline from methanol in one step," *Chem. Tech.*, **686** (1976).
48. J. Scherzer, *Octane enhancing zeolite FCC catalysts; Scientific and Technological aspects*, Marcel Dekker, Inc. New York (1976).
49. C. Braddock, "Novel recyclable catalysts for atom economic aromatic nitration.", *Green Chemistry.*, **G26** (2001).

50. K. Qiao and C. Yokoyama, "Nitration of aromatic compounds with nitric acid catalyzed by ionic liquids.", *Chem Lett.*, **33**, 808 (2004)
- 51 (a) K. Ishihara, M. Kubota and H. Yamamoto, "A new scandium complexes an extremely active acylation catalyst.", *Synlett.*, **265** (1996); (b) K. Ishihara, Y. Karumi, M. Kubota and H. Yamamoto, "Scandium trifluoromethanesulfonimide and scandium trifluoromethanesulfonate as extremely active acetalization catalysts.", *Synlett.*, **839** (1996).
52. Min Shi and Shi-Cong Cui, "A new method for nitration of phenolic compounds.", *Adv. Synth. Catal.*, **345**, 1329 (2003).
53. Kirk Othmer, *Encyclopedia of Chemical Technology*, John Wiley & Sons Inc., New Jersey, 5th Edn, (2004).
54. S. P. Dagade, S. B. Waghmode, V. S. Kadam and M. K. Dongare, "Vapor phase nitration of toluene using dilute acid and molecular modeling studies over Beta zeolite.", *Appl. Catal. A: Gen.*, **226**, 49 (2002).
55. D. Akolar, A. Glemay and S. Kaliaguine, *Res. Chem. Iterm.*, **21**, 7 (1995).
56. A. Germain, T. Akouz and F. Figuaras, "Vapor phase nitration of fluorobenzene with N₂O₄ over aluminosilicates: Effects of structure and acidity of the catalyst.", *Appl. Catal. A: Gen.*, **136**, 57 (1996).
57. L. Bertia, H. W. Kouwenhoven and R. Prins, "Vapor phase nitration of benzene over modified mordenite catalysts.", *Appl. Catal. A: Gen.*, **129** 229 (1995).
58. K. Smith, *Bull. Soc. Chim. Fr.*, (1989) 272.
59. S. M. Nagy, K. A. Yaravoy, V. G. Shubin and L. A. Vostrikova, "Selectivity of nitration reactions of organic reactions of organic compounds on zeolites H-Y and H-ZSM-11.", *J. Phys. Org. Chem.*, **7** (1994) 385.
60. N. F. Salakhutdinov, N. F. Ione, E. A. Kobzar and L. V. Malysheva, "Gas phase nitration of aromatic compounds at zeolites with nitrogen dioxide.", *J. Org. Chem. USSR.*, **29**, 457 (1993).
61. O. L. Wright, J. Teipel and D. Thoennes, "The nitration of toluene by means of nitric acid and an ion exchange resin.", *J. Org. Chem.*, **30**, 301 (1965).
62. G. A. Olah, R. Malhotra and S. C. Narang, "Aromatic substitution 43 perflourinated resin sulfonic acid catalyzed nitration of aromatics.", *J. Org. Chem.*, **43**, 4628 (1978).

63. L. Delaude, P. Laszlo and K. Smith, "Heightened selectivity in aromatic nitrations and chlorinations by the use of solid supports and catalysts.", *Acc. Chem. Res.*, **26**, 993 (1993).
64. P. Laszlo and P. Vondorneal, "Regioselective nitration of aromatic hydrocarbons by metallic nitrates on the K10 montmorillonite under menke conditions.", *Chem. Lett.*, **1843** (1988).
65. B. M. Choudhary, M. Ravichandra Sharma and K. Vijaya kumar, "Fe³⁺ montmorillonite catalyst for selective nitration of chlorobenzene.", *J. Mol. Catal.*, **87**, 33 (1994)
66. T. Kameo, S. Nishimura and O. Manabe, "HNO₃ over polystyrenesulfonic acid alone or supported on celite.", *Nippon kagaku kaishi.*, **1**, 122, (1974).
67. J. M. Riego, Z. Sedin, J. M. Zaldivar, N. C. Marziano and C. Tortato, "Sulfuric acid on silica gel: an expensive catalyst for aromatic nitration.", *Tetrahedron letters.*, **37**, 513 (1996).
68. E. Suzuki, K. Tohmori and Y. Ono, "Vapor phase nitration of benzene over silica supported sulfonic acid catalyst.", *Chem. Lett.*, **2273** (1987).
69. H. Schubert and F. Wunder, "Process for nitrating toluene", *US Patent* 4,112 006 (1978).
70. Radoslaw, R. Bak, and A. J. Smallridge, "A fast and mild method for the nitration of aromatic rings," *Tetrahedron letters.*, **42**, 6767 (2001).
71. B. M. Choudhary, M. Sateesh, M. Lakshmikantam, K. Koteswara Rao, K. V. Ramprasad, K. V. Raghavan and J. A. R. P. Sharma, "Selective nitration of aromatic compounds by solid acid catalysts.", *Chem. Comm.*, **1**, 25 (2000).
72. D. Vassena, D. Malossa, A. Kogelbauer and R. Prins, "Zeolites as catalysts for the selective para nitration of toluene," *Proceedings of 12th Inter.Zeol. Conf.* (Eds: M. M. J. Treacy, B. K. Markus, M. E. Bisher and J. B. Higgins, Materials Research Society Warrendale, Pennsylvania, USA) 1909 (1999).
73. C. Perego and S. Peratello, "Experimental methods in catalytic kinetics.", *Catal Today.*, **52**, 133 (1999).

74. S. K. Bej, A. K. Dalai and S. K. Maity, "Effect of diluent size on the performance of a microscale fixed bed multiphase reactor in up-flow and down-flow modes of operation.", *Catal Today.*, **64**, 333 (2001).
75. G. D. Bellos and N. G. Papayannakos, "The use of a three phase microreactor to investigate HDS kinetics.", *Catal Today.*, **79-80**, 349 (2003).
76. S. Ishiagaki and S. Goto, "Vapor phase kinetics and its contribution to global three phase reaction rate in hydrogenation of 1-methylnaphthalene.", *Catal Today.*, **48**, 31 (1999).
77. S. Caravieilhas, D. Schweich and C. de Bellefon, "Transient operation of a catalytic liquid-liquid plug flow reactor for kinetics measurements.", *Chem. Eng. Sci.*, **57**, 2697 (2002).
78. A. Chamoyou, H. Delmas and G. Casamatta, "Kinetic of a liquid/liquid/solid fine chemicals reactions-modelling of a continuous pilot plant reactor.", *Chem. Eng. Technol.*, **19**, 67 (1996).
79. J. M. Zaldivar, E. Molga, M. A. Alos, H. Hernandez and K. R. Westerterp, "Aromatic nitrations by mixed acid. Slow liquid-liquid reaction regime.", *Chemical Engineering and Processing.*, **34**, 543 (1995).
80. J. M. Zaldivar, E. Molga, M. A. Alos, H. Hernandez and K. R. Westerterp, "Aromatic nitrations by mixed acid. Fast liquid-liquid reaction regime.", *Chemical Engineering and Processing.*, **35**, 91 (1996).
81. I. Pitault, P. Fongarland, M. Mitrovic, D. Ronze and M. Forissier, "Choice of laboratory scale reactors for HDT kinetic studies or catalytic tests.", *Catal Today.*, **98**, 31 (2004).
82. Chun-Yu Chen and Chia-Wei Wu, "Thermal hazard assessment and macrokinetics analysis of toluene mononitration in a batch reactor.", *J. Loss Prev. Process Ind.*, **9**, 309 (1996).
83. K. Luo and J. Chang, "The stability of toluene mononitration in a reaction calorimeter reactor.", *J. Loss Prev. Process Ind.*, **11**, 81 (1998).
84. N. C. Deno and R. Stein, "Carbonium Ions.III. Aromatic nitration and the C_o acidity function.", *J. Am. Chem. Soc.*, **578** (1956).

85. R. G. Coombes, R. B. Moodie and K. Schofield, "Electrophilic aromatic substitution. Part 1. The nitration of some reactive aromatic compounds in concentrated sulfuric and perchloric acids.", *J. Chem. Soc. B.*, **800** (1968).
86. J. W. Chapman, P. R. Cox and A. N. Strachan, "Two phase nitration of toluene-III.", *Chem. Eng. Sci.*, **29**, 1247 (1974).
87. N. G. Papayannakos and P. Petrolekas, "Kinetic studies of homogeneous nitration of toluene.", *Ind. Eng. Chem. Res.* **31**, 1457 (1992).
88. D. R. Lide, *C.R.C. Handbook of Chemistry and Physics.*, **78th** edn, CRC Press, NY, (1997).
89. T.E. Daubert and R.P. Danner, *Physical and Thermodynamic Properties of Pure Chemicals.*, Hemisphere Pub. Corp. USA, (1989).
90. J. M. Smith, H. C. Vanness and M. M. Abbott, *Introduction to Chemical Engineering Thermodynamics.*, **6th** edn, (2001).
91. R. H. Perry and C. H. Chilton: *Chemical Engineers' Handbook.*, **7th** edn, McGrawHill, USA (1997).
92. M. A. Delichatsios and R. F. Probst, "The effect of coalescence on the average drop size in liquid-liquid dispersions.", *Ind. Eng. Chem. Fundam.*, **15**, 134 (1976).
93. M. Arashmid and G. V. Jeffreys, "Analysis of phase inversion characteristics of liquid-liquid dispersions.", *AIChE J.*, **26**, 51 (1980).
94. L. R. Perkins and C. J. Geankoplis, "Molecular diffusion in a ternary liquid system with the diffusing component dilute.", *Chem. Eng. Sci.*, **24**, 1035 (1969).
95. P. R. Cox and A. N. Strachan, "Two phase nitration of toluene-I.", *Chem. Eng. Sci.*, **27**, 457 (1972).
96. V. R. Balmoos, *Collection of Stimulated XRD Powder Patterns of Zeolites*, Butterworths, London, (1984).
97. W. M. Meier, *Molecular Sieves*, Soc. Chem. Ind, London, 283 (1968).
98. J. J. Pluth, J. V. Smith and J. M. Bennett, "Microporous aluminophosphate number 17 with encapsulated piperidine, topological similarity to erionite.", *Acta. Crystallogr.* **C42**, 283 (1986).
99. J. F. Charnell, "Gel growth of large crystals of sodium A and sodium X zeolites.", *J. Cryst. Growth*, **8**, 291 (1971).

100. H. M. Rietveld, "A profile refinement method for nuclear and magnetic structures.", *J. Appl. Crystallogr.* **2**, 65 (1969).
101. E. G. Derouane, S. Detremmerie, Z. Gabelica and N. Blom, "Synthesis and characterization of ZSM-5 catalysts. 1. Physicochemical properties of precursors and intermediates.", *Appl. Catal.* **1**, 20 (1981).
102. R. M. Barrer and D. A. Langley, "Reactions and stability of chabazite-like phases. Part I. Ion exchanged forms of natural chabazite.", *J. Chem. Soc.*, 3804 (1958).
103. L. S. de Saldarriaga, C. Saldarrage and M. E. Davies, "Investigations into the nature of a silicoaluminophosphate.", *J. Am. Chem. Soc.*, **109**, 109 (1987).
104. H. Knozinger, "Specific poisoning and characterization of catalytically active surface.", *Adv. Catal.* **25**, 184 (1976).
105. E. M. Flanigen, H. Khatami and H.A. Seymenski, *Molecular Sieve Zeolites-1*, ACS Monograph, (Eds. Seymenski, H. A.), **101**, 201 (1971).
106. E. M. Flanigen, *Zeolite Chemistry and Catalysis*, ACS Monograph, (Eds. Rabo, J. A., et.al.), **171**, 180 (1976).
107. N. Kutz, *Heterogeneous Catalysis -II*, (Eds. Shrpiro, B. L.), 121 (1984).
108. P. A. Jacobs and V. Ballmoos, "Framework hydroxyl groups of H-ZSM-5 zeolites.", *J. Phys. Chem.*, **86**, 3050 (1982).
109. C. T-W. Chu and C.D. Chang, "Isomorphous substitution in zeolite frameworks. 1. Acidity of surface hydroxyls in [B]-, [Fe]-, [Ga]- and [Al]- ZSM-5.", *J. Phys. Chem.* **89**, 1569 (1985).
110. N. Y. Topsoe, K. Pederson and E. G. Derouane, "Infrared and temperature programmed desorption study of the acidic properties of ZSM-5 type zeolites.", *J. Catal.* **70**, 41 (1981).
111. M.W. Anderson and J. Klinowski, "Zeolites treated with silicon tetrachloride vapour. IV: Acidity.", *Zeolites*, **6**, 455 (1986).
112. E. Lippmaa, M. Magi, A. Samason, G. Engelhardt and A.R. Grimmer, "Structural studies of silicates by solid-state high resolution silicon-29 NMR.", *J. Am. Chem. Soc.*, **102**, 4889 (1983).

113. C. A. Fyfe, G. C. Gobbi, J. Klinowski, J. M. Thomas and S. Ramdas, "Resolving crystallographically distinct tetrahedral sites in silicalite and ZSM-5 by solid state NMR.", *Nature*, (London), **296**, 530 (1982).
114. C. A. Fyfe, G. C. Gobbi, J. K. Hartman, J. Klinowski and J. M. Thomas, "Solid-State Magic-Angle spinning Aluminur-27 Nuclear magnetic resonance studies of zeolites using a 400-MHz high resolution spectrometer.", *J.Phys. Chem*", **86**, 1247 (1982).
115. D. Freude, M. Hunger and H. Pfeifer, *Z. Phys. Chemie (Neue Folge)*, **152**, 429 (1987).
116. K. F. M. G. J. Scholle, W. S. Veeman, J. G. Post and Van Hoof, "The adsorption of water by H-ZSM-5 zeolite studied by magic angle spinning proton NMR.", *Zeolites*, **3**, 214 (1983).
117. R. B. Borade, S. G. Hegde, S. B. Kulkarni and P. Ratnaswamy, "Active centers over H-ZSM-5 zeolites for paraffin cracking.", *Appl. Catal*, **13**, 27 (1984).
118. G.A. Olah, S.C. Narang, J.A. Olah and K. Lammertsma, "Recent aspects of nitration: New preparative methods and mechanistic studies (A Review).", *Proc. Natl. Acad. Sci. USA.*, **79**, 4487 (1982).
119. K. Smith and K. Fry, "Para selective mononitration of alkyl benzenes under mild conditions by use of benzoyl nitrate in the presence of a zeolite catalyst.", *Tetrahedron letters.*, **30**, 5333 (1989).
120. S. Bernasconi, G. D. Pirngruber and R. Prins, "Influence of the properties of zeolite BEA on its performance in the nitration of toluene and nitrotoluene," *J. Catal.*, **224**, 297 (2004).
121. S. Bernasconi, G. D. Pirngruber and R. Prins, "Factors determining the suitability of zeolite BEA as para-selective nitration catalyst.", *J. Catal.*, **219**, 231 (2003).
122. M. Haouas, A. Kogelbauer and R. Prins, "The effect of flexible lattice aluminium in zeolite beta during the nitration of toluene with nitric acid and acetic anhydride.", *Catalysis letters.*, **70**, 61 (2000).
123. K. Smith, A. Musson and G. A. Deboos, "Superior methodology for the nitration of simple aromatic compounds.", *J.Chem.Soc. Chemical Communications.*, **4**, 469 (1996).

124. D. W. Breck, W. G. Eversole, R. M. Milton, T. B. Reed and T. L. Thomas, "Crystalline zeolites. I. The properties of a new synthetic zeolite, type A.", *J. Am. Chem. Soc.*, **78**, 5963 (1956).
125. S. J. X. He, M. A. Long, M. I. Atalla and M. A. Wilson, "Methylation of naphthalene by methane over substituted aluminophosphate molecular sieves.", *Energy Fuels*, **6**, 498 (1992).
126. J. M. Zaldivar, M. A. Alos, E. Molga, H. Hernandez and K.R. Westerterp., "The effect of phase inversion in during semibatch aromatic nitrations.", *Chemical Engineering and Processing.*, **34**, 529 (1995).
127. J. M. Zaldivar, C. Barcons, H. Hernandez, E. Molga and T. J. Snee, "Modelling and optimization of semi batch toluene mononitration with mixed acid from performance and safety viewpoints.", *Chem. Engg. Sci.*, **47**, 2517 (1992).
128. J. A. Quinn and D. B. Sigloh, "Phase inversion in the mixing of immiscible liquids.", *Can. J. Chem. Eng.*, **41**, 15 (1963).
129. A. H. Selkar and J. Sleicher, "Factors affecting which phase will disperse when immiscible liquids are stirred together.", *Can. J. Chem. Eng.*, **43**, 298 (1965).
130. S. Kumar, "On phase inversion characteristics of stirred dispersions," *Chem. Eng. Sci.*, **51**, 831 (1996).
131. M. A. Norato, C. Tsouris and L. L. Tavlarides, "Phase inversion studies in liquid-liquid dispersions: Engineering research on mixing.", *Can. J. Chem. Eng.*, **76**, 486 (1998).
132. Y. Yeo. Leslie, K Omar, E. M. Susana, Perez de Ortiz and F.H. Geoffrey, "A simple predictive tool for modeling phase inversion in liquid-liquid dispersions," *Chem. Eng. Sci.*, **57**, 1069 (2002).
133. (a) C. Hanson, H.A.M. Ismail, *Journal of Applied Chemistry and Biotechnology* **25**, 319 (1975)
(b) C. Hanson, H.A.M. Ismail, *Journal of Applied Chemistry and Biotechnology.*, **26**, 111 (1976).
134. K. B. Deshpande and S. Kumar, "A new characteristic of liquid-liquid systems--inversion holdup of intensely agitated dispersions.", *Chem Eng. Sci.*, **58**, 3829 (2003).

135. F. Rieger, Ditzl and V. Novak, "Vortex depth in mixed agitated vessels.", *Chem. Eng. Sci.*, **34**, 397 (1979).
136. S. M. Nagy, K. A. Yarovoy, M. M. Shakirov, V. G. Shubin, L. A. Vostrikova and K. G. Ione, "Nitration of aromatic compounds with benzyl nitrate on zeolites.", *J. Mol. Catal.*, **64**, L31 (1991).
137. A. Cornelis, L. Delaude, A. Gerstmans and P. Laszlo, "A procedure for quantitative regioselective nitration of aromatic hydrocarbons in the laboratory.", *Tetrahedron Letters.*, **29**, 5909 (1988).
138. McKinley et al. *AIChE Trans.*, 40 (1944).
139. H. M. Brennecke and K. A. Kobe, *Ind. Eng. Chem.*, "Mixed acid nitration of toluene.", **48**, 1298 (1956).
140. L F Albright, *AIChE Symposium.*, 1969
141. A. J. Engel and O. A. Hougen, "Mass transfer and contactor efficiency in a stirred liquid-liquid reactor.", *AIChE J.*, **9**, 724 (1963).
142. S. V. Jadhav and V. G. Pangarkar, "Particle liquid mass transfer in mechanically agitated contactors.", *Ind. Eng. Chem. Res.*, **30**, 2496 (1991).
143. E. Molga and R. Cherbanski, "Catalytic reaction performed in the liquid-liquid system at batch and semi batch operating mode.", *Catalysis Today.*, **66**, 325 (2001).
144. A. H. P. Skelland and H. Xien., "Dispersed-phase mass transfer in agitated liquid-liquid systems.", *Ind Eng. Chem. Res.*, **29**, 415 (1990).
145. V. G. Pangarkar, A. A. Yawalkar, M. M. Sharma and A. A. C. M. Beenackers, "Particle-liquid mass transfer coefficient in two-/three-phase stirred tank reactors.", *Ind. Eng. Chem. Res.*, **41**, 4141 (2002).
146. P. H. Calderbank and M. B. Moo Young, "The continuous phase heat and mass transfer properties of dispersions.", *Chem. Eng. Sci.*, **16**, 39 (1961).
147. H. S. Fogler, *Elements of Chemical Reaction Engineering.*, **2nd** edn; PH Inc USA, (2000).

APPENDIX A

PHOTOGRAPHS OF EXPERIMENTAL SET-UP AND REACTION CALORIMETER

1. Experimental set-up

2. Reaction calorimeter

PUBLICATIONS FROM THE STUDY

1. I. Sreedhar, K. S. Reddy, M. Ramakrishna, S. J. Kulkarni and K. V. Raghavan, “Studies on *para*-selectivity and yield enhancement in zeolite catalyzed toluene nitration.”, *The Can. J. Chem. Eng.*, (2007) (**Accepted, In Press**).
2. I. Sreedhar, K. S. Reddy and K. V. Raghavan, “Studies on physico-chemical changes of zeolites in mononitration of toluene.”, *Kinetics and Catalysis.*, (2007) (**Communicated**).
3. I. Sreedhar, K. S. Reddy, M. Ramakrishna and K. V. Raghavan, “Catalyst Characterization Studies of Zeolites in mononitration of toluene.”, *8th International Symposium on Catalysis Applied to Fine Chemicals (CAFC-8)*., September 2007, Verbania, Italy, September 17-20 (2007). (**Accepted**).
4. I. Sreedhar, K. S. Reddy, M. Ramakrishna, S.J. Kulkarni and K.V. Raghavan, “Process analysis of solid acid catalyzed mononitration of toluene.”, *Proceedings of International Symposium & 58th Annual Session of IChE in association with International Partners (CHEMCON 2005)*, New Delhi, Dec 14-17, (2005).
5. I. Sreedhar, K. S. Reddy and K. V. Raghavan, “Physico-chemical effects on zeolites in toluene mononitration.”, *International Symposium & 60th Annual Session of IChE in association with International Partners (CHEMCON 2007)*, Kolkata, Dec 27-30 (2007). (**Accepted**)
6. I. Sreedhar, K. S. Reddy and K. V. Raghavan, “Kinetic and Phase Inversion Studies of Zeolite Catalyzed Toluene Nitration.”, *International Journal of Chemical Reactor Engineering* (To be Communicated).
7. K. S. Reddy, I. Sreedhar, S. J. Kulkarni, N. Narendar and K. V. Raghavan, *8th International Symposium on Catalysis Applied to Fine Chemicals (CAFC-8)*., Verbania, Italy, September 17-20 (2007). (**Accepted**).

8. K. S. Reddy, I. Sreedhar and K. V. Raghavan, "Interrelationship of process parameters in vapor phase pyridine synthesis.", "Optimization of vapor phase pyridine synthesis from acetaldehyde, formadehyde and ammonia.", *International Symposium & 60th Annual Session of IChE in association with International Partners (CHEMCON 2007).*, Kolkata, Dec 27-30 (2007). (**Accepted**).
9. K. S. Reddy, I. Sreedhar, M. Ramakrishna, S. J. Kulkarni and K. V. Raghavan, "Optimization of vapor phase pyridine synthesis hindered by rapid catalyst deactivation.", *Chem. Eng. J.*, (**Communicated 2007**).

Brief Biography of the Candidate

I did my B.Tech in Chemical Engineering from N.I.T Warangal (1989-93) and M.Tech in Chemical Engineering from IIT, Delhi (1993-94). Henceforth, I worked as Research Associate from 1994 to 1996 at IIT Delhi, as a senior process Engineer at Grindwell Norton Ltd, Mumbai from 1996 to 1999 and as a lecturer in Chemical Engineering at Bapatla Engineering College. Currently, I have been working as a lecturer in Chemical Engineering in BITS, Pilani from Dec 2001 till date. I have published 6 papers in Journals / conferences apart from two papers communicated to International Journals.

Brief Biography of the Supervisor

DR K V RAGHAVAN (DOB: 01.10.1943) is a Fellow of the National Academy of Engineering, Indian Institute of Chemical Engineers (IChE) and A.P. Akademi of Sciences and a Distinguished Fellow of University Grants Commission (UGC). He did his B.Tech. from Osmania University in 1964; M.S. and Ph.D from the Indian Institute of Technology (IIT), Madras. He joined CSIR service in 1964 and worked in three national laboratories. He became the Director of Central Leather Research Institute (CLRI), Chennai in 1994. He was the Director of Indian Institute of Chemical Technology, Hyderabad from 1996 to 2003. Currently he is the Chairman of the Recruitment and Assessment Centre, DRDO, New Delhi

Chemical process development and design, reaction engineering, simulation and modeling and chemical hazard analysis are broad areas of his specialization. His basic research contributions have been simulation of complex reaction in fixed bed reactors, hydrodynamics of multiphase reaction system, envirocatalysis for clean processing, zeolite catalysis for macromolecules, thermochemistry and kinetics of charge transfer polymerization and modeling of chemical accidents.

He published more than 100 papers, filed 45 patents and edited 3 books. His applied research efforts, covering a time span of three decades, contributed to the development of

more than 25 chemical processes with high industrial impact in bulk organics, speciality chemicals, essential oil field chemicals and fluoroorganics. He made significant scientific contribution to the technological upgradation of leather and drugs/pharma sectors.

Dr Raghavan represented on the Syndicate and Academic Councils of Anna University, BITS (Pilani) and School of Chemistry of Hyderabad University. He was the Honorary Professor of Anna University and Indian Institute of Technology (Kharagpur) and Member of the Research Councils of NCL (Pune), RRL (Bhubaneswar), CFRI (Dhanbad) and CPPRI (Saharanpur). Currently, Dr Raghavan is the Member of Atomic Energy Regulatory Board, Director of Heavy Water Board, Central Insecticides Board (CIB), Bureau of Indian Standards (BIS), Project Advisory Committee of DOD on New Bioactives from Ocean Sources, High Powered Committee on Disaster Management, Govt. of India and Scientific Advisory Committees (SAC) of Petroleum and Health Ministries of Govt. of India. He is the Member of the High Level Task Force for Drugs and Pharmaceutical Industry in A.P. He is a Member of Asia Pacific Council for Chemical Engineering, American and Indian Institute of Chemical Engineers (IICChE), Catalysis Society of India and other professional bodies. He was the President of IICChE in 1997 and Currently, he is the President of AP Akademi of Sciences.

Dr Raghavan visited more than 25 countries in North and South America, Europe, Russia, Caribbean, Africa, Middle East, Far East, South East and South Asian regions under bilateral and multilateral programs supported by CSIR, NSF (USA), European Commission (Brussels), Hungarian and USSR Academy of Sciences, UNDP, UNIDO, Commonwealth Science Council, Japanese Institute of Chemical Research, Asia Pacific Council for Chemical Engineering.

Dr Raghavan is the recipient of the Hindustan Lever Award of the Most Outstanding Chemical Engineer of the Year, NRDC Invention Promotion Award, Pilot Officer DV Ranga Reddy Gold Medal, J N Sinha Roy Memorial, ChemTech Foundation and A.P. Akademi of Science Awards.